Coordination Chemistry and Applications of Medium/High Oxidation State Metal and Non-Metal Fluoride and Oxide-Fluoride Complexes with Neutral Donor Ligands.

William Levason,* Francesco M. Monzittu and Gillian Reid

School of Chemistry, University of Southampton, Southampton SO17 1BJ UK

Abstract

Most high and medium oxidation state (O.S. ≥ 3) metal and non-metal fluorides and oxide fluorides have Lewis acidic properties although detailed exploration of their chemistry with neutral ligands, which differs significantly from that with chloride, bromide or iodide co-ligands, has only been undertaken in recent years. The previous review (Benjamin et. al. Chem. Soc. Rev. 42 (2013) 1460) covered work published up to ~ 2011, and the present article covers new work up to early 2019, a period which has seen many new contributions to the field. This article describes work on the coordination chemistry of d, f and p-block fluorides and oxide fluorides with neutral ligands containing donor atoms drawn from Groups 15 (N, P, As or Sb) and 16 (O, S, Se or Te) and including N-heterocyclic carbenes. The incorporation of the radionuclide ^{18}F into neutral metal complexes and their use in medical diagnosis via positron emission tomography (PET) is described, along with briefer coverage of other potential applications.

Keywords: fluoride; oxide fluoride; complexes; ^{18}F radiopharmaceuticals;

Contents

* Corresponding author. E-mail wxl@soton.ac.uk

Abbreviations: those which appear only once are defined in the text, more common abbreviations are: py = pyridine, 2,2'-bipy = 2,2'-bipyridyl, 4,4'bipy = 4,4'-bipyridyl, 4,4'-Me_2-2,2'-bipy = 4,4'-Me_2-2,2'-bipyridyl, 1,10-phen = 1,10-phenanthroline, terpy = 2,2',6',2''-terpyridine, PMDTA = N,N,N'N"-pentamethyldiethylenetriamine, tacn = 1,4,7-triazacyclononane, Me_3-tacn = 1,4,7-trimethyl-1,4,7-triazacyclonane, BnMe_2-tacn = 1-benzyl-4,7-dimethyl-1,4,7-triazacyclonane, Rpy = substituted pyridine, e.g. 3-Mepy = 3-methylpyridine, 4-Me_2Npy = 4-dimethylaminopyridine, pyNO = pyridine N-oxide, 2Meimid = 2-methylimidazole, en = 1,2-ethanediamine, tmeda = tetramethylethylenediamine, acacH = acetylacetone, 12-crown-4 = 1,4,7,10-tetraoxacyclododecane, 15-crown-5 = 1,4,7,10,13-pentaoxacyclopentadecane, 18-crown-6 = 1,4,7,10,13,16-hexaoxacyclooctadecane, [18]aneO_4S_2 = 1,10-dithia-4,7,13,16-tetraoxacyclohexadecane, [15]aneO_3S_2 = 1,4-dithia-7,10,13-trioxacyclopentadecane, [18]aneO_4Se_2 = 1,10-diselena-4,7,13,16-tetraoxacyclohexadecane, dmso = dimethylsulfoxide, dmf = N,N-dimethylformamide, thf = tetrahydrofuran, AHF = anhydrous hydrogen fluoride, 2,3,2-tet = 1,4,8,11-tetraazaundecane, 2,2,3-tet = 1,4,7,11-tetraazaundecane**,** $BIMEt_3$ = tris(1-ethyl-benzoimidazol-2-ylmethyl)amine, NHC = N-heterocyclic carbene (specific formulae of NHC's and other carbenes are shown below).

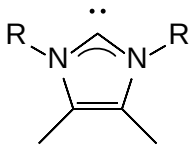

R = Me, Et, ^{i}Pr

[$NHCMe_2R_2$]

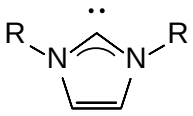

R,R' = Me [$NHCMe_2$]

R = Et, R' = Me [NHCEtMe]

R,R' = ^{i}Pr [$NHCIP_2$]

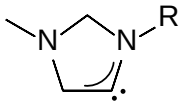

R = Me, Et, ^{i}Pr

[NNHC]

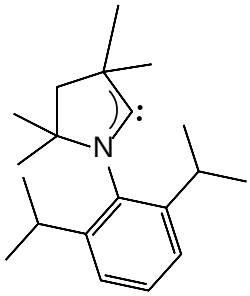

[NHCAAC]

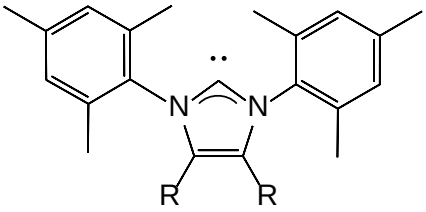

R=H [$NHCMes_2$]

R=Cl [$NHCCl_2Mes_2$]

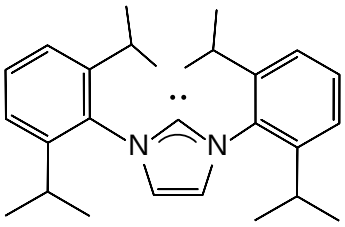

[$NHCD^{i}PP_2$]

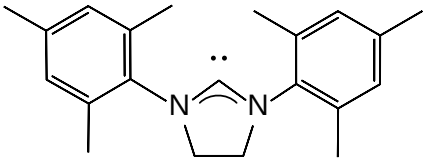

[$SNHCMes_2$]

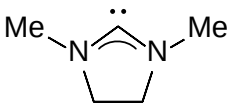

[$SNHCMe_2$]

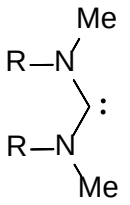

R = Me_2

[CAMe]

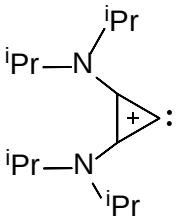

[$NC^{i}Pr_4$]

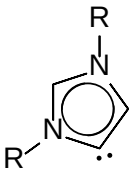

[ANHC]

1. Introduction and Scope

The coordination chemistry of metal fluorides and oxide fluorides has traditionally developed separately from that of the heavier halides, and, until the last twenty-five years, the characterisation of the complexes was often poor and the properties were not investigated in any detail [1,2]. Recent years have seen much renewed interest in this area of chemistry, which results both from the recognition that the chemistry of metal fluoride complexes is fundamentally different to that of other halides [3,4,5,6,7] and from applications such as the use of ^{18}F in radiochemical diagnostics (PET imaging) [8,9,10]. Metal fluorides are also popular building blocks for molecular magnets, although only in a small minority of these cases are neutral ligands involved. This work is reviewed elsewhere [11,12] and is therefore not discussed in detail in the present article. Metal fluoride complexes in catalysis have been receiving increased attention [13,14]. In a review published in 2013 [7], we discussed the chemistry of metal and non-metal fluoride and oxide fluoride complexes containing neutral donor ligands with the metal/non-metal Lewis acid in oxidation states ≥ 3. Complexes in the higher oxidation states demonstrate the very significant differences imposed by the fluoride ligands on the metal/non-metal centre and result in quite different stabilities and reactivities compared to complexes containing the heavier halides, alkoxides, amides, etc. The unique ability of fluorine to stabilise very high oxidation states results, in many cases, in complexes that have no chloride or bromide analogues.

There has been significant new work in this area and the present article is an update covering the literature published from late 2011 to early 2019; earlier work is only discussed where needed to place recent results in context. The current article excludes organometallic or low-valent compounds, specifically compounds with M-C bonds, metal carbonyls, metallocenes, etc., that are dealt with in other articles. Relevant neutral ligands are those with donor atoms from Group 15 (N, P, As or Sb) and Group 16 (O, S, Se or Te) and we also include N-heterocyclic carbenes (NHCs). The aim is to showcase the new work published in this period, rather than provide fully comprehensive coverage, although we aim to include all new compounds and significant new studies of existing complexes. Fluoride complexes containing the softest donor ligands are very rare, but the recent characterisation of tertiary arsine complexes of WF_6 [15] and a telluroether complex of TaF_5 [16], demonstrate that some complexes of this type are obtainable. Other recent reviews covering aspects of fluorine chemistry are: *Crystal Chemistry and Selected Physical Properties of Inorganic Fluorides and Oxide-Fluorides* [17]; *Molecular Hexafluorides* [18]; *A survey of titanium fluoride complexes, their preparation, reactivity and applications* [14]; and *Highly reactive carbenes as ligands for main group element fluorides* [19]. Reviews covering relevant aspects of the chemistry of single elements are listed in the appropriate sections below.

2. Synthesis

All the elements in the periodic table, except He, Ne and Ar, form fluorides and many also form oxide fluorides, so a wide variety of synthesis routes for their complexes are possible, although often only one or two will be suitable for a specific complex. The Lewis acidity of these metal/non-metal fluorides is most easily demonstrated by their formation of the corresponding fluoroanions, which form for almost all examples [17]. Typically fluoroanions are formed from aqueous or anhydrous HF, or alkali metal fluorides in water or in melts, none of which are generally suitable routes for the synthesis of neutral ligand complexes. The few cases where fluoroanions do not form are mostly associated with "coordinatively saturated" fluorides such as SF_6. For complexes with neutral donor ligands a number of other factors need to be considered in addition to the Lewis acidity of the metal. A key factor is that fluorine forms very strong bridges between metal centres, often of type M-(μ^2-F)-M, and competition between coordination of an MF_n fragment to a neutral ligand and polymerisation to form (or reform) the binary fluoride *via* such fluorine bridges is competitive in many systems. For the heavier halogens the generally weaker bridge bonds makes this competition much less important. Neutral ligands containing the heavier (soft) donor atoms, are reducing agents in the free state, and may promote reduction of the metal if readily dissociated from the metal centre in solution or if present in the synthesis in excess. Many of the parent fluorides and the complexes described are sensitive to water; in some cases water competes with the neutral ligand for the metal centre, in others trace water causes hydrolysis of the M-F bonds and decomposition. In marked contrast, in a limited number of cases, complexes may be prepared in water, sometimes using hydrothermal methods.

In the previous review [7] we suggested a pragmatic "classification" of the metal fluoride/oxide fluorides from the viewpoint of synthesising their metal complexes, and an updated version of this is shown below

- No Lewis acidity – examples are NF_3 or CF_4;
- Probably incompatible with neutral organic ligands due to their extremely strong oxidising/fluorinating power, e.g. IrF_6, RuF_6, BiF_5, $CrOF_4$, CrF_5, PbF_4;
- Molecular fluorides or oxide fluorides that may react directly with neutral ligands, sometimes dispersed in an inert solvent or even in the absence of solvent, e.g. SiF_4, GeF_4, AsF_5, BF_3, PF_5, WF_6;
- Weakly polymerised fluorides or oxide fluorides, which may react directly in a suitable non-polar or weakly polar solvent, e.g. TaF_5, NbF_5, VOF_3, SbF_5;
- Strongly polymerised fluorides that may be converted into a suitable (molecular and soluble) synthon – examples are SnF_4 (as $[SnF_4(MeCN)_2]$), TiF_4 (as $[TiF_4(thf)_2]$); the synthon here contains a readily substituted neutral co-ligand;

- Very strongly polymerised, but may form synthons of more limited utility – examples are $[ZrF_4(dmso)_2]$ or $[HfF_4(dmf)_2]$; the strongly coordinating dmso or dmf are necessary to break up the parent fluoride polymer, but are consequently more difficult to substitute by other ligands;
- Sometimes the anhydrous binary metal fluoride is inert, but a hydrated form may provide an entry into the coordination chemistry, e.g. $MF_3{\cdot}3H_2O$ (M = Al, Ga), often using hydrothermal routes.
- Inert polymers where no suitable molecular synthons are known, e.g. WO_2F_2, VO_2F, ScF_3. Complexes of these metal fluorides may be accessible *via* Cl/F exchange from the corresponding chloro-complex or, for oxide fluorides, *via* O/F exchange from the binary fluoro-complex;
- Inert and intractable, e.g. BiF_3, PbF_2, and the 4f-block trifluorides, for which there are no reports of successful complex formation with neutral ligands.
- For complexes stable to water and dilute acid, addition of an alcohol solution of the ligand to the metal ion in dilute aqueous HF may be possible, e.g $[MO_2F_2(L)_2]$ (M = Mo or W).

The majority of the complexes discussed in this article are prepared from the parent fluoride or oxide fluoride directly, by reaction with the neutral ligand, or *via* use of an intermediate synthon. The latter is often a discrete, molecular nitrile or ether complex, formed by dissolution of the fluoride in the appropriate solvent. The solution may be reacted directly with the new ligand, or after isolation of the solvent adduct. The latter can be reacted subsequently with other neutral ligands in a non-coordinating solvent, which avoids competition between the donor nitrile or ether solvent present in large excess and the incoming ligand.

As indicated above, some metal fluoride hydrates, including $MF_3{\cdot}3H_2O$ (M= Al, Ga, In), can be complexed with N-donor ligands using hydrothermal vessels (180°C, 15h) [20]. The same approach fails with $MF_3{\cdot}xH_2O$ (M = Sc, Y, La), when the reagents are recovered unchanged [21]. The differences may result from the different constitution of the trifluoride "hydrates". Whilst those of Group 13 contain water coordinated to the metal centre, the Group 3 compounds were shown by PXRD to have the extensively polymerised structure of the anhydrous trifluorides with the water on the surface or interstitial [21]. The hydrated tetrafluorides of Zr and Hf, in which the water is also coordinated to the metal, dissolve in refluxing dmso or dmf to form $[ZrF_4(dmso)_2]$ or $[HfF_4(dmf)_2]$, which are useful synthons [22]. The anhydrous tetrafluorides appear to be completely inert. A variant on this approach is the synthesis of complexes of VOF_2 from VF_4 and O- or N-donor ligands under hydrothermal conditions [23].

An alternative approach is Cl/F exchange from a pre-formed chloro-complex with the neutral ligand(s) already installed. Since many of the highest oxidation state fluorides do not have isolable chloride analogues, this limits the systems for which Cl/F exchange is possible. Typical fluoride sources are Me_3SnF [24], $[R_4N]F$,

[PPh_4]F, or [K(18-crown-6)]F. A rare and unexpected result of using Me_3SnF as fluorinating agent was the coordination of the Me_3SnCl formed (as a weak Lewis acid) to the M-F unit formed, as in [Sc(Me_3-tacn)F_2(μ-F)$SnMe_3Cl$] [21]. Fluorinating agents such as XeF_2 or SF_4 may work in some systems, but may be too aggressive in others. AHF has been used to fluorinate chloro-complexes, but requires metal or fluoroplastic equipment and can result in unwanted bond cleavage. Displacement of F^- from a fluoroanion by a neutral ligand is seldom used, as it requires breaking of the strong M–F bond, and separation of the [cation]F by-product. A rare example is the formation of [VO_2F(2,2'-bipy)], from [Ph_4As][VO_2F_2] and 2,2'-bipyridyl in refluxing MeCN [25].

Oxide fluorides can also be intractable and therefore growing use is being made of O/F exchange from the binary fluoride complex and $(Me_3Si)_2O$, since the volatile by-product, Me_3SiF, is easily removed, e.g. the synthesis of [WOF_4(MeCN)] from WF_6 and $(Me_3Si)_2O$ in anhydrous MeCN. The [WOF_4(MeCN)] can then be reacted with other ligands (L) to generate [WOF_4(L)] [26]. WO_2F_2 and $NbOF_3$ are intractable polymers and do not react with neutral ligands, but [$WO_2F_2(L)_2$] complexes can be made from [WOF_4(MeCN)] + 2L and a further equivalent of $(Me_3Si)_2O$ [26], whilst [$NbOF_3(L)_2$] are obtained from NbF_5, $(Me_3Si)_2O$ and 2L in MeCN [27].

Some very aggressive systems require fluoroplastic or metal equipment (e.g. the higher fluorides of the platinum metals) or systems using (or generating) HF, but in many cases borosilicate glass vessels fitted with PFTE taps that are common in modern organometallic laboratories are adequate, along with glass vacuum lines and high quality glove box facilities. For the most reactive systems the key requirement is to use rigorously anhydrous conditions, thoroughly dried glassware, dried solvents and purified/dried ligands. Water not only competes successfully with many ligands for the metal fluoride, but also may initiate a downward spiral of attack on the glass, formation of HF, SiF_4, and in some cases, ready protonation of the ligand (especially with N-donor functions). It can also introduce HF_2^- or fluorosilicate anions into the products. One benefit of the hydrothermal reactions (above) is that the fluoroplastic vessels used mean any HF that is generated is not a problem.

3. Structural and Spectroscopic Characterisation

The species described in this article are mostly molecular coordination complexes, and their characterisation uses the usual suite of structural and spectroscopic techniques. We have discussed the key features of their application to metal fluoride complexes elsewhere [7]. Some new points to consider are mentioned here.

Single crystal X-ray diffraction: The continuing improvements in diffractometers and computing power means that the main challenge in the area is now the growth and handling of often very reactive and moisture sensitive crystals. One should also bear in mind that particularly with very reactive systems the species found in the single crystal X-ray structure may not be characteristic of the bulk. Often spectroscopic data on the

bulk sample may provide the required assurance, while PXRD can be used to confirm whether the bulk sample is (or is not) the same as that found in the single crystal structure [23]. Examples of the problems in very reactive systems are the W(VI) complexes $[WF_4(L\text{-}L)_2][WF_7]_2$ (L-L = 2,2'-bipy, *o*-$C_6H_4(PMe_2)_2$), where the microanalysis and spectroscopic data on the bulk samples clearly identify them as the heptafluorotungstate(VI) salts, but whilst the few crystals grown from batches of these complexes in MeCN show the expected dodecahedral cations, the anions present in individual crystals were $[WOF_5]^-$, $[W_2O_2F_9]^-$, or $[WF_8]^{2-}$, clearly resulting from trace hydrolysis during the crystal growth [15,28].

NMR and EPR Spectroscopy: ^{19}F NMR spectroscopy (I = ½, 100%) provides a very sensitive specific probe in diamagnetic complexes; the other halogens have only quadrupolar nuclei that are not observable in the low symmetry environments of coordinated halide groups. ^{19}F NMR spectroscopy is also very useful in identifying decomposition products or impurities formed by fluorination of the neutral ligands. For example, the reaction of Me_2Te and TeF_4 produced Me_2TeF_2 and elemental tellurium rather than a complex of TeF_4 [29]. Triphenylarsine oxide forms complexes with some metal fluorides, but in other systems it is converted to Ph_3AsF_2, which is most easily identified by the characteristic ^{19}F NMR chemical shift [30]. Although usually not identified, the other product is probably the corresponding metal oxide fluoride (i.e. the arsine oxide is functioning as an O/F exchange reagent rather than a ligand). Many of the complexes described in this review, especially those of weakly bound soft donor ligands, are labile and undergo rapid reversible dissociation at ambient temperatures in non-donor solvents. In order to resolve the resonances of inequivalent fluorines or spin-spin couplings, it is often necessary to record NMR spectra at low temperatures. CH_2Cl_2/CD_2Cl_2 (m.p. –97°C) is particularly useful in this respect and under anhydrous conditions often reacts only slowly, even with highly reactive fluorides. Very little work has been reported using solid state ^{19}F NMR spectroscopy, which presumably reflects limited access to the appropriate hardware (a specific solid state probe is necessary to observe ^{19}F NMR resonances). For paramagnetic complexes, for which NMR spectroscopy is unavailable, EPR may provide an alternative. Depending upon the d^n configuration, EPR spectroscopy can prove very useful. One possible problem in very reactive systems is the very high sensitivity of the EPR technique, which may produce credible resonances from minor species/impurities. A good example of this is in the (non-fluoride) vanadium(IV) systems where the EPR signals attributed to $[VCl_4(PR_3)_2]$ species were in fact due to phosphine oxide impurities with the major constituent being the V(III) $[VCl_4(PR_3)_2]^-$, which are EPR silent [31].

4. f-block complexes

There appear to be no known simple adducts of lanthanide(III) fluoride complexes containing neutral ligands. The "hydrate" $LaF_3{\cdot}xH_2O$ does not react with neutral ligands, including Me_3-tacn or terpy, even under hydrothermal conditions (180°C). PXRD showed the "hydrate" had the same polymeric structure as

anhydrous LaF_3 indicating that the water is interstitial or surface and not coordinated to the lanthanum, which accounts for its lack of reactivity [21]. Treatment of $[LaCl_3(Me_3\text{-tacn})(OH_2)]$ with $[NMe_4]F$ in MeCN resulted in displacement of the Me_3-tacn and precipitation of LaF_3 [21].

Cerium(IV) fluoride dissolves sparingly in liquid ammonia to form $[CeF_4(NH_3)_4]\cdot NH_3$, which has a distorted square antiprismatic structure [32] and is isomorphous with $[MF_4(NH_3)_4]\cdot NH_3$ (M = U, Zr, Hf) [33]. $CeF_4\cdot xH_2O$ does not dissolve in or react with MeCN or dmf even on prolonged reflux, but dissolves slowly in refluxing dmso to give a yellow solution from which yellow crystals $[CeF_4(dmso)_2]$ were isolated [34]. The structure (Fig. 1) reveals a distorted square antiprismatic cerium environment with two *cis* disposed O-coordinated dmso molecules, linked into a zig-zag chain by fluorine bridges. Attempts to use this complex as a synthon for other complexes were unsuccessful, the dmso was not displaced by phosphine oxides or diimines in dmf solution.

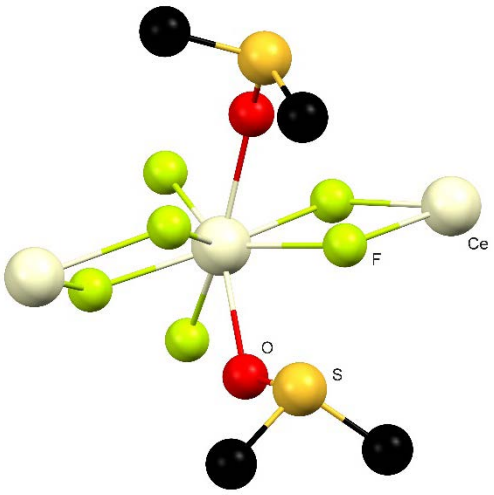

Fig. 1 The structure of $[CeF_4(dmso)_2]$, showing part of the fluoro-bridged chain structure (including the next Ce neighbours), redrawn from reference 34. The dmso groups were disordered and only the major component is shown. [Hydrogen atoms are omitted for clarity from this and subsequent structures unless needed to identify ligands]

Actinide fluoride complexes with neutral donor ligands are more numerous, but mostly limited to uranium. Attempts to produce thorium complexes from $ThF_4\cdot xH_2O$ were unsuccessful, the hydrate proved to be insoluble even in refluxing dmso [34]. The reaction of UF_4 with $K_2Th(NO_3)_6$ in liquid ammonia gave the large cluster $[Th_{10}(\mu\text{-}F)_{16}(\mu\text{-}O)_8(NH_3)_{32}](NO_3)_8\cdot 19{\cdot}6NH_3$, which has a $Th_{10}(\mu\text{-}O)_4$ core with edge-bridging fluorides [35].The reaction of $[Th(SPh)_x(SC_6F_5)_{4-x}]$ with AgF in pyridine solution gave colourless crystals of $[Th_2(\mu\text{-}F)_3F_2(py)_7(SC_6F_5)_3]\cdot 2py$ (Fig. 2) containing nine-coordinate thorium [36].

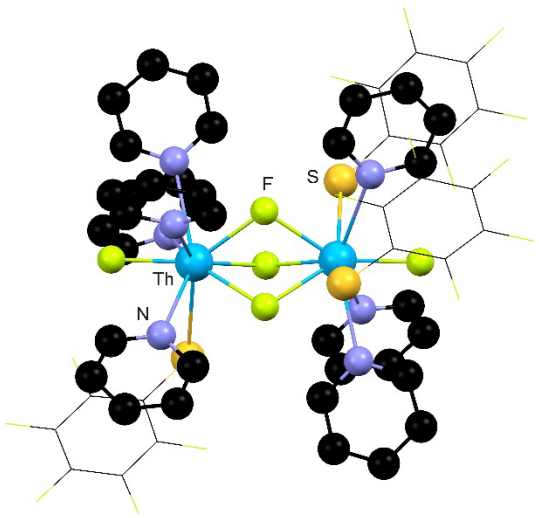

Fig. 2 The structure of $[Th_2(\mu\text{-}F)_3F_2(py)_7(SC_6F_5)_3]$ redrawn from Reference 36.

The reaction of UF_6 with liquid ammonia gave a mixture of green crystals, identified as $[NH_4]_3[UF_7(NH_3)]\cdot NH_3$, and $[UF_4(NH_3)_4]\cdot NH_3$ in an approximate ratio of 2:1, which could be separated manually [33]. $[UF_4(NH_3)_4]\cdot NH_3$ could also be made from UF_4 and liquid ammonia and loses the ammonia solvate molecule at room temperature. The structure of $[UF_4(NH_3)_4]\cdot NH_3$ is a square antiprism like the Ce, Zr and Hf analogues [33] whilst the $[UF_7(NH_3)]^-$ anion is a bicapped trigonal prism. The tricapped trigonal prismatic cation in $[UF(NH_3)_8]Cl_3$ is formed from the reaction of excess $TiCl_3$ with UF_4 in liquid ammonia [37]. Dissolution of UO_2F_2 in liquid ammonia produces the yellow $[UO_2F_2(NH_3)_3]\cdot 2NH_3$ the structure of which shows a pentagonal bipyramidal geometry with a *trans* UO_2 group [38]. The $[UO_2F_2(NH_3)_3]\cdot 2NH_3$ loses the solvated NH_3 below room temperature to form yellow $[UO_2F_2(NH_3)_3]$ of unknown structure. Uranium pentafluoride dissolves in liquid HCN to produce turquoise $[UF_5(HCN)_2]$ which is a 1D polymer with the uranium coordinated to four terminal and two bridging fluorides and two N-coordinated hydrogen cyanide molecules [39].

The reaction of uranium metal, iodine and AgF_2 in pyridine solution gives green $[UF_2I_2(py)_4]\cdot 2py$ (Fig. 3) which is soluble in pyridine and thf and is potentially a useful synthon to prepare other U(IV) fluoride complexes [36]. The corresponding $[UF_2Cl_2(py)_4]$ was obtained as a by-product from reaction of a uranium pincer carbene with PhCOF [40]. The hydrothermal reaction of $UO_2(NO_3)_2$, 1,10-phen and HF gave yellow crystals of $[\{UO_2(1,10\text{-phen})(\mu\text{-}F)F\}_2]$, which contains a dimer structure with edge-sharing pentagonal bipyramidal molecules [41]. Extensive DFT calculations on $[\{MO_2(L\text{-}L)(\mu\text{-}F)F\}_2]$ (M = U, Np or Pu, L-L = 1,10-phen, $2NH_3$, 2F) exploring the predicted structures and electronic properties were also reported [41].

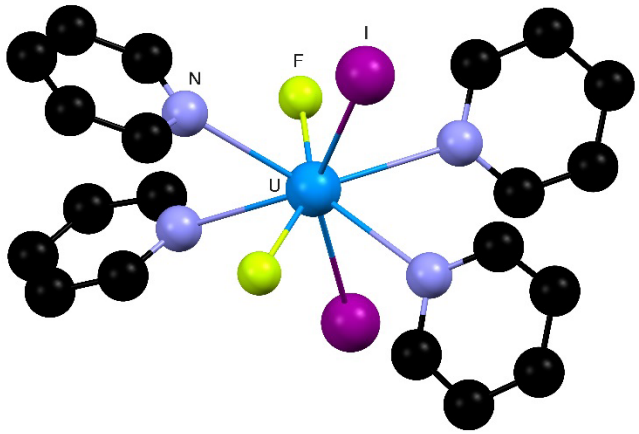

Fig. 3 Structure of $[UF_2I_2(py)_4]$ redrawn from reference 36.

Trimethyltin fluoride converts the uranocene halides, $[U(\eta^5\text{-}Me_5C_5)_2X_2]$ (X = Cl, Br) in toluene solution containing R_3PO (R = Me, Ph, Cy), to the phosphine oxide complexes $[U(\eta^5\text{-}Me_5C_5)_2F_2(OPR_3)]$, which have the structure shown in Fig. 4 [42].

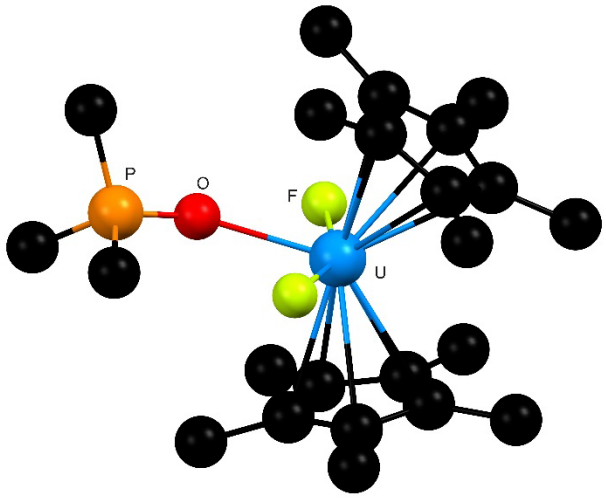

Fig. 4 Structure of $[U(\eta^5\text{-}Me_5C_5)_2F_2(OPMe_3)]$ redrawn from Reference 42.

5. d-block complexes

Group 3

The "hydrates", $ScF_3{\cdot}xH_2O$ and $YF_3{\cdot}xH_2O$ do not react with neutral N- or O-donor ligands even under hydrothermal conditions, and like the $LaF_3{\cdot}xH_2O$ discussed above, PXRD shows them to have the same structures as the anhydrous trifluorides, explaining their inert nature [21]. Although a few examples of Sc-F bonds are known in complexes with charged C or N donor co-ligands, the first examples of neutral N-donor complexes have been obtained only very recently [21]. These are $[ScF_3(R_3\text{-tacn})]$ (R_3 = Me_3 or $BnMe_2$) and $[ScF_3(terpy)]$, which were made from the corresponding chloro-complexes and either $[Me_4N]F$ or Me_3SnF in

anhydrous MeCN. The Me_3SnF route results in isolation of adducts with the Me_3SnCl formed, *viz* [Sc(Me_3-tacn)F_2(μ-F)$SnMe_3Cl$] and [Sc(terpy)F(μ-F)$_2$($SnMe_3Cl$)$_2$]; the structure of the former is shown in Fig. 5.

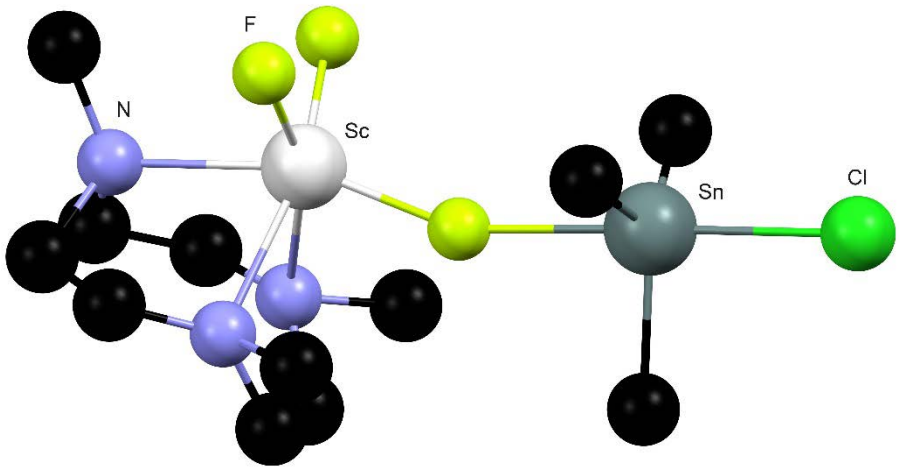

Fig. 5 Structure of [Sc(Me_3-tacn)F_2(μ-F)$SnMe_3Cl$] redrawn from Reference 21. Carbon atoms in the macrocycle and Me_3SnCl were disordered and only one component is shown.

The terpy complex decomposes in solution, but although $^{19}F\{^1H\}$ and ^{45}Sc NMR spectra show the [Sc(Me_3-tacn)F_2(μ-F)$SnMe_3Cl$] is dissociated in solution, it reforms on evaporation [21]. Using a deficit of $[Me_4N]F$ in the Cl/F exchange reaction shows the intermediate formation of $[ScF_{3-x}Cl_x(Me_3\text{-tacn})]$ (x = 2,1,0) (Fig. 6), and the structure of $[ScF_2Cl(Me_3\text{-tacn})]$ was determined. Although they must be prepared under anhydrous conditions, multinuclear NMR studies show that once formed, the $[ScF_3(R_3\text{-tacn})]$ are stable in water at pH = 7 for many weeks, are not decomposed by neutral water at 80°C or by chloride or acetate. They are however decomposed by water at high pH and by excess F^-. Attempted Cl/F exchange using $[YCl_3(Me_3\text{-tacn})]$ or $[YCl_3(terpy)]$ and $[Me_4N]F$ or Me_3SnF found that loss of the N-donor ligand and precipitation of YF_3 occurred and neutral ligand complexes of YF_3 are still unknown [21]. Similarly, reaction of $[ScI_3\{o\text{-}C_6H_4(PMe_2)_2\}_2]$ with $[Me_4N]F$ in anhydrous CH_2Cl_2 solution resulted in liberation of the diphosphine and precipitation of ScF_3 [43].

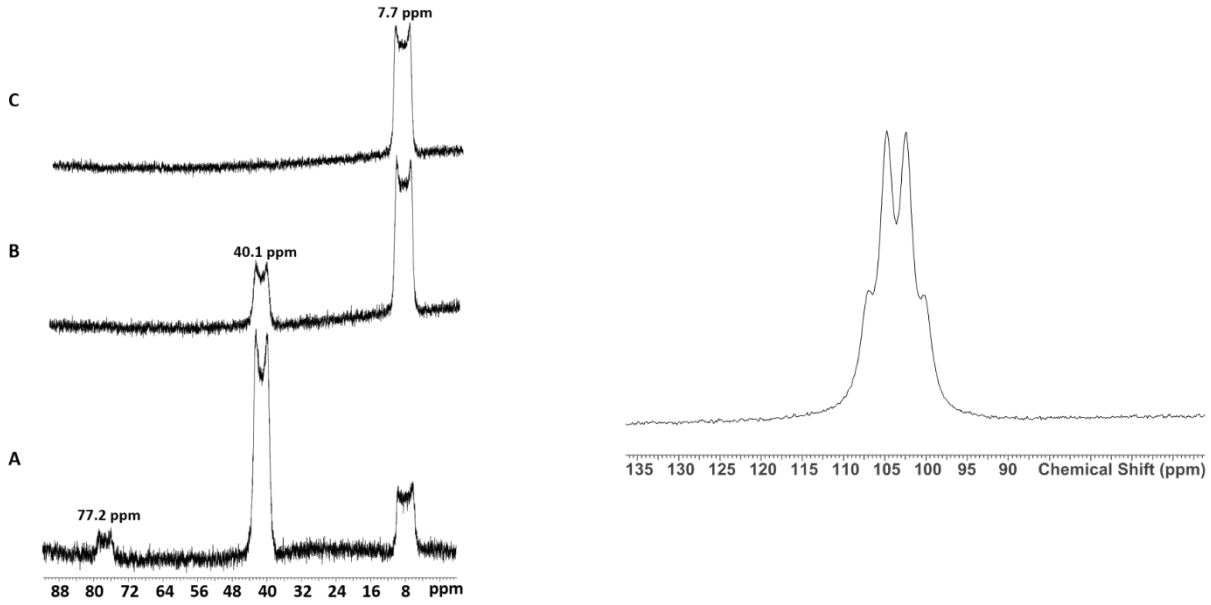

Fig. 6 **Left**: $^{19}F\{^{1}H\}$ NMR spectra of $[ScFCl_2(Me_3\text{-tacn})]$ (77.2 ppm), $[ScF_2Cl(Me_3\text{-tacn})]$ (40.1 ppm) and $[ScF_3(Me_3\text{-tacn})]$ (7.7 ppm). ~ 2.5 mol. equiv. (**A**), <3 mol. equiv. (**B**) and >3 mol. equiv. (**C**) of Me_3SnF were added to a CD_3CN solution of $[ScCl_3(Me_3tacn)]$; **Right**: ^{45}Sc NMR spectrum of *fac*-$[ScF_3(Me_3\text{-tacn})]$. [$^{45}Sc$ is 100% abundant and has I = 7/2, Ξ = 29.24 MHz, Dc = 1710, Q = -0.22×10^{-28} m^2. Reproduced from Reference 21 with permission from the Royal Society of Chemistry.

Group 4

The coordination chemistry of TiF_4 is relatively well developed [7,14] and little new work has appeared. The excellent review by Nikiforov *et.al.* [14] provides a very detailed account of the synthesis, reactivity and applications of complexes derived from TiF_4. It also uses DFT calculations to probe the structures and relative stability of isomers of types $[TiF_{4-n}Cl_nL_2]$ (n = 1-3), $[TiCl_{3-n}F_nL_3]^+$ (n = 1-3), $[TiCl_{5-n}F_n(L)]^-$ (n = 1-4), and compares the results with experimental data where available. In general, a linear L-Ti-F arrangement is the most stable in each case, which maximises the Ti-F pπ-dπ bonding [14].

The colourless Ti(IV) carbene $[TiF_4(NHCD^iPP_2)_2]$ was prepared in good yield from TiF_4 and the carbene in thf solution [44]. The structure (Fig. 7) shows an octahedral titanium centre with the bulky carbenes in a *trans* arrangement. The Ti-C bonds are shorter (2.26 Å) than those in the corresponding $[TiCl_4(NHCD^iPP_2)_2]$ (2.32 Å).

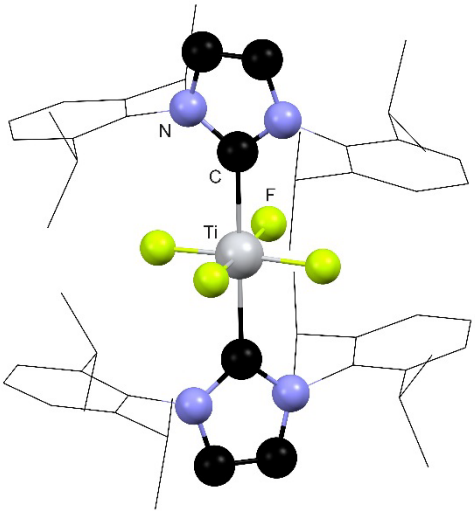

Fig. 7 Structure of $[TiF_4(NHCD^iPP_2)_2]$ redrawn from Reference 44.

^{19}F NMR spectroscopy has been used to identify the formation in MeCN solution of complexes with picolinic acid and picolinic acid esters - $[TiF_4(\kappa^2\text{-}C_5H_5NCOOEt)]$, $[TiF_4(\kappa^2\text{-}C_5H_5NCOOH)]$, *trans*-$[TiF_4(C_5H_5NCOOEt)_2]$ and $[TiF_5(C_5H_5NCOOEt)]^-$ [45]. The ligands, $Ph_2P(O)CH_2C(O)Me$ and $Ph_2P(O)(CH_2)_2C(O)NMe_2$, (L-L), behave as chelating O,O donors producing six-coordinate $[TiF_4(L\text{-}L)]$ [46,47]. In solution excess ligand produces some $[TiF_4(L\text{-}L)_2]$, which on the basis of their ^{19}F and ^{31}P NMR spectra, contain monodentate L-L coordinated through the phosphoryl group. The X-ray structure of $[TiF_4\{Ph_2P(O)(CH_2)_2CONMe_2\}]$ confirmed the presence of a seven membered chelate ring [48]. The chemistry of lower oxidation state titanium fluorides with neutral ligands remains unexplored.

The coordination chemistry of ZrF_4 and HfF_4 is less extensive than that of TiF_4, but the structures of known compounds have been reviewed in detail [49]. The majority of the structural work described concerns fluoro-zirconate(IV) and -hafnate(IV) anions, but the limited structural data on complexes with neutral ligands were also included. The structure of the monoclinic form of $ZrF_4{\cdot}3H_2O$ has been shown to be a polymer with $ZrF_6(H_2O)_2$ groups [50], which contrasts with the known structure of the triclinic form, which is a discrete dimer. The structure of monoclinic $HfF_4{\cdot}3H_2O$ has a similar polymer unit to the zirconium [50]. A new hafnium anion obtained with a 4-amino-1,2,4-triazolium cation is $[C_2H_5N_4][HfF_5(H_2O)_2]{\cdot}H_2O$ which has a pentagonal bipyramidal geometry with axial fluorides and a donor atom sequence of FFOFO in the equatorial plane [51]. The solution speciation of ZrF_4 complexes with Ph_3PO, $^nBu_3PO$ and $(Me_2N)_3PO$ (L) has been explored by variable temperature ^{19}F NMR spectroscopy in CH_2Cl_2 [52]. The species identified were *cis*-$[ZrF_4(L)_2]$, $[ZrF_5(L)]^-$ and *mer*- and *fac*-$[ZrF_3(L)_3]^+$, although the relative amounts of the different species varies with L.

Group 5

Vanadium

High valent vanadium fluoride chemistry is unusual in that whilst complexes of the oxide fluorides VOF_3 and VO_2F are well established [7], and that of VOF_2 has recently been explored (see below), neutral ligand complexes of VF_5 and VF_4 are restricted to work in a few very old reports, although some data on VF_3 adducts is available [7].

The first carbene complex of VOF_3 has been obtained very recently. The $[VOF_3(NHCD^iPP_2)]$ was made by combining VOF_3 and $NHCD^iPP_2$ in thf and the X-ray structure showed a square pyramidal geometry with the oxido group occupying the apical position [53]. Attempts to convert this complex into $[VO_2F(NHCD^iPP_2)]$ by reaction with $O(SiMe_3)_2$ was unsuccessful, with the starting materials recovered unchanged. Combination of $[(NHCD^iPP_2)H]F$ and VOF_3 in MeCN gave the salt $[(NHCD^iPP_2)H][VOF_4]$, which contains a discrete square pyramidal anion (salts containing smaller cations are oligomeric in the solid state), and this hydrolyses in solution to $[(NHCD^iPP_2)H][VO_2F_2]$ [53]. The mixed fluoride-alkoxide complex, $[VOF_2(O^iPr)(^iPrOH)_2]$, crystallised from a $CDCl_3$ solution of the product from reacting $[VO(O^iPr)_3]$ with HF in a $H_2O/^iPrOH$ mixture [54]. The structure is shown in Fig. 8.

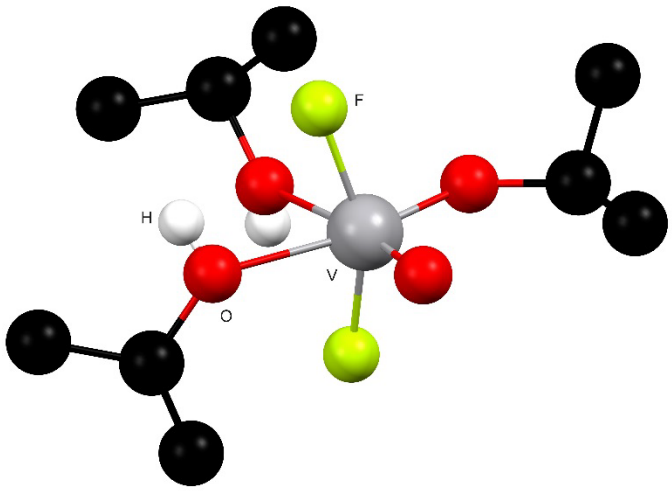

Fig. 8 Structure of $[VOF_2(O^iPr)(^iPrOH)_2]$ redrawn from Reference 54.

A popular synthesis of extended lattice structures or frameworks containing vanadium oxide-fluoride anions is to combine polydentate amines or nitrogen heterocycles, a vanadium source, and aqueous HF, in hydrothermal or solvothermal vessels. The majority of products contain protonated organonitrogen cations, but in some cases the base is also incorporated into the framework. An example is the pyrazine complex $[V_2(N_2C_4H_4)O_2F_4]$, made hydrothermally from pyrazine, VOF_3 and aqueous HF [55]. The structure is a 2D polymer with zig-zag chains of $V^{IV}_2O_2F_4$ linked to adjacent dimers by fluorine bridges and with coordinated pyrazine linking the chains to form a sheet structure. Hydrothermal syntheses were also used to prepare a series of Ag-V^V MOFs with $[Ag_2(VO_2F_2)_2(triazole)_4]$ building blocks [56]. Several mixed valence (V^VV^{IV})

polyoxofluorovanadate clusters containing coordinated pyridine or imidazole have been prepared and their structures determined [57].

Although vanadyl (V^{IV}) oxide fluoride complexes were described in the older literature, characterisation was mostly sketchy and syntheses rather haphazard. Now two series, one containing neutral VOF_2 complexes [23], and the second, VOF^+ cations [58], have been described and characterised in detail (Scheme 1).

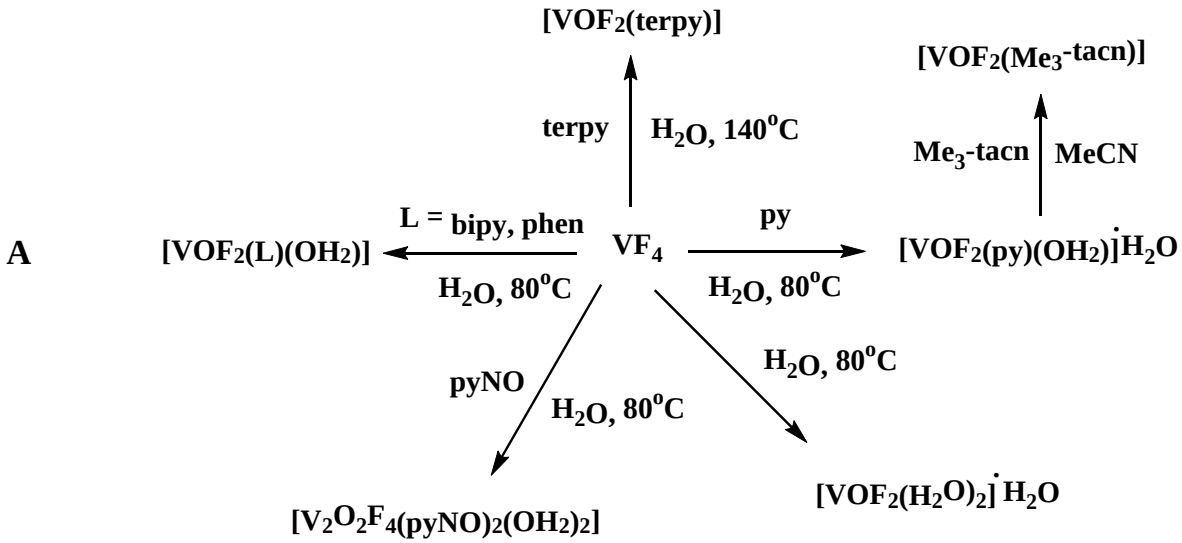

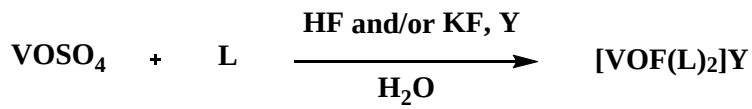

B

L = bipy, 4,4'-Me_2-2,2'-bipy, 4,4'-$^tBu_2$-2,2'-bipy, phen;
Y = BF_4 , ClO_4 , SbF_6

Scheme 1 Synthesis of the VOF_2 and VOF^+ Complexes.

The dissolution of VF_4 in hot water followed by allowing the blue solution formed to evaporate in air, gave blue crystals of $[VOF_2(H_2O)_2]\cdot H_2O$ [23]. The structure consists of square pyramidal molecules with disordered F/H_2O in the basal plane, weakly linked into chains *via* the apical V=O with asymmetric V···O–V bridges. A different hydrate, $[V_2O_2F_4(H_2O)_2]\cdot H_2O$, isolated serendipitously during hydrothermal synthesis of vanadium selenites, has a 2D layered structure [59]. Heating VF_4 with a variety of nitrogen donor ligands either under reflux or in a hydrothermal vessel (80°C) is a convenient way of making VOF_2 complexes (Scheme 1) [23]. Isolated examples include $[VOF_2(terpy)]\cdot 3H_2O$, $[VOF_2(2,2'\text{-bipy})(H_2O)]$, $[VOF_2(1,10\text{-phen})(H_2O)]$, $[VOF_2(py)_2(H_2O)]$ and $[VOF_2(py)_2(H_2O)]\cdot H_2O$. The complex, $[VOF_2(Me_3\text{-tacn})]$, was produced from

$[VOF_2(py)_2(H_2O)]$ and Me_3-tacn in MeCN. The pyridine N-oxide complex, $[V_2O_2F_4(pyNO)_2(H_2O)_2]$, was obtained by the hydrothermal route, but attempts to form complexes with phosphine oxides or $MeOCH_2CH_2OMe$ failed. The complexes have magnetic moments ~ 1.7-1.9 B.M., consistent with $d^1 V^{IV}$ and strong IR absorptions in the range 945-975 cm^{-1} assigned as ν(V=O). The structures of three examples are shown in Figs. 9-11.

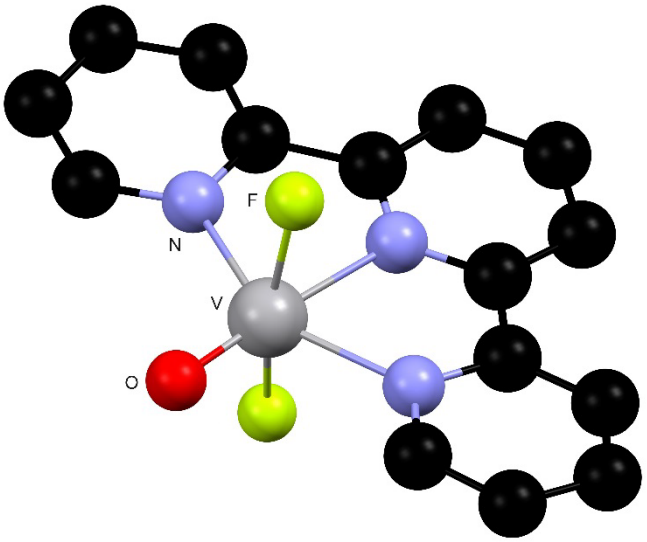

Fig. 9 Structure of $[VOF_2(terpy)]$ redrawn from Reference 23.

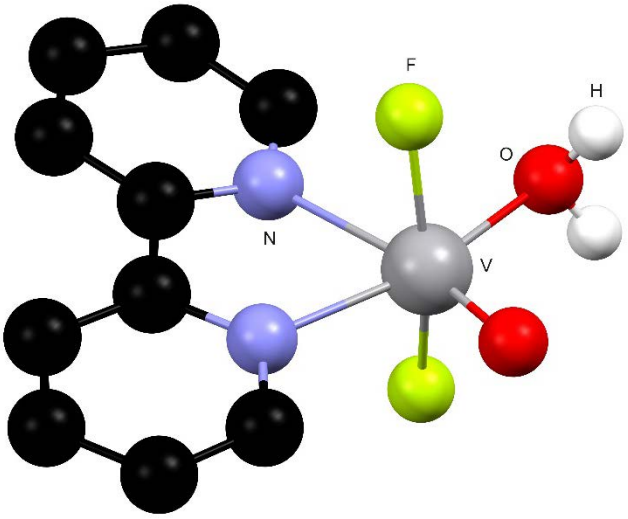

Fig. 10 Structure of $[VOF_2(2,2'\text{-bipy})(H_2O)]$ redrawn from reference 23.

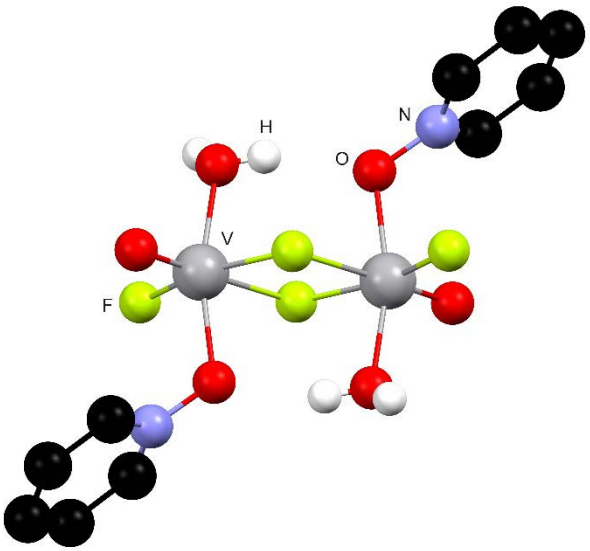

Fig. 11 Structure of $[V_2O_2F_4(pyNO)_2(H_2O)_2]$ redrawn from reference 23.

Using hydrothermal methods at higher temperature (or extended reaction times) produced mixtures, including some V^V compounds, and to confirm that the single crystal structures were characteristic of the bulk products, PXRD data were collected on bulk samples and compared with patterns simulated from the single crystal data [23]. The six-coordinate $[VOF(diimine)_2]Y$ (diimine = 2,2'-bipy, 4,4'-Me_2-2,2'-bipy, 4,4'-$^tBu_2$-2,2'-bipy, 1,10-phen; Y = BF_4, ClO_4, SbF_6) were obtained by combining $VOSO_4$, the diimine, HF or KF and the appropriate anion in aqueous solution [58]. The structures of $[VOF(diimine)_2]Y$ (diimine = 2,2'-bipy, 4,4'-$^tBu_2$-2,2'-bipy) revealed distorted octahedral vanadium centres with *cis* O,F ligands (Fig 12). The reaction of $[VOF(4,4'-^tBu_2\text{-}2,2'\text{-bipy})_2]^+$ with Me_3SiCl resulted in exchange to form Me_3SiF and $[VOCl(4,4'-^tBu_2\text{-}2,2'\text{-bipy})_2]^+$ [58].

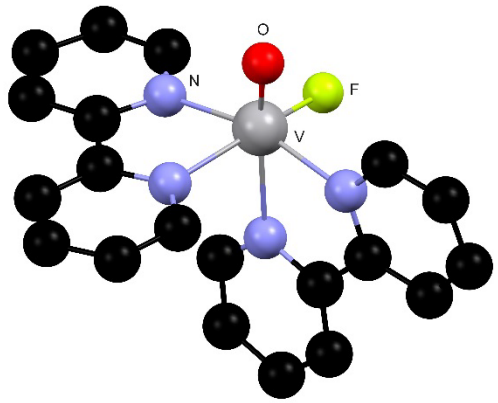

Fig. 12 Structure of the cation $[VOF(2,2'\text{-bipy})_2]^+$ redrawn from Reference 58.

Lilac *mer*-$[VF_3(NH_3)_3]$ is formed by dissolving VF_3 in liquid ammonia [60]. The reaction of $[V(acac)_3]$, LiO^tBu and HF in an organic solvent, followed by pyrolysis under N_2, has been used to form Li_3VF_6 for use in batteries

[61]. Dissolving the product (before pyrolysis) in pyridine, followed by crystallisation gave a variety of V^{III}-py complexes: red $[V(acac)F_2(py)_2]$, blue-green *trans*-$[VF_2(py)_4]BF_4$, purple *mer*-$[VF_3(py)_3]$, blue $[pyH][trans\text{-}VF_2(py)_4]SiF_6$, and green-black $[pyH][trans\text{-}VF_4(py)_2]$ (the reactions were carried out in glass vessels and the $[BF_4]^-$ and $[SiF_6]^{2-}$ arise from HF attack on the glass) [61]. The structures of all five complexes were determined; all are octahedral with typical bond lengths, but they do provide a significant addition to the list of known VF_3 derived complexes.

Niobium and Tantalum

There has been significant new work on the pentafluorides of both elements, including the first NHC complexes, and the first characterisation of phosphine and arsine complexes, which add a second group of soft donor ligands to the thioether and selenoether complexes reported a few years ago [7]. The first complexes of $NbOF_3$ have also been prepared, but those of $TaOF_3$ have proved elusive. Complexes of fluorides in lower oxidation states, or of other oxide fluorides, also remain unknown. Table 1 lists the new reports of Nb(V) and Ta(V) fluoride complexes.

Table 1 Complexes of NbF_5 and TaF_5

Complex	Comments	Reference
$[TaF_5(NH_3)_3]$	Square antiprism	62
$[MF_5(NCC_6H_4p\text{-}F)]$	M = Nb and Ta	63
$[MF_4(py)_4][MF_6]$	M = Nb and Ta; square antiprismatic cations	64
$[MF_5(OPR_3)]$	M = Nb and Ta (R = Me, Ph)	27
$[MF_5(OAsPh_3)]$	M = Nb and Ta	27
$[TaF_5(MeNCO)]$	N- and O-coordinated isomers in solution	65
$[NbF_5(L)]$	L = Et_2O, thf, MeOH, EtOH	66
$[NbF_4(MeCN)_4][NbF_6]$		66
$[(MF_5)_2\{\mu\text{-}1,3\text{-}C_6H_4(OMe)_2\}]$	M = Nb and Ta	67
$[MF_4(Ph_2CO)_2][MF_6]$	M = Nb and Ta	63
$[TaF_4(2\text{-}HOC_6H_4PPh_2)][TaF_6]$	Ligand is O,P-coordinated	63
$[MF_4(diimine)_2][MF_6]$	M = Nb and Ta; diimine = 2,2'-bipy, 1,10-phen	27,64
$[MF_4(2,2'\text{-}bipy_2][M(N_3)_6]$	M = Nb and Ta	68
$[MF_5(PR_3)]$	M = Nb and Ta; R = Me, Ph	69
$[MF_5(AsR_3)]$	M = Nb and Ta, R = Me, Et	69
$[MF_4(PMe_3)_2][MF_6]$	M = Nb and Ta; six-coordinate cations	69

$[MF_4(diphosphine)_2][MF_6]$	M= Nb and Ta; diphosphine = $R_2P(CH_2)_2PR_2$ R = Me, Et, Ph; *o*-$C_6H_4(PR_2)_2$ R = Me, Ph	64, 70
$[MF_4\{o\text{-}C_6H_4(AsMe_2)_2\}_2][MF_6]$	M = Nb and Ta	70
$[NbF_5(\kappa^1\text{-L-L})]$	L-L = $OC_6H_4CH{=}NHC_6H_3(CHMe_2)_2$	71
$[NbF_4(\kappa^1\text{-L-L})_2][NbF_6]$	L-L = $ONH{=}CHC_6H_4OH$	71
$[TaF_3(NMe_2)_2(NHC)]$	NHC = $NHCMes_2$, $SNHCMes_2$	72
$[MF_5(NHC^iPP_2)]$	M = Nb and Ta	73
$[TaF_4(Me_2NC_6H_5)_2][TaF_6]$		74
$[NbF_4(L\text{-}L)_2][NbF_6]$	L-L = α-diimines (1,4-diaza-1,3-dienes)	76

As can be seen from Table 1, the complexes are of three main types, six-coordinate neutral $[MF_5(L)]$, eight-coordinate cations $[MF_4L_4]^+$ and $[MF_4(L\text{-}L)_2]^+$ and more rarely, six-coordinate cations $[MF_4L_2]^+$. The $[NbF_5(L)]$ type are often rather unstable and only one example has been structurally authenticated, the $[NbF_5(\kappa^1\text{-}OC_6H_4CH{=}NHC_6H_3(CHMe_2)_2)]$, where the structure (Fig. 13) is stabilised by intramolecular hydrogen bonding [71].

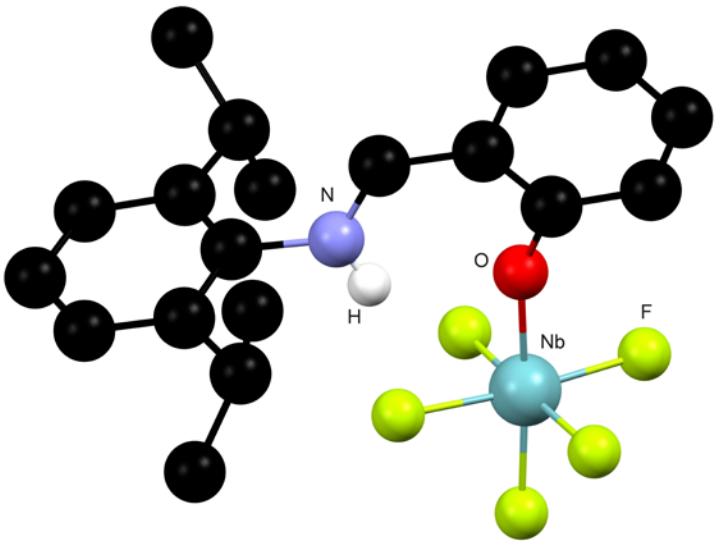

Fig. 13 Structure of $[NbF_5(\kappa^1\text{-}OC_6H_4CH{=}NHC_6H_3(CHMe_2)_2)]$ redrawn from Reference 71.

The white $[TaF_5(NH_3)_3]$, which appears to be the first ammine complex of TaF_5, was isolated from the reaction of $[Sr(HF)_3(TaF_6)_2]$ with liquid ammonia over several months; it is surprisingly unstable and decomposes below room temperature [62]. The $[MF_4(py)_4][MF_6]$ have square antiprismatic cations established by X-ray structures of both [64] (Fig. 14). The diimine complexes $[MF_4(diimine)_2][MF_6]$ (2,2'-bipy, 1,10-phen) were

originally assumed to be seven-coordinate neutral species, but although poorly soluble in most solvents, which seems to have prevented crystal growth for X-ray studies, the IR and $^{19}F\{^{1}H\}$ NMR spectra clearly show they contain the familiar $[MF_6]^-$ anions and hence eight coordinate cations [27,64].

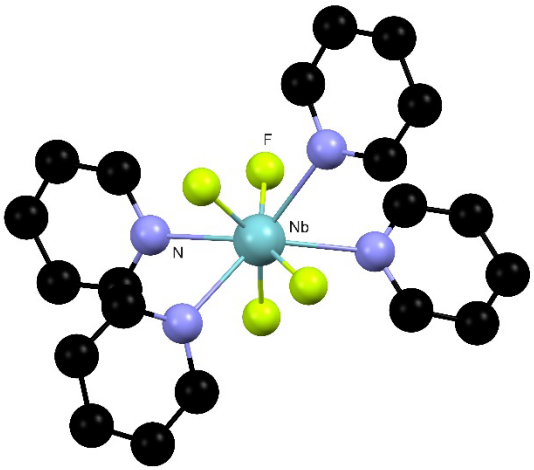

Fig. 14 Structure of the cation $[NbF_4(py)_4]^+$ redrawn from Reference 64.

Phosphine and arsine complexes of the pentafluorides have also finally been identified (Scheme 2).

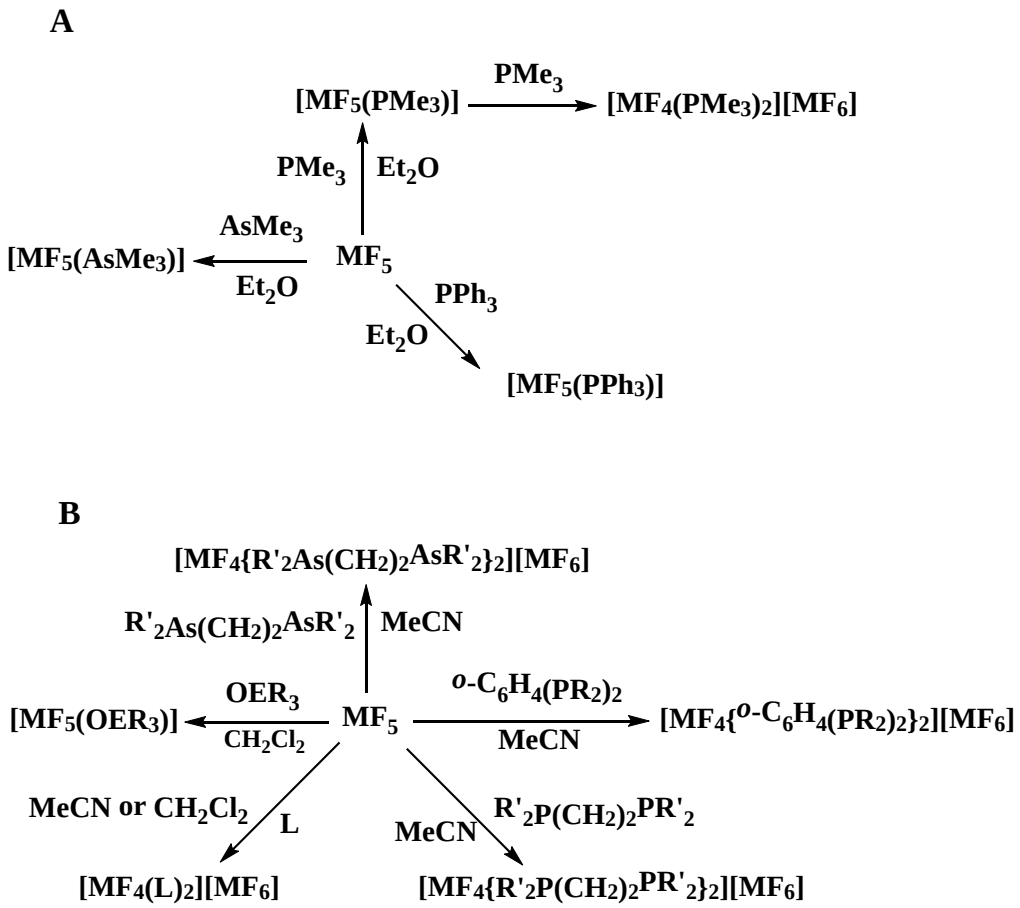

M = **Nb, Ta**
L = **bipy, phen**
E = **P, As**
R = **Me, Ph**
R' = **R, Et**

Scheme 2. NbF_5 and TaF_5 complexes of phosphorus and arsenic ligands.

The $[MF_5(L)]$ (L = PMe_3, PPh_3, $AsMe_3$, $AsEt_3$) are obtained as colourless solids by reaction of the MF_5 with the ligands in anhydrous Et_2O [69]. Attempts to obtain analogues with $SbMe_3$ were unsuccessful. The complexes are decomposed by MeCN and are extremely moisture sensitive, hydrolysing rapidly on exposure to air. They are unstable in solution and the formulation as six-coordinate neutral complexes is based upon the $^{19}F\{^1H\}$ NMR spectra [69]. The reaction of MF_5 with excess PMe_3 in Et_2O, initially forms the $[MF_5(L)]$, but using longer reaction times, white complexes, identified as $[MF_4(PMe_3)_2][MF_6]$ precipitate from solution, confirmed by microanalysis and multinuclear NMR spectroscopy. The arsine ligands do not form similar cations. The diphosphine complexes $[MF_4(diphosphine)_2][MF_6]$ (diphosphine = $R_2P(CH_2)_2PR_2$; R = Me, Et, Ph; *o*-$C_6H_4(PR_2)_2$ R = Me, Ph) are robust although moisture sensitive, and form by combining a 1:1 ratio of MF_5 and the ligands

in anhydrous MeCN [64,70]. The NMR spectra show that unlike the PR_3 complexes, the diphosphine complexes do not dissociate the ligand in solution in MeCN or CH_2Cl_2 and both the $^{19}F\{^1H\}$ and $^{31}P\{^1H\}$ NMR spectra show binomial quintet couplings in the cations, demonstrating the equivalency of the P and F atoms (Fig. 15). This was confirmed by X-ray crystal structures determined for five of the complexes, all of which reveal dodecahedral cations [64,70] (Fig. 16). The corresponding reactions of the MF_5 with *o*-$C_6H_4(AsMe_2)_2$ produced analogous $[MF_4(o\text{-}C_6H_4(AsMe_2)_2)_2][MF_6]$ [70] (Fig. 17), which are partially decomposed in MeCN solution, but stable in CH_2Cl_2. The formation of these diarsine complexes with Nb and Ta contrasts with the case of TiF_4 [75], where diphosphine complexes form, but no diarsine analogue could be obtained.

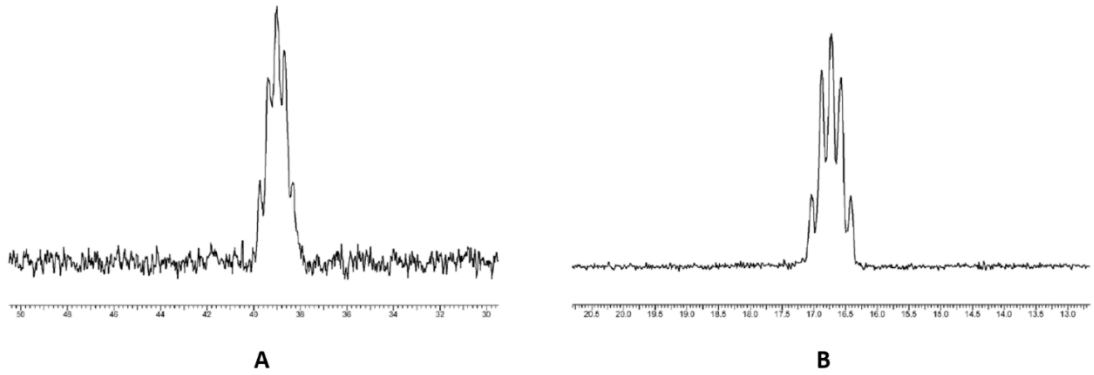

Fig. 15 $^{31}P\{^1H\}$ P (**A**) and $^{19}F\{^1H\}$ (**B**) NMR spectra of $[TaF_4(o\text{-}C_6H_4(PMe_2)_2)_2]^+$. Reproduced from Reference 70 with permission from the Royal Society of Chemistry.

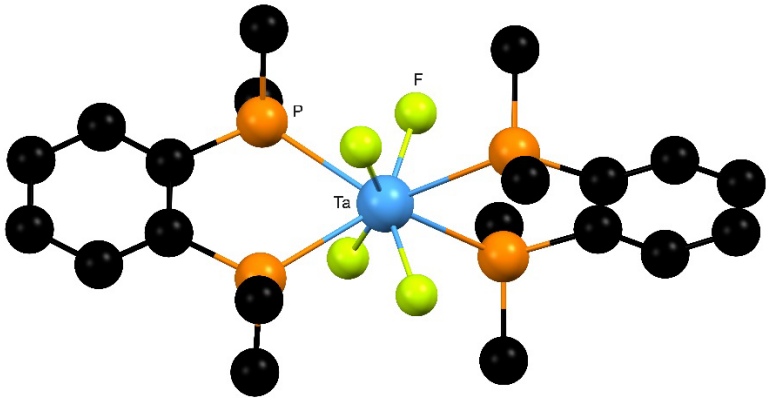

Fig. 16 Structure of the cation $[TaF_4(o\text{-}C_6H_4(PMe_2)_2)_2]^+$ redrawn from Reference 70.

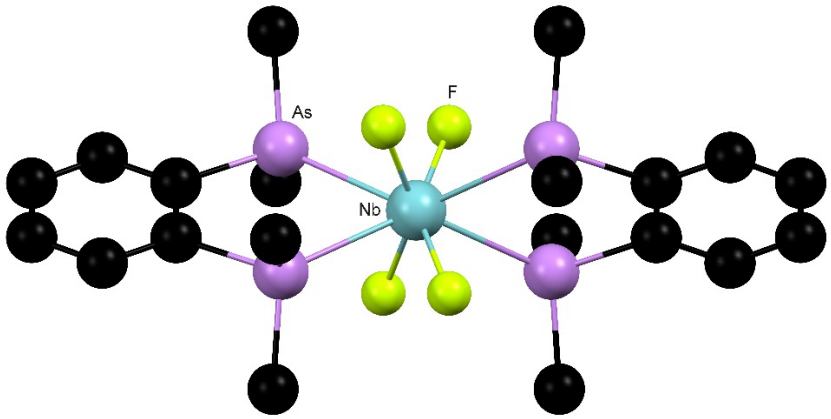

Fig. 17 Structure of $[NbF_4(o\text{-}C_6H_4(AsMe_2)_2)_2]^+$ redrawn from Reference 70.

The reaction of TaF_5 with $TeMe_2$ in CH_2Cl_2 at 0°C gave an unstable yellow solid identified spectroscopically as $[TaF_5(TeMe_2)]$; this is the first telluroether complex of a high valent d-block fluoride [16]. It decomposes in a few hours at room temperature, forming Me_2TeF_2 among other products. The corresponding reaction with NbF_5 gives only a black sticky decomposition product.

NHC complexes of type $[MF_5(NHCD^iPP_2)]$ have been prepared from toluene solution [73]. They contain an unusually high metal oxidation state for carbene complexes. Tantalum amido carbene complexes $[TaF_3(NMe_2)_2(NHC)]$ (NHC = $NHCMes_2$, $SNHCMes_2$) are formed by reaction of $[Ta(NMe_2)_5]$ with $NHC{\cdot}HBF_4$, the fluoride ligands coming from degradation of the fluoroborate [72]. The crystal structure (Fig. 18) of $[TaF_3(NMe_2)_2(SNHCMes_2)]$ shows *mer*-fluorine and *cis*-amides.

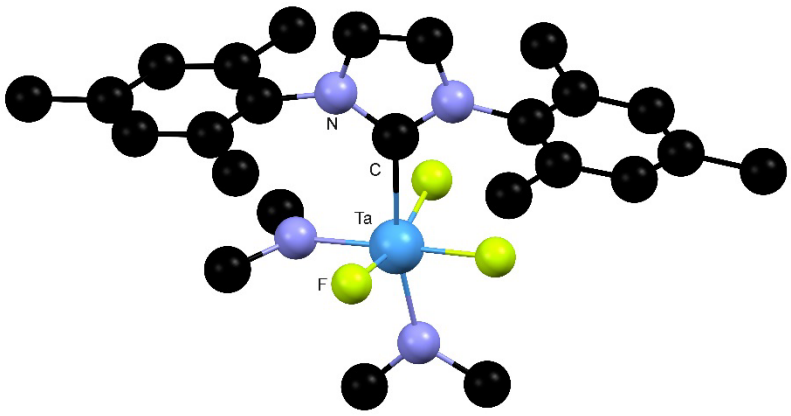

Fig. 18 Structure of $[TaF_3(NMe_2)_2(SNHCMes_2)]$ redrawn from Reference 72.

Niobium oxide trifluoride, $NbOF_3$, is an inert polymer that does not react with neutral ligands, although it does hydrolyse slowly in air. However, reaction of $[NbF_5(L)]$ (L = $OPPh_3$, $OPMe_3$, dmso) with a further equivalent of L and the siloxane, $O(SiMe_3)_2$, in CH_2Cl_2/MeCN solution produced white $[NbOF_3(L)_2]$ complexes [27] (Scheme 3). Treatment of NbF_5 with 2L or L-L (L-L = $Me_2N(CH_2)_2NMe_2$, $Ph_2P(O)CH_2P(O)Ph_2$, 2,2'-bipy, 1,10-

phen) in the same solvent mixture, followed by addition of $O(SiMe_3)_2$, gave the complexes $[NbOF_3(L)_2]$ or $[NbOF_3(L\text{-}L)]$ directly.

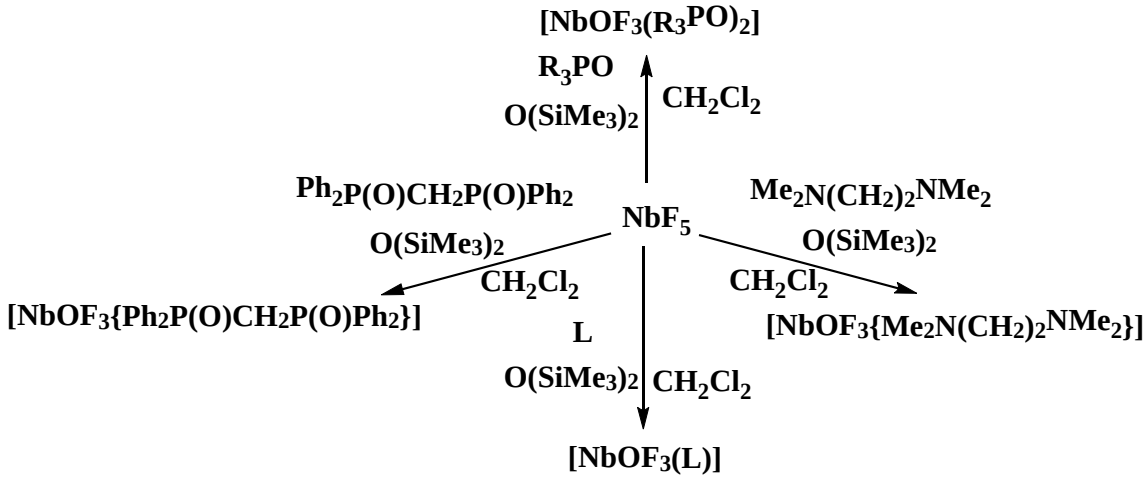

L = bipy, phen
R = Me, Ph

Scheme 3 Synthesis of $NbOF_3$ complexes.

However, attempts to make complexes with thf, $MeOCH_2CH_2OMe$, PMe_3 or $MeSCH_2CH_2SMe$ failed, with $NbOF_3$ precipitating, indicating that these ligands do not bind sufficiently strongly to the oxide fluoride to prevent dissociation and polymerisation [27,69]. In contrast, the diphosphine complexes $[MF_4(diphosphine)_2][MF_6]$ (diphosphine = $R_2P(CH_2)_2PR_2$; R = Me, Et: *o*-$C_6H_4(PMe_2)_2$) did not react with $O(SiMe_3)_2$ in CH_2Cl_2/MeCN [70]. The reason for this failure is unclear. X-ray structures of $[NbOF_3(OPR_3)_2]$ (R = Me, Ph) and $[NbOF_3\{Ph_2P(O)CH_2P(O)Ph_2\}]$ show *mer*-fluorines with the neutral donor ligands *trans* to O/F (Fig. 19).

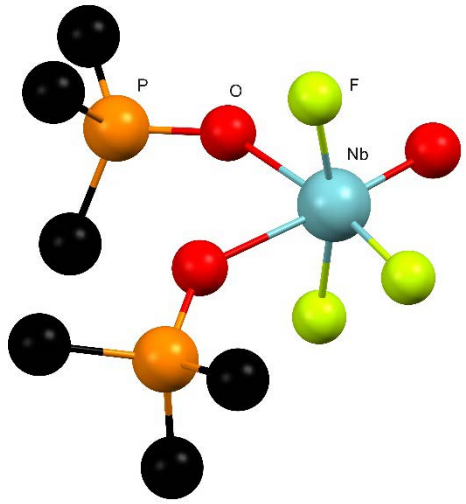

Fig. 19 Structure of $[NbOF_3(OPMe_3)_2]$ redrawn from Reference 27.

In contrast, the product formed by slow hydrolysis of a mixture of NbF_5 and the carbene, $NHCD^iPP_2$, in toluene in moist air, is the dinuclear complex, $[(NbOF_3)_2(NHCD^iPP_2)_2]$ (Fig. 20) [77]. All attempts so far to obtain complexes of $TaOF_3$, either from TaF_5-$O(SiMe_3)_2$ and a variety of ligands, or from Ta_2O_5 in aqueous HF (*cf* $NbOF_3$ [78]) have failed [27].

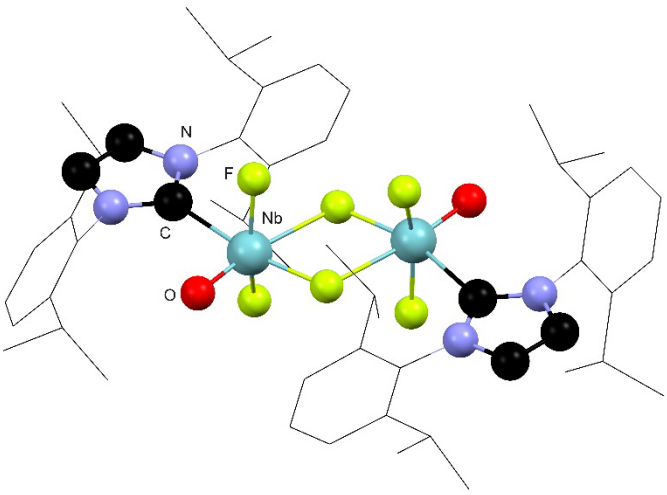

Fig. 20 Structure of $[(NbOF_3)_2(NHCD^iPP_2)_2]$ redrawn from Reference 77.

Group 6

Chromium

There are no complexes of chromium fluorides or oxide fluorides in oxidation states >3; it seems possible that N-bases could coordinate to CrF_4 or $CrOF_3$ if an appropriate synthetic entry can be found. Chromium(III) fluoride complexes, especially $[CrF_3(py)_3]$, are useful building blocks for the synthesis of heterobimetallic magnets, particularly those containing lanthanide ions. The work has been reviewed [11] and some exemplar

reports [79-81] should be consulted for details. A different system making molecular magnetic refrigerants with fluoride bridged Cr^{III}_2-Gd^{III}_3 cores used *fac*-[CrF_3(Me_3-tacn)] as the source of chromium [82]. Chromium(III) fluoride is of technological interest in solid state lasers, and in connection with this work, the crystal structures have been reported for several complexes using synchrotron data – *trans*-[$CrF_2(py)_4]_2[ZnCl_4]\cdot Na[ClO_4]$ [83], *trans*-$[CrF_2(py)_4]ClO_4$ [84] and *trans*-$[CrF_2(py)_4][ZnCl_3(py)]\cdot H_2O$ [85], with emphasis on the intermolecular hydrogen bonding and the crystal packing. The X-ray structure and spectroscopic properties of the tetra-aza macrocyclic complex, *trans*-$[CrF_2$(2,2,3-tet)$]ClO_4$, has been reported [86]. The complex, *fac*-$[CrF_3(Me_3\text{-tacn})]\cdot 3.5H_2O$, was explored as a potential carrier for ^{18}F for PET imaging (see Section 7), but although it has the necessary stability to water and towards common anions, the Cl/F exchange from *fac*-$[CrCl_3(Me_3\text{-tacn})]$ and F^- is incomplete after 24 h and thus it is not a viable route for radiolabelling [87].

Molybdenum

In contrast to WF_6 (below), no neutral ligand complexes of MoF_6 have been isolated, and Mo(VI) complexes are limited to those of the two oxide fluorides. The first neutral ligand complexes of $MoOF_4$ have been made from *trans*-$[MoOF_4(MeCN)]$, which is conveniently obtained from MoF_6 and $O(SiMe_3)_2$ in anhydrous MeCN as a white extremely moisture sensitive solid [88]. Reaction of $[MoOF_4(MeCN)]$ in anhydrous MeCN with $OPPh_3$, $OPMe_3$, dmso and dmf resulted in the corresponding *trans*-$[MoOF_4(L)]$. Dissolution of $[MoOF_4(MeCN)]$ in thf and removal of the volatiles *in vacuo* produced unstable $[MoOF_4(thf)]$ which decomposed in ~24 h, turning blue. The complexes are all very moisture sensitive, hydrolysis producing the $[MoO_2F_2(L)_2]$ complexes (and other products, see below). All exhibit strong ν(Mo=O) vibrations in the IR spectra in the range 990-1020 cm^{-1} and binomial quintet ^{95}Mo NMR resonances due to coupling with four equivalent fluorines, showing the structures have *trans*-O=Mo-L units. This was confirmed by the X-ray structure of *trans*-$[MoOF_4(OPPh_3)]$ (Fig. 21). $[MoOF_4(MeCN)]$ fluorinates Ph_3AsO to Ph_3AsF_2. The reaction of $[MoOF_4(MeCN)]$ with 2,2'-bipyridyl gave an insoluble white solid, $[MoOF_4$(2,2'-bipy)], which was air stable and is probably seven-coordinate [88]. In contrast to the behaviour of the tungsten systems (below), the reaction of $[MoOF_4(MeCN)]$ with soft ligands, including PMe_3, $Me_2PCH_2CH_2PMe_2$, $AsMe_3$ and SMe_2 in Et_2O or MeCN immediately produced deep red or brown paramagnetic species, indicating reduction of the molybdenum on contact.

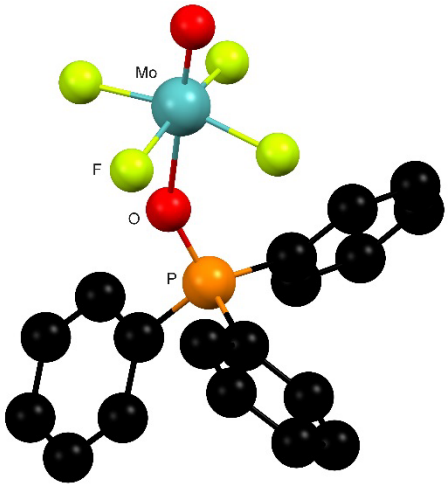

Fig. 21 Structure of $[MoOF_4(OPPh_3)]$ redrawn from Reference 88.

Complexes of MoO_2F_2 have long been known and can be prepared from $MoO_3{\cdot}nH_2O$ in aqueous HF and ethanolic solutions of the ligands [89], or by Cl/F exchange from $[MoO_2Cl_2(L)_2]$ and Me_3SnF [90]. The reaction of $[MoOF_4(L)]$ with $O(SiMe_3)_2$ and a further equivalent of L also produces $[MoO_2F_2(L)_2]$ (L = $OPPh_3$, $OPMe_3$, dmso), and indeed the reaction of $[MoOF_4(MeCN)]$ with 2L in "wet" solvents also generates $[MoO_2F_2(L)_2]$ demonstrating the great contrast between the highly moisture sensitive $[MoOF_4(L)]$ and the much more robust $[MoO_2F_2(L)_2]$ [88]. Attempts to isolate $[MoO_2F_2(MeCN)_2]$ by reaction of $[MoOF_4(MeCN)]$ with $O(SiMe_3)_2$ in MeCN solution, produced white solids which turned blue over time and appeared to be mixtures of MoO_2F_2 (polymer) and $[MoO_2F_2(MeCN)_2]$. Serendipitously, one attempt to grow crystals of $[MoOF_4(MeCN)]$ by evaporation of an MeCN solution, gave a few colourless crystals of $[MoO_2F_2(MeCN)_2]$ (Fig. 22), no doubt a result of trace hydrolysis. It appears that $[MoO_2F_2(MeCN)_2]$ is unstable and loses MeCN to form MoO_2F_2 polymer, even in MeCN solution [88]. The structure of $[MoO_2F_2(OPPh_3)_2]$ shows the $OPPh_3$ ligands *trans* to the oxido groups. Three structures of minor by-products from the $[MoOF_4(OPMe_3)]$ synthesis were $[MoO_2F_2(OPMe_3)(OH_2)]$, $[Mo_2O_4F_2(\mu\text{-}F)_2(OPMe_3)_2]$ (Fig. 23) and the anion in $[Me_3POH]_2[Mo_2O_4F_4(\mu\text{-}F)_2]$.

The products of solvothermal syntheses (MoO_3, aq. HF, ethylenediamine and ethylene glycol) of molybdenum oxide fluoride species include an unusual dimer $[Mo_2O_4F_2(en)_2]$ (Fig. 24) with the terminal O/F disordered (assigned by bond valence analysis) [91].

The complexes of molybdenum fluorides in lower oxidation states remain largely unexplored. Recently characterised complexes include the seven-coordinate, purple-black $[Mo^{IV}F(4,4'\text{-}Me_2\text{-}2,2'\text{-}bipy)(4,4'\text{-}Me_2\text{-}2,2'\text{-}bipy^*)_2][PF_6]$ (4,4'-Me_2-2,2'-bipy* is the radical anion of the diimine) obtained by $[Cp_2Fe][PF_6]$ oxidation of $[Mo(4,4'\text{-}Me_2\text{-}2,2'\text{-}bipy)_3]$ in thf [92]. The structure of the Mo(III) complex $[MoF_2(Ph_2PCH_2CH_2PPh_2)_2]BF_4$ has also been reported [93].

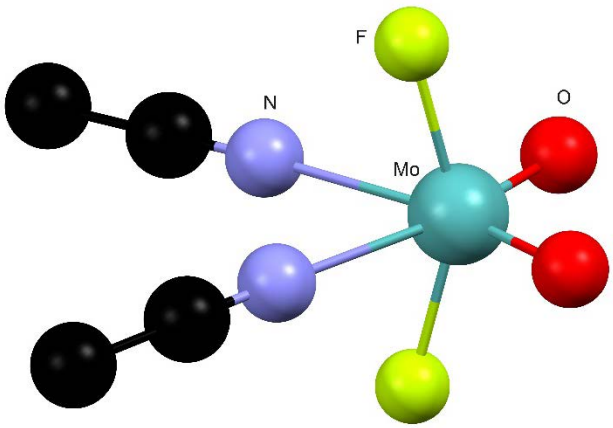

Fig. 22 Structure of $[MoO_2F_2(MeCN)_2]$ redrawn from Reference 88.

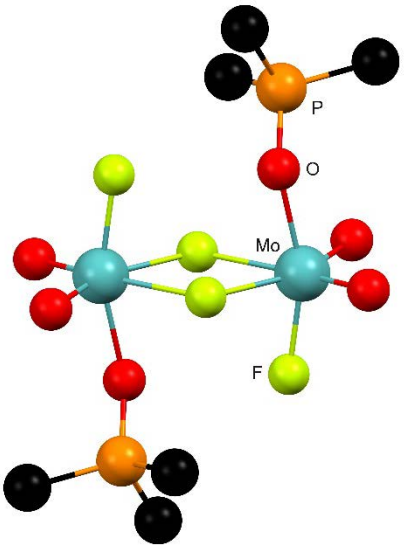

Fig. 23 Structure of $[Mo_2O_4F_2(\mu\text{-}F)_2(OPMe_3)_2]$ redrawn from Reference 88.

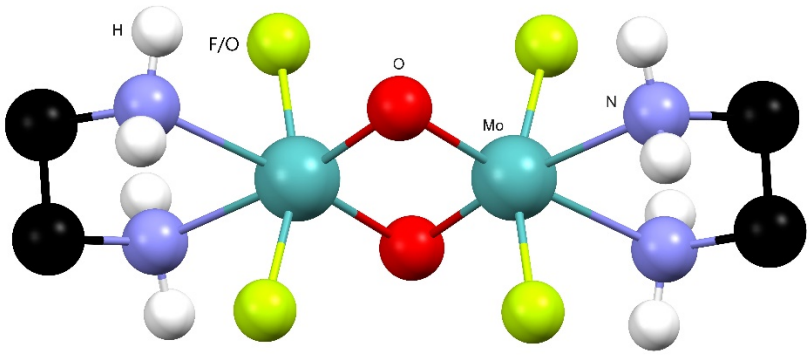

Fig. 24 Structure of $[Mo_2O_4F_2(en)_2]$ redrawn from Reference 91. Note the terminal O/F disorder.

Tungsten

Tungsten hexafluoride is the only one of the metal hexafluorides known to form complexes with neutral organic ligands. The structures of $[WF_6(Rpy)]$ (Rpy = py, 4-Mepy, 4-Me_2Npy) are all capped trigonal prisms

with identical W-N bonds for the first two and a slightly shorter bond for the last [94]. With 4,4'-bipy the complex formed is $[F_6W(\mu\text{-}4,4'\text{-bipy})WF_6]$ [94]. Curiously, whilst the other WF_6 adducts of pyridyl bases are white, $[WF_6(4\text{-}Me_2Npy)]$ is dark red. Seven-coordinate tertiary phosphine complexes, $[WF_6(PR_3)]$ ($R_3 = Me_3$, Me_2Ph), were characterised in 2010 [95], and the tertiary arsine analogues $[WF_6(AsR_3)]$ (R = Me, Et) have been obtained very recently [15], the former as an orange-red powder, the latter an orange oil. Neither $AsPh_3$ nor $SbEt_3$ formed similar complexes. The $[WF_6(AsR_3)]$ are extremely sensitive to moisture and decompose on standing at room temperature. The $^{19}F\{^1H\}$ NMR spectra in CD_2Cl_2 are singlets down to 180 K, indicating fluxionality even at low temperatures. The orange-red colour was assigned as a As(σ)→W(d) charge transfer band. More unexpectedly, the reaction of WF_6 with *o*-$C_6H_4(EMe_2)_2$ (E = P, As) in anhydrous CH_2Cl_2 solution gave very moisture sensitive orange $[WF_4\{o\text{-}C_6H_4(EMe_2)_2\}_2][WF_7]_2$. Crystals of both were grown from CH_2Cl_2 solution by evaporation, and the structures revealed dodecahedral cations (Fig. 25) [15]. The cations are surprisingly robust, but trace moisture converts some of the $[WF_7]^-$ anions into $[WOF_5]^-$ or $[WF_8]^{2-}$, found in the crystals studied. The cations are stable in solution under anhydrous conditions with both the $^{19}F\{^1H\}$ and $^{31}P\{^1H\}$ NMR spectra of the diphosphine complex showing binomial quintet patterns (Fig. 26). The flexible diphosphine $Me_2PCH_2CH_2PMe_2$ produced an inseparable mixture of $[WF_4(Me_2PCH_2CH_2PMe_2)_2][WF_7]_2$ and $[F_6W(\mu\text{-}Me_2PCH_2CH_2PMe_2)WF_6]$. Reaction of the dithioethers $RSCH_2CH_2SR$ (R = Me, ^{i}Pr) with WF_6 in CH_2Cl_2 at 180 K gave orange-brown solutions indicative of adduct formation, but the colour faded on warming and removal of the volatiles *in vacuo* led to recovery of the dithioether [15].

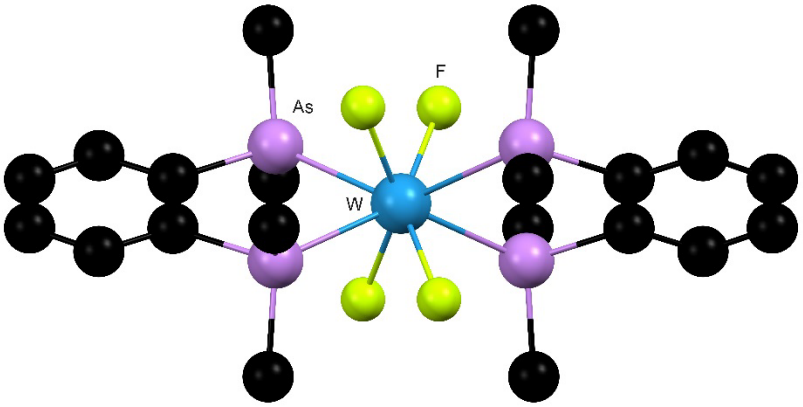

Fig. 25 Structure of the cation $[WF_4\{o\text{-}C_6H_4(AsMe_2)_2\}_2]^{2+}$ redrawn from Reference 15.

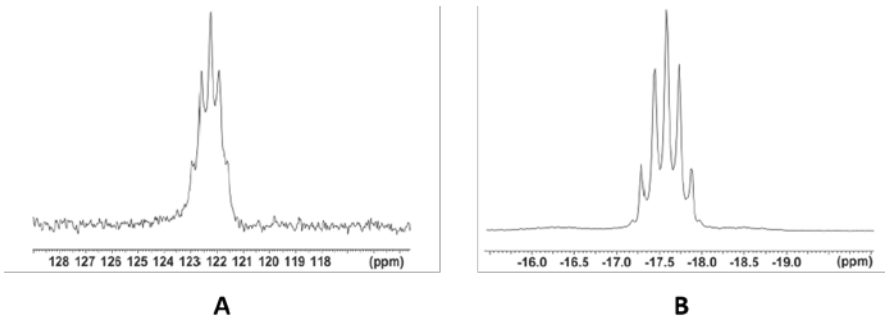

Fig. 26 $^{31}P\{^{1}H\}$ (**A**) and $^{19}F\{^{1}H\}$ (**B**) NMR spectra of $[WF_4\{o\text{-}C_6H_4(PMe_2)_2\}_2]^{2+}]^{+}$, Reproduced from Reference 15 with permission from the Royal Society of Chemistry.

A number of complexes of WOF_4 and WO_2F_2 are described in the earlier literature [7], but a new versatile route from WF_6 and $O(SiMe_3)_2$ has been developed [26]. The reaction of WF_6 and $O(SiMe_3)_2$ in a 1:1 molar ratio in anhydrous MeCN solution produces $[WOF_4(MeCN)]$, which reacts with various ligands (L= $OPPh_3$, $OPMe_3$, dmso, dmf, py, thf) to form $[WOF_4(L)]$. Attempts to synthesise $[WO_2F_2(MeCN)_2]$ by reaction with a further equivalent of $O(SiMe_3)_2$ failed, with only (polymeric) WO_2F_2 precipitation (*cf* $[MoO_2F_2(MeCN)_2]$ above). However, treatment of $[WOF_4(MeCN)]$ with 2L and $O(SiMe_3)_2$ gave $[WO_2F_2(L)_2]$ (L = $OPPh_3$, $OPMe_3$, pyNO, dmso) (Scheme 4) [26].

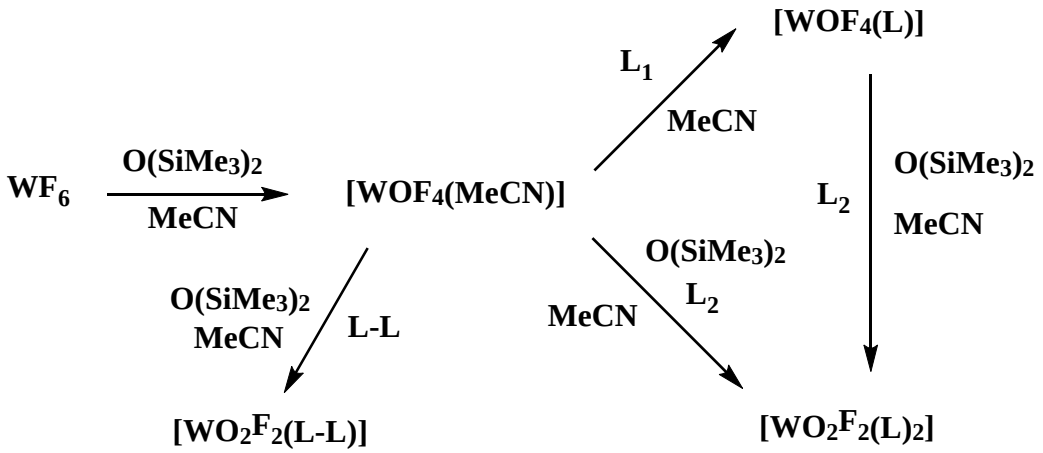

L_1 = $OPPh_3$, $OPMe_3$, py, dmso, thf
L_2 = $OPPh_3$, pyNO, dmso
L-L = 2,2'-bipy, 10-phen, $Ph_2P(O)CH_2P(O)Ph_2$

Scheme 4 Synthesis of the tungsten oxide fluoride complexes.

The IR and NMR spectroscopic data, together with the X-ray structure of $[WOF_4(OPPh_3)]$, show all of the $[WOF_4(L)]$ have the expected octahedral structures with L *trans* to W=O. The structures of $[WO_2F_2(L)_2]$ (L = pyNO, $OPPh_3$) also show the presence of an octahedral geometry (Fig 27), again with L *trans* to W=O.

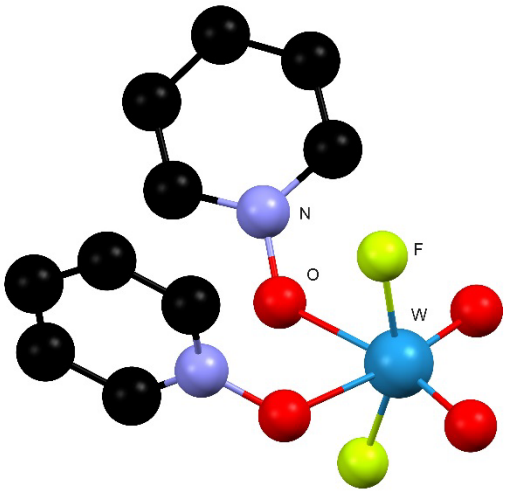

Fig. 27 Structure of $[WO_2F_2(pyNO)_2]$ redrawn from Reference 26.

The $[WOF_4(L)]$ are moisture sensitive in solution and as solids, but the $[WO_2F_2(L)_2]$ are air stable. The complexes $[WO_2F_2(L\text{-}L)]$ (L-L = 2,2'-bipy, 10-phen, $Ph_2P(O)CH_2P(O)Ph_2$) were also obtained from reaction of $[WOF_4(MeCN)]$, L-L and $O(SiMe_3)_2$ in a 1:1:1 molar ratio. Attempts to react $[WOF_4(MeCN)]$ with soft donors including Me_2S, Me_2Se, Me_3As, $MeSCH_2CH_2SMe$ and $MeSeCH_2CH_2SeMe$ in MeCN solution, failed with the ligands unable to displace MeCN, whilst on standing the solutions decomposed becoming blue or green, probably due to reduction of the tungsten. The corresponding reactions with phosphine ligands proved to be very sensitive to the phosphine and the solvents used [96]. Addition of PMe_3 to a suspension of $[WOF_4(MeCN)]$ in a 1:1 molar ratio in anhydrous Et_2O precipitated white $[WOF_4(PMe_3)]$; use of excess phosphine produced a blue paramagnetic oil, indicative of reduction of the tungsten. The microanalysis, IR and NMR spectra identified the white complex as $[WOF_4(PMe_3)]$, but it proved too unstable in solution to grow crystals for an X-ray study. Use of other phosphines, including P^nPr_3, $PPhMe_2$, initially produced white solids, which are probably the analogous complexes, but these rapidly turned yellow and then brown and appear to be too unstable to isolate in a pure state [96]. The use of alkyl diphosphines was more successful and $[WOF_4(L\text{-}L)]$ (L-L = *o*-$C_6H_4(PMe_2)_2$, $Me_2PCH_2CH_2PMe_2$) were isolated from Et_2O solution as very moisture sensitive powders. The structures of both were determined and revealed pentagonal bipyramidal geometries (Fig. 28) with the axial O/F disordered [96].

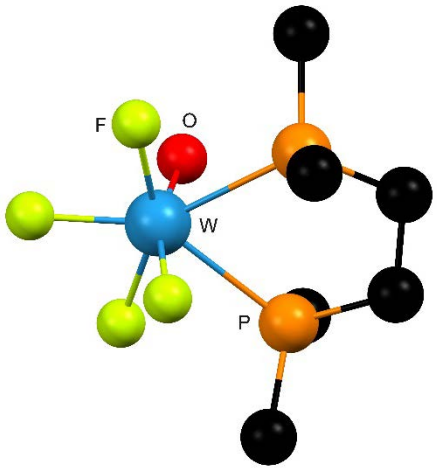

Fig. 28 Structure of $[WOF_4(Me_2PCH_2CH_2PMe_2)]$ redrawn from Reference 96.

The $^{19}F\{^1H\}$ and $^{31}P\{^1H\}$ NMR show the structures are retained in solution, and the complex second order spectra were successfully modelled. Analogous complexes did not form with *o*-$C_6H_4(PPh_2)_2$, *o*-$C_6H_4(AsMe_2)_2$, or *o*-$C_6H_4(SMe)_2$ [96]. No reaction occurred between the $[WOF_4(L\text{-}L)]$ (L-L = *o*-$C_6H_4(PMe_2)_2$, $Me_2PCH_2CH_2PMe_2$) and $O(SiMe_3)_2$ in Et_2O or Et_2O/MeCN and phosphine complexes of WO_2F_2 remain unknown, although would probably be relatively stable if an entry can be found. Little is known about complexes of WSF_4, with only $[WSF_4(MeCN)]$ [97] and $[WSF_4(py)]$ [98] being known; both have the expected octahedral structure with the neutral ligand *trans* to W=S. In contrast to the $[WOF_4(py)_2]$ [99], there was no evidence for a 2:1 adduct for WSF_4 [98] which is probably due to its slightly decreased Lewis acidity.

Oxidation of $[W(terpy)_2]$ with $Ag[PF_6]$ in CH_2Cl_2 produces diamagnetic $[WF(terpy)_2][PF_6]$, with the cation having a distorted pentagonal bipyramidal geometry with an equatorial fluorine. The formulation is uncertain, $[W^{VI}F(terpy^{2-})_2]^+$, $[W^{IV}F(terpy^*)_2]^+$ and $[W^{V}(terpy)(terpy^{2-})]^+$ (terpy* is the radical monoanion, and $terpy^{2-}$ the dianion) all being possible [92].

Group 7

There appear to be no new reports of neutral ligand complexes of Tc or Re fluorides in oxidation states >3. In part this probably reflects the difficulties in accessing the metal fluorides.

Manganese

When Li_2MnF_5 was suspended in neat pyridine in a glass vessel for several days, orange brown crystals of *trans*-$[MnF_2(py)_4][SiF_5(py)]$ formed and *mer*-$[MnF_3(py)_3]$ was isolated from the mother liquor; both were identified by the X-ray crystal structures [61]. The direct reaction of MnF_3 with a range of diimines (L-L = 2,2'-bipy, 1,10-phen, 6-Me-2,2'-bipy, 4,4'Me_2-2,2'-bipy, 5,5'-Me_2-2,2'-bipy, 5-Cl-1,10-phen) in methanol gave $[MnF_3(diimine)(H_2O)]\cdot xH_2O$ [100]. The structures of all six have *mer* fluorines and the water *trans* to one nitrogen atom (Fig. 29); detailed magnetic and EPR measurements were reported.

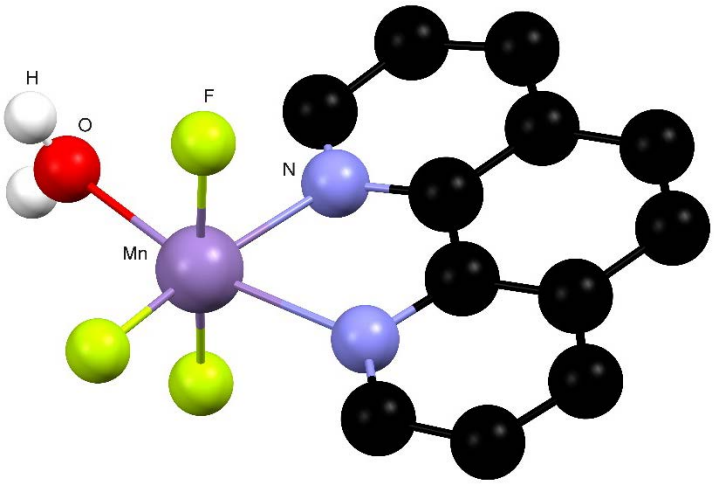

Fig. 29 Structure of [MnF_3(phen)(H_2O)] redrawn from Reference 100.

Orange [MnF_3(terpy)]·2.5H_2O [7] and red *fac*- [MnF_3(Me_3-tacn)]·2H_2O were obtained from reaction of MnF_3 with the ligand in MeOH [87]. The structure of the latter (Fig. 30) shows a distorted octahedron as expected from the Jahn-Teller effect on a high spin d^4 complex. If the reaction of MnF_3 and Me_3-tacn in methanol was carried out with added [NH_4]PF_6, the product was the dimer [Mn_2F_4(μ-F)(Me_3-tacn)$_2$]PF_6 with the two manganese centres linked by a single fluorine bridge [101]. Detailed theoretical studies of the superexchange mechanism in this dimer have been reported [102].

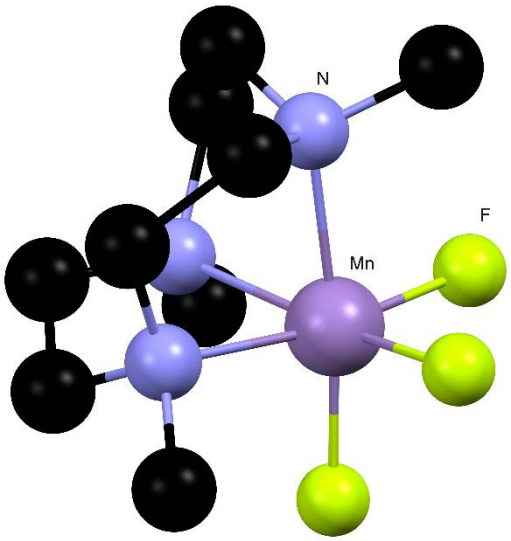

Fig. 30 Structure of [MnF_3(Me_3-tacn)] redrawn from Reference 87. Carbon atoms in the ring were disordered and only one component is shown.

A rare Mn(V) carbene complex is [(TIMENxyl)Mn(N)(F)]BPh_4 (TIMENxyl = tris[2-(3-xylylimidazol-2-ylidene)ethyl]-amine), obtained by oxidation of the Mn(IV) nitride [(TIMENxyl)Mn(N)]BPh_4 with AgF [103]. It has an octahedral geometry with the three carbene donors and the fluoride in one plane (Fig. 31) and is diamagnetic.

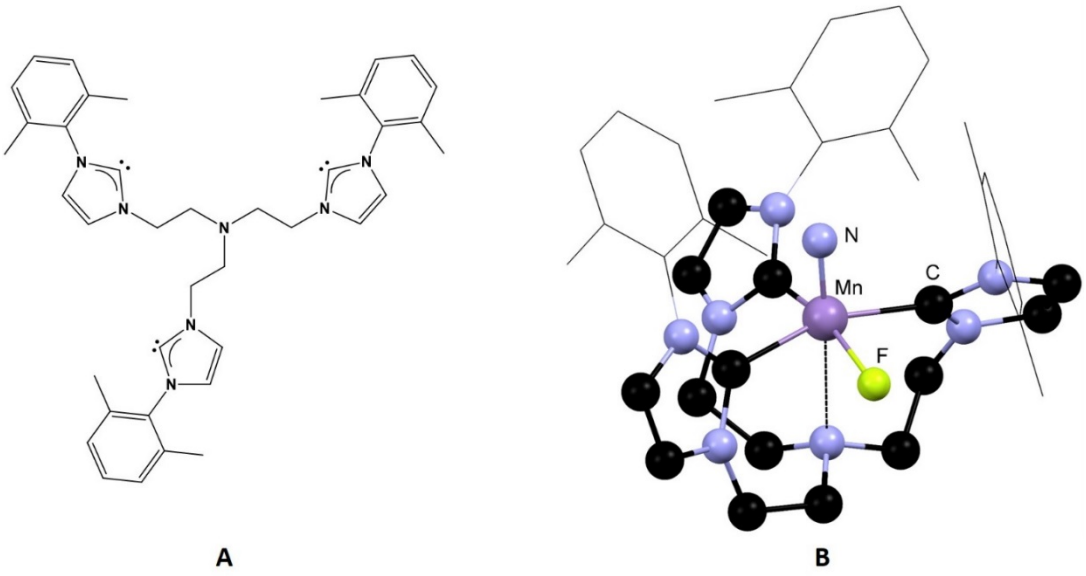

Fig. 31 **A** ligand TIMENxyl and **B** the structure of the cation $[(TIMENxyl)Mn(N)(F)]^+$ redrawn from Reference 103.

Group 8

There appears to be no new work on complexes of ruthenium or osmium fluorides, which probably reflects the difficulty of accessing the fluorides and the need for metal or fluoroplastic vessels to handle these aggressive species.

Iron

The reaction of $FeF_3 \cdot 3H_2O$ with terpy, Me_3-tacn or $BnMe_2$-tacn in ^{n}BuOH gave purple *mer*-$[FeF_3(terpy)] \cdot 2H_2O$, yellow *fac*-$[FeF_3(Me_3\text{-tacn})] \cdot H_2O$ and yellow *fac*-$[FeF_3(BnMe_2\text{-tacn})] \cdot 3.5H_2O$. The structures of the three complexes were determined [81,87]. The *fac*-$[FeF_3(Me_3\text{-tacn})]$ is stable in water and *fac*-$[FeCl_3(Me_3\text{-tacn})]$ can be rapidly fluorinated in aqueous or anhydrous MeCN [87] (Section 7).

Most of the other work involving nitrogen base complexes of FeF_3 involves the syntheses and studies of magnetic materials [11,12]. Green crystals of $[FeF_3(4,4'\text{-bipy})]$ were obtained by a hydrothermal method from a mixture of Fe_2O_3, 4,4'-bipy and aqueous HF [104]. The structure is built from FeF_4N_2 octahedra sharing *trans* fluorine atoms to form chains and with the chains cross-linked by the diimine; the compound is a 1D antiferromagnet. The reaction of $Fe(BF_4)_2 \cdot 6H_2O$ with 2-amino-4-(2-pyridyl)thiazole (H_2apt) in MeCN in air, gave a red Fe(III) complex $[(H_2apt)_2FFe(\mu\text{-}O)FeF(H_2apt)_2][BF_4]_2$ the fluoride being extracted from the fluoroborate ions [105].

Under slightly different conditions from MeOH a mononuclear $[FeF_2(H_2apt)_2]BF_4$ was isolated. The structures of both complexes reveal the thiazole ligand coordinated as a chelate through the heterocyclic nitrogens (Fig. 32).

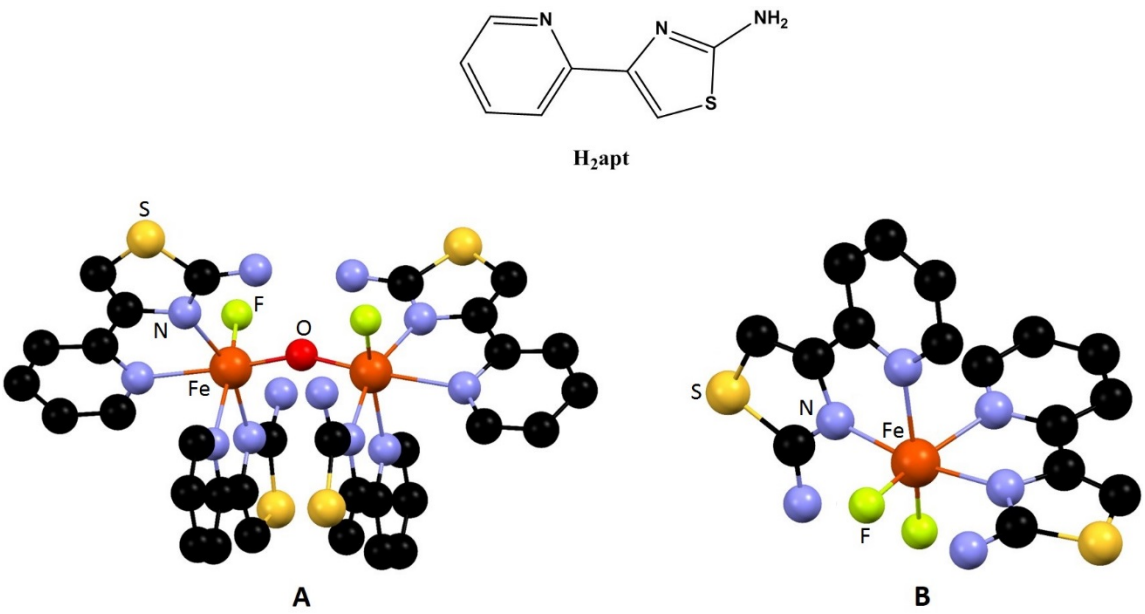

Fig. 32 The ligand H_2apt (top) and structures of cations $[(H_2apt)_2FFe(\mu\text{-}O)FeF(H_2apt)_2]^{2+}$ (**A**) and $[FeF_2(H_2apt)_2]^{+}$ (**B**) redrawn from Reference 105.

Magnetic and Mössbauer data show both complexes contain high spin Fe(III), the dimer with strong antiferromagnetic coupling. Triazole and tetrazoles have been used to assemble MOFs based upon iron(III) fluoride or mixed valence Fe(III)/Fe(II) fluorides [106,107,108,109]. In some systems the organic moiety is present only as a cation linked to the iron fluoride anions by hydrogen bonding, but in others Fe-N coordination is present. A new dinucleating ligand ($Susan^{6Me}$) (Fig. 33) reacts with $Fe(BF_4)_2{\cdot}6H_2O$ and NEt_3 under argon to give a green Fe(II) dimer, but in air the mixed valence brown $[(Susan^{6Me})Fe^{II}F(\mu\text{-}F)Fe^{III}F][BF_4]_2$ was obtained, which contains a single fluoride bridge with each iron N_4F_2 coordinated; magnetic and Mössbauer data confirm the mixed valence description [110]. Magnetic materials containing FeF_3 in combination with Gd [81] or a range of 3d metal fluorides [111] have also been described.

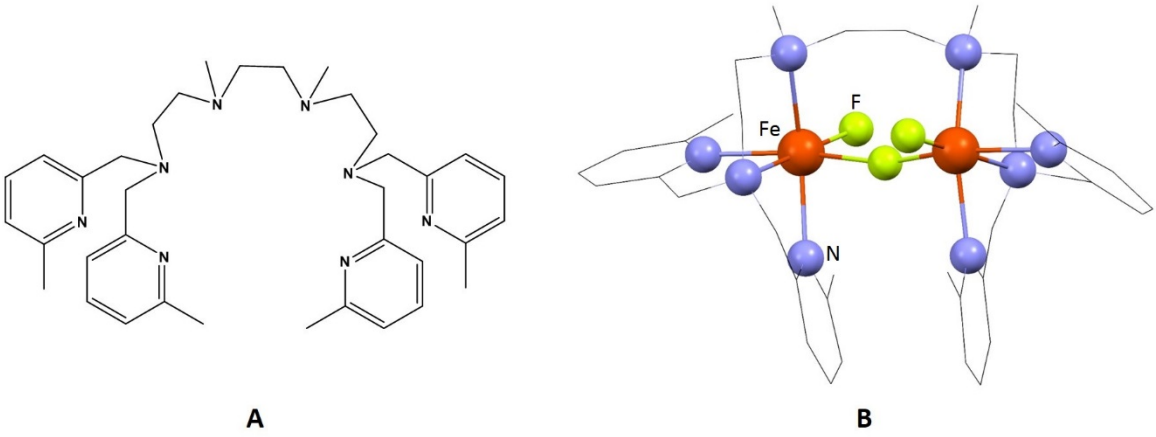

Fig. 33 **A**: the ligand $Susan^{6Me}$; **B**: Structure of the cation $[(Susan^{6Me})Fe^{II}F(\mu\text{-}F)Fe^{III}F]^{+}$ redrawn from Reference 110.

Group 9

Cobalt

Although cobalt(III) amines with fluoride co-ligands were first reported over 100 years ago, complexes with other ligand types are very rare and little new work has appeared in recent years. Two new compounds are $[CoF_3(terpy)]\cdot MeOH\cdot 2H_2O$ and $[CoF_3(Me_3\text{-}tacn)]\cdot 2H_2O$, obtained by air oxidation of a mixture of the ligand, CoF_2 and NaF in MeOH solution [87]. Neutral trihalocobalt(III) complexes are much rarer than the cationic mono- or di-halocobalt(III) cations with any of the halogens. Both complexes are low spin d^6 systems and exhibited very broad resonances in the ^{59}Co NMR spectra ($w½ > 15000$ Hz) due to the large quadrupole moment of ^{59}Co (I = 7/2) which rule out observation of $^1J_{Co\text{-}F}$ couplings. The $[CoF_3(Me_3\text{-}tacn)]\cdot 2H_2O$ is isomorphous with the manganese(III) complex (Fig. 34).

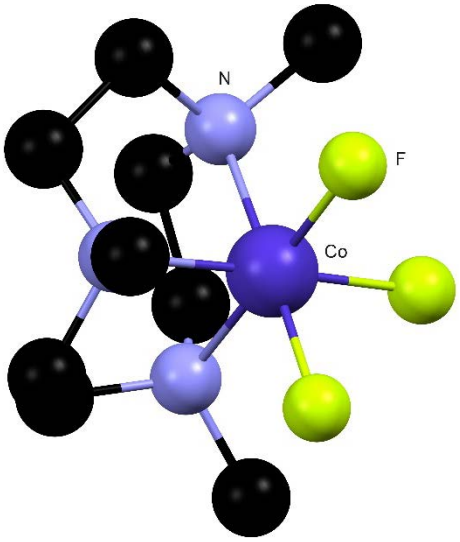

Fig. 34 Structure of $[CoF_3(Me_3\text{-}tacn)]$ redrawn from Reference 87. The carbon atoms in the ring were disordered, only one component is shown.

Rhodium and Iridium

There are no reports of the direct reaction of rhodium or iridium fluorides with neutral ligands, and the relatively few examples of complexes with $Rh^{III}F$ or $Ir^{III}F$ bonds are organometallic species often derived from oxidation of Rh^{I} or Ir^{I} compounds [112,113,114,115] which fall outside the scope of the present article.

Group 10

Nickel, Palladium and Platinum

High valent nickel species have been suggested as intermediates in some nickel catalysed organic transformations, but only very rarely has the species been experimentally identified or isolated. One example is the surprisingly stable yellow (formally) Ni(IV) complex $[NiF_2(py)_2(CF_3)_2]$ obtained by oxidation of

$[Ni(py)_2(CF_3)_2]$ with XeF_2 [116]. The crystal structure shows an octahedral nickel environment with *trans* fluorines, and *cis* pyridines (Fig. 35). Two Ni(III) complexes were isolated under slightly different conditions – $[NiF(py)_3(CF_3)_2]$ and $[(CF_3)_2(py)Ni(\mu\text{-}F)_2Ni(py)_2(CF_3)_2]$, the first octahedral, the dimer with unusual five- and six-coordinate nickel centres (Fig. 36).

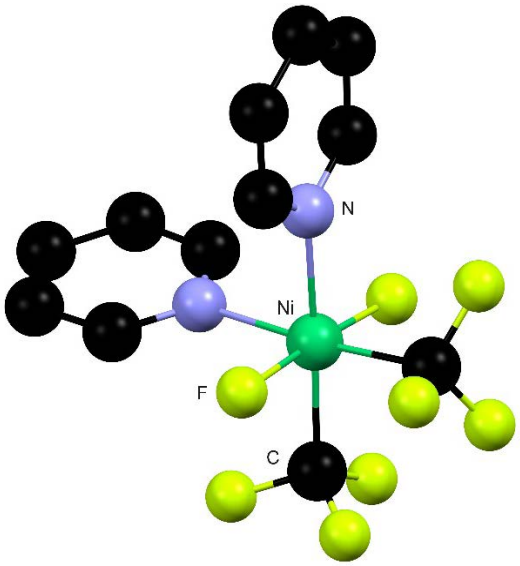

Fig. 35 Structure of $[NiF_2(py)_2(CF_3)_2]$ redrawn from Reference 116.

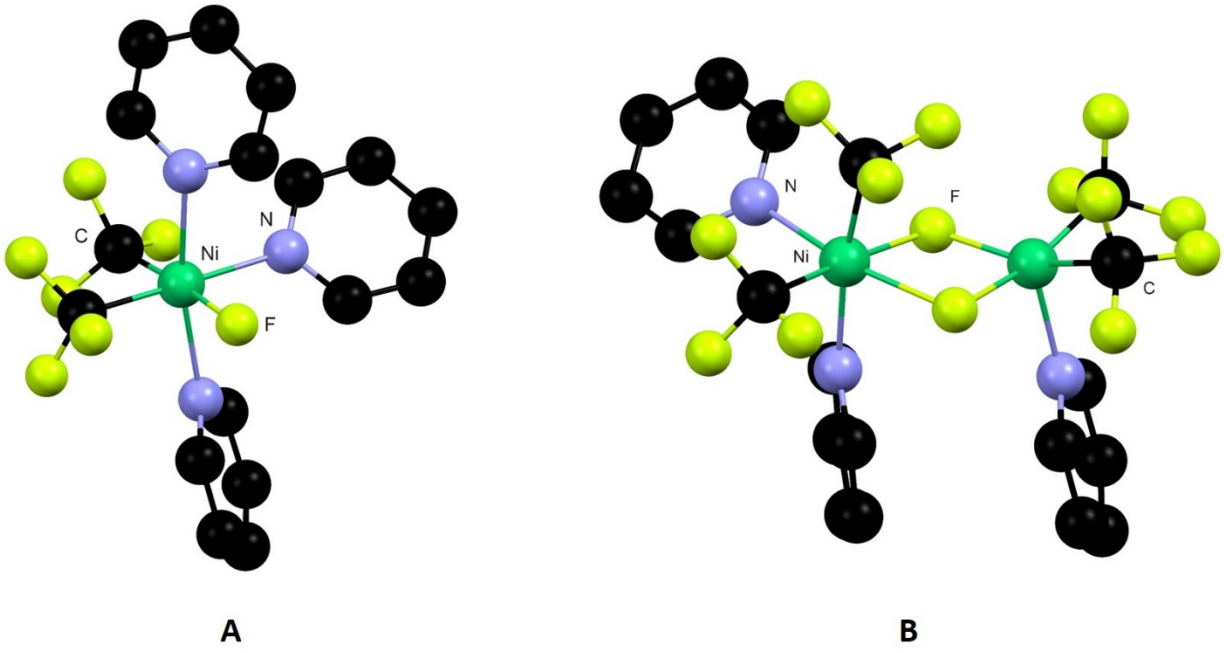

Fig. 36 Structure of $[NiF(py)_3(CF_3)_2]$ (**A**) and $[(CF_3)_2(py)Ni(\mu\text{-}F)_2Ni(py)_2(CF_3)_2]$ (**B**) redrawn from Reference 116.

Similarly, Pd(II) catalysed conversions of aryl-H bonds to aryl-F have been suggested to involve Pd(IV) intermediates, but only in a few cases have the latter been isolated and/or characterised [117,118]. The strong ligand field produced by Ni-C σ or Pd-C σ bonds and the presence of bulky ligands help to stabilise the

high oxidation states, but it seems quite unlikely that simple coordination complexes of the metal fluorides with neutral ligands will be isolable. The possibility of obtaining complexes of N-donor ligands with PtF_4 does not seem to have been examined.

Group 11

Copper, Silver and Gold.

Complexes of copper and silver in oxidation states ≥3 are not expected to form, but gold(III) complexes with N-donor ligands have been described. The use of gold catalysts in the synthesis of fluoro-organics has been reviewed very recently [119] and this article should be consulted for details. The dissolution of AuF_3 in anhydrous MeCN at low temperatures gave $[AuF_3(MeCN)]$, which decomposed > –25°C, whilst dissolving $Cs[AuF_4]$ in pyridine gave three complexes $[AuF_3(py)]$, $[AuF_2(py)_2]^+$ and $[F(py)Au(\mu\text{-}F)_2AuF(py)]^{2+}$ identified spectroscopically in solution (although not isolated) [120]. The first trifluoro-gold complex isolated was the carbene, $[AuF_3(SNHCMes_2)]$, which was formed, along with some $[AuF_2(SNHCMes_2)_2]^+$, by reaction of $[NMe_4][AuF_4]$ with $SNHCMes_2$ in CH_2Cl_2 [121]. The structure of $[AuF_3(SNHCMes_2)]$ (Fig. 37) shows a square planar gold centre.

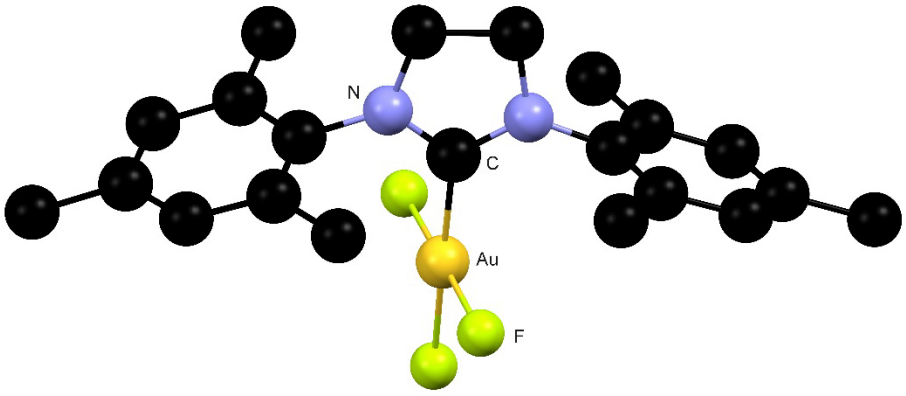

Fig. 37 Structure of $[AuF_3(SNHCMes_2)]$ redrawn from Reference 121.

Treatment of $[AuF_3(SNHCMes_2)]$ with Me_3SiCl or $Me_3SiOTeF_5$ cleanly replaces the fluoride *trans* to the carbene to form $[AuClF_2(SNHCMes_2)]$ or $[AuF_2(SNHCMes_2)(OTeF_5)]$ [122]. Difluorogold(III) cations are somewhat more easily prepared by XeF_2 oxidation of Au(I) precursors [123]. The reaction of $[Au(Rpy)_2][Y]$ (Rpy = py or 4-Me_2Npy; Y = BF_4 or O_3SCF_3) with XeF_2 in $CHCl_3$ gave yellow *trans*-$[AuF_2(Rpy)_2][Y]$, whilst the same reaction using the 2-methylimidazole complex $[Au(2Meimid)_2][O_3SCF_3]$ gave $[AuF_2(2Meimid)_2][O_3SCF_3]$, which was sufficiently stable for crystallographic analysis (Fig. 38).

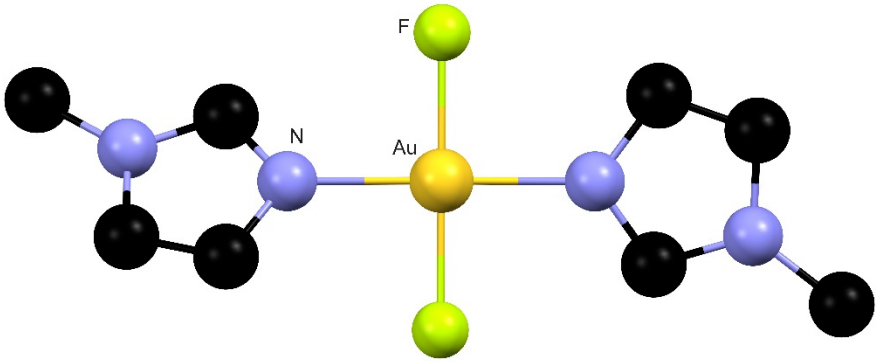

Fig. 38 Structure of the cation $[AuF_2(2Meimid)_2]^+$ redrawn from Reference 123.

An alternative synthesis is from $[Au(L)_4][O_3SCF_3]_3$ (L = 4-Me_2Npy, 2Meimid) and KF in the presence of 18-crown-6 in MeCN [123]. Alkylgold(III) fluorides $[AuRF_2(NHC)]$ (NHC = $SNHCMes_2$, $NHCD^iPP_2$) are also made by XeF_2 oxidation of the gold(I) [AuR(NHC)]; in solution they are present as an equilibrium mixture with the dimers $[R(NHC)Au(\mu\text{-}F)_2AuR(NHC)]F_2$ and the structure of $[Me(NHCD^iPP_2)Au(\mu\text{-}F)_2AuMe(NHCD^iPP_2)]F_2$ was determined [124]. Reductive elimination of RF from some of the $[AuRF_2(NHC)]$ complexes has been examined, the products depending upon the R group [125].

6. p-block complexes

Group 13

Boron trifluoride is a reactive gas, but the anhydrous trifluorides of aluminium, gallium and indium are inert polymers containing octahedrally coordinated metal ions. No complexes of TlF_3 have been described. Boron, aluminium and gallium fluoro-complexes have been developed as potential carriers for the radioisotope ^{18}F in medical diagnostics (PET imaging), and this is discussed in Section 7.

Boron

BF_3, or its more conveniently handled, commercially available adducts, including $[BF_3(OEt_2)]$, $[BF_3(SMe_2)]$, $[BF_3(MeOH)]$ and $[BF_3(thf)]$, are widely used Lewis acids in organic synthesis [126]. Many other similar adducts are known [7]; all are distorted tetrahedral monomers. Although the Lewis base involved is also important, in most cases the Lewis acidity of the boron halides falls $BI_3 > BBr_3 > BCl_3 > BF_3$, which was for many years attributed to π-backbonding from the halogen lone pairs into the empty boron p-orbital. Considerable effort using DFT methods has led to the view that the order arises from σ-bonding effects and sometimes a steric component [126,127], and the π-backbonding explanation has been discarded. Whilst further examples of BF_3 adducts with N- or O-donor ligands continue to be reported, with a few exceptions discussed below, they are not much different to known examples. More notable has been the recent detailed studies of BF_3 adducts with the heavier donor ligands of Groups 15 and 16 and with various types of NHC.

Detailed electrochemical and spectroscopic studies have been carried out on a range of BF_3 adducts with nitrogen heterocycles, with the aim of understanding how the heterocycle structures affect the electrochemical properties [128,129]. Adducts of this type have been examined as electrolyte additives to increase the lifetime of Li-ion batteries [130,131,132].

Phosphine complexes of BF_3 are less stable than analogues with the other three boron halides. The complex $[BF_3(PMe_3)]$ was prepared some years ago and characterised spectroscopically [7], and its structure has recently been obtained. It shows the expected distorted tetrahedral arrangement about boron with an eclipsed conformation [133]. The bond lengths are identical with those found in $[BF_3(PEt_3)]$, the only other reported structure of a tertiary phosphine-BF_3 adduct [134]. Whilst $[BF_3(PMe_3)]$ is stable as a solid and in solution in anhydrous non-coordinating solvents, solid $[BF_3(AsMe_3)]$ has a significant vapour pressure at ambient temperatures, and in solution shows only singlets in the ^{11}B and $^{19}F\{^1H\}$ NMR spectra, with no $^1J_{BF}$ couplings, indicating fast reversible arsine exchange [133]. The tertiary stibine complexes are even less stable, and although $[BF_3(SbR_3)]$ (R = Et, ^{i}Pr) have been isolated by reaction of BF_3 with n-hexane solutions of the stibines, the complexes fume in air and lose BF_3 rapidly on standing at room temperature [135]. They were identified by multinuclear NMR spectroscopy (^1H, $^{13}C\{^1H\}$, ^{11}B and $^{19}F\{^1H\}$) in anhydrous CD_2Cl_2 solution.

Ditertiary phosphine complexes are more stable. The reaction of $R_2PCH_2CH_2PR_2$ (R = Me, Et) with BF_3 in n-hexane or with $[BF_3(SMe_2)]$ in CH_2Cl_2, produced white $[F_3B(\mu\text{-}R_2PCH_2CH_2PR_2)BF_3]$ (Fig. 39). Comparison of the structure with those of the other $[X_3B(\mu\text{-}Et_2PCH_2CH_2PEt_2)BX_3]$ (X = Cl, Br, I), shows the B-P bond is ~ 0.06 Å longer in the fluoride complex, consistent with weaker B-P bonding in the fluoride. Both complexes were also characterised by multinuclear NMR spectroscopy [133].

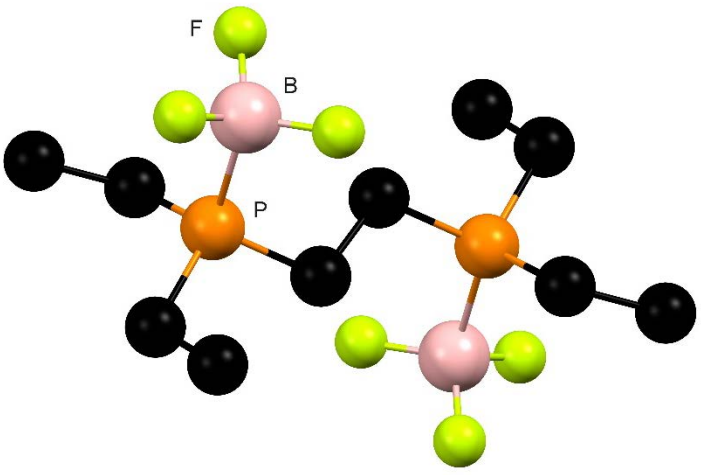

Fig. 39 Structure of $[F_3B(\mu\text{-}Et_2PCH_2CH_2PEt_2)BF_3]$ redrawn from Reference 133.

In contrast, the more rigid diphosphine *o*-$C_6H_4(PMe_2)_2$ produced the first phosphine containing example of a difluoroboronium cation in $[BF_2\{o\text{-}C_6H_4(PMe_2)_2\}][BF_4]$. The white complex is insoluble in CH_2Cl_2 and

decomposed by dmso, or MeCN. Multinuclear NMR spectra (^{1}H, $^{19}F\{^{1}H\}$ and ^{11}B) were obtained from freshly prepared $MeNO_2$ solutions, but slow decomposition prevented growth of crystals for an X-ray study [133]. The constitution follows from the NMR data (Fig. 40) and by comparison with the structures of more stable $[BX_2\{o\text{-}C_6H_4(PMe_2)_2\}]^+$ (X = Cl, Br, I). The diarsine ligand $o\text{-}C_6H_4(AsMe_2)_2$ also formed a difluoroboronium cation $[BF_2\{o\text{-}C_6H_4(AsMe_2)_2\}][B_2F_7]$, which appears to be partially dissociated in solution in $MeNO_2$.

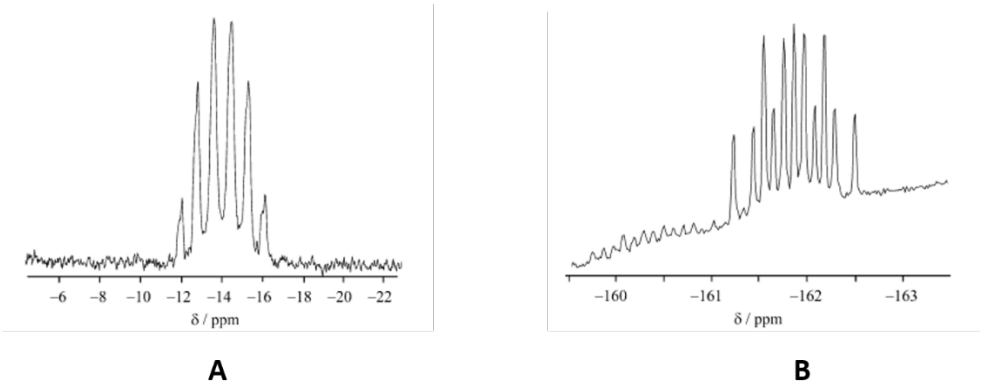

Fig. 40 $^{31}P\{^{1}H\}$ (A) and $^{19}F\{^{1}H\}$ (B) NMR spectra of $[BF_2\{o\text{-}C_6H_4(PMe_2)_2\}]^+$. Reprinted with permission from Reference 133. Copyright (2016) American Chemical Society.

The ambidentate $HN(P^iPr_2)_2$ reacts with BF_3 in Et_2O to form $[BF_3\{N(P^iPr_2)(P^iPr_2H)\}]$ in which the BF_3 is coordinated to the nitrogen and the proton has been switched onto one phosphorus (Fig. 41) [136], which contrasts with the phosphine donor coordination by this ligand found with most heavier Group 13 centres.

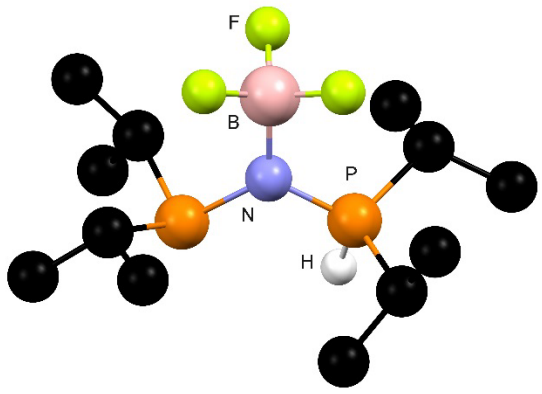

Fig. 41 Structure of $[BF_3\{N(P^iPr_2)(P^iPr_2H)\}]$ redrawn from Reference 136.

The reaction of the diphosphine dioxide, $Ph_2P(O)CH_2P(O)Ph_2$, with BF_3 gave both $[(BF_3)_2\{\mu\text{-}Ph_2P(O)CH_2P(O)Ph_2\}]$ and $[BF_2\{Ph_2P(O)CH_2P(O)Ph_2\}][B_2F_7]$; an X-ray crystal structure of the latter showed it to contain a chelating diphosphine dioxide and a rare crystallographically authenticated example of the $[B_2F_7]^-$ anion [133]. The structure of the secondary phosphine oxide complex, $[BF_3(OPHMe^tBu)]$, has also been determined [137].

The weaker Lewis acidity of BF_3 compared to the heavier boron trihalides is also evident in the complexes with thio-, seleno- and telluro-ethers [138,139]. Whilst the heavier halides form solid complexes $[BX_3(EMe_2)]$ (E = S, Se, Te; X = Cl, Br, I), which are stable in the absence of moisture for E = S or Se and slowly decomposed on standing in the case of E = Te, the $[BF_3(SMe_2)]$ and $[BF_3(SeMe_2)]$ are moisture sensitive liquids that fume in air and have a significant vapour pressure of BF_3 at room temperature. Passing BF_3 into neat $TeMe_2$ or a solution of $TeMe_2$ in CH_2Cl_2 at 0°C, afforded a yellow liquid and some red solid. The yellow oil was identified as $[BF_3(TeMe_2)]$ by multinuclear NMR spectroscopy, but could not be obtained pure and decomposed in a few hours [138]. Similarly, the complexes $[BF_3(\mu\text{-L-L})BF_3]$ (L-L = $EtSCH_2CH_2SEt$, $MeSeCH_2CH_2SeMe$, $MeTeCH_2CH_2CH_2TeMe$, *o*-$C_6H_4(SMe)_2$ and *o*-$C_6H_4(SeMe)_2$) are viscous oils which lose BF_3 at ambient temperatures [139]. Their identity was confirmed by ^{1}H, ^{11}B, $^{19}F\{^{1}H\}$, ^{77}Se, ^{125}Te NMR spectroscopy. The complexes with $MeSeCH_2CH_2SeMe$ and $MeTeCH_2CH_2CH_2TeMe$ decompose in solution by C-Se/Te bond fission.

NHC complexes of BF_3 have attracted significant effort [140]. They can be viewed either as boron trifluoride adducts of a neutral carbene, or as zwitterionic imidazolium trifluoroborates. The air and moisture stable complex, $[BF_3(SNHCMe_2)]$, is conveniently made from $[SiCl_4(SNHCMe_2)]$ and $[BF_3(Et_2O)]$ [141]. Unexpectedly, thermolysis of the corresponding imidazolium tetrafluoroborates yields $[BF_3(NHC)]$ (NHC = NHCMeEt, $NHCMe_2$), rather than eliminating RF as might have been expected; the complexes hydrolyse only very slowly in water and can even be recrystallised quickly from hot water without significant decomposition [142,143]. Functionalised derivatives have been used to generate potential ^{18}F carriers (Section 7). The N,N'-diamidocarbene complex $[BF_3(DAC)]$ (DAC = N,N'-dimesityl-4,6-diketo-5,5-dimethylpyrimidin-2-ylidene) has also been synthesised and structurally characterised [144]. DFT calculations on B, Al and Ga complexes with both normal and abnormal NHC's have shown that the carbene-Lewis acid bond is strongly influenced by the substituents on the acceptor atom and that the covalent character increases Al < Ga < B [145]. Boron trifluoride-carbene adducts have also been investigated as electrolyte additives for Li-ion batteries [146].

Aluminium

As indicated above, AlF_3 is an inert polymer that neither dissolves in nor reacts with neutral ligands, and entry into its complexes is either via Cl/F exchange from corresponding chloro-complexes or from the hydrate $AlF_3{\cdot}3H_2O$. Aluminium trifluoride hydrate exists in two crystalline forms, the α-form made by precipitation of an aqueous solution of an aluminium salt with HF contains discrete octahedral molecules $[AlF_3(H_2O)_3]$, whilst the more stable β-form, into which it transforms on heating, is a chain polymer $[\{AlF_2(H_2O)_2(\mu\text{-}F)\}_n]{\cdot}nH_2O$. Use of the more reactive α-$[AlF_3(H_2O)_3]$ is preferable in making complexes. Using hydrothermal vessels (180°C, 15 h), a range of N-donor complexes were made in high yields from α-$[AlF_3(H_2O)_3]$ and the ligands [20,147]. Complexes made in this way include *mer*-$[AlF_3(terpy)]{\cdot}3H_2O$, *mer*-$[AlF_3(2,2'\text{-bipy})(H_2O)]{\cdot}2H_2O$, and *mer*-

[AlF_3(1,10-phen)(H_2O)] [147]. The structure of [AlF_3(terpy)]·3H_2O is shown in Fig 42, which also shows the π-stacking and the extensive H-bonding typical of these metal fluoride complexes.

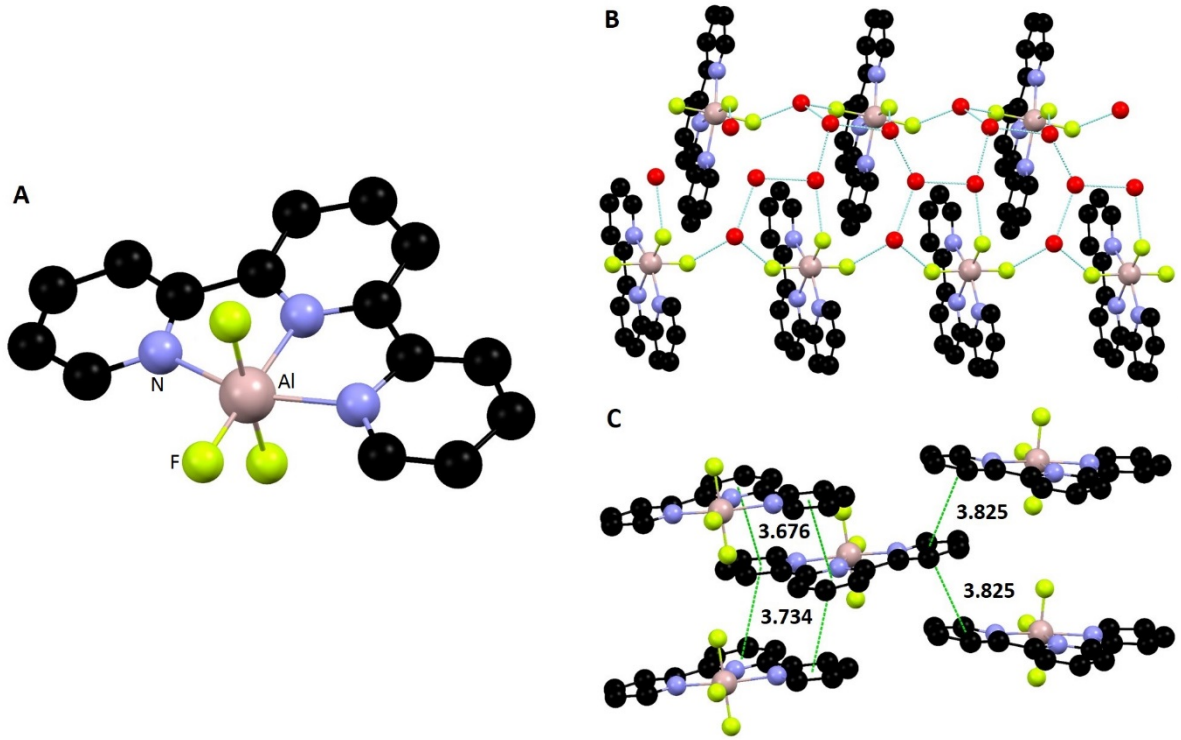

Fig. 42 Structure of [AlF_3(terpy)]·3H_2O redrawn from Reference 147 (**A**) and H-bonding (**B**) and π-stacking (**C**) present in the lattice.

Using the same hydrothermal conditions with the open chain triamine PMDTA, resulted in cleavage of the amine and ring closure to form the 1,1,4-trimethylpiperazinium cation, isolated as the [⊂-$Me_2N(CH_2)_2NMe(CH_2)_2$][$Al_2F_8(H_2O)_2$]·2H_2O salt [147]. The aza-macrocycle complex, *fac*-[AlF_3(Me_3-tacn)]·xH_2O, was obtained by the hydrothermal route and also by Cl/F exchange from [$AlCl_3$(Me_3-tacn)] and KF in aqueous solution; *fac*-[AlF_3($BnMe_2$-tacn)]·xH_2O was also made by Cl/F exchange in water, whereas the [$AlCl_3$(R_3-tacn)] fail to react with [R_4N]F in MeCN solution [20]. The fluorination of *fac*-[$AlCl_3$($BnMe_2$-tacn)] by [^{18}F]KF in water at pH = 4 has also been used to incorporate the ^{18}F radionuclide (Section 7) [148].

Use of the hydrothermal approach to make complexes with oxygen donor ligands, including phosphine oxides, pyNO, dmso and crown ethers, failed, with the reactants being recovered unchanged, indicating that the ligands cannot compete with the excess water present for the aluminium centre [149]. However, [$AlF_3(H_2O)_3$] dissolved in hot dmso to form [AlF_3(dmso)(H_2O)$_2$] [149]; curiously, further dmso is not incorporated even after prolonged heating. Reaction of [AlF_3(dmso)(H_2O)$_2$] with pyNO in MeOH generated [AlF_3(pyNO)(H_2O)$_2$], but a similar reaction failed to produce phosphine oxide adducts probably reflecting the lower basicity of the phosphine oxides [149].

The $[AlF_3(H_2O)_3]$ or $[AlF_3(dmso)(H_2O)_2]$ also fail to react with soft donor ligands such as phosphines or thioethers and attempted Cl/F exchange from preformed chloro-complexes containing the soft donor results in liberation of the soft donor ligands and precipitation of AlF_3 polymer [149]. Further studies of the reaction of $[AlX_3(py)_3]$ (X = Cl, Br, I) with Me_3SiF confirmed the products as $[AlF_2(py)_4]X$ [150]. X-ray structures for all three show the expected *trans*-difluoro structure for the cations and the presence of the same cation in each was also confirmed by solid state ^{27}Al NMR spectroscopy. Hydrolysis in dilute HCl-MeOH converted $[AlF_2(py)_4]Cl$ to *trans*- $[AlF_2(H_2O)_4]^+$.

Gallium

Hydrated gallium fluoride, $GaF_3{\cdot}3H_2O$, prepared by dissolving $Ga(OH)_3$ in aqueous HF, has the α-$[AlF_3(H_2O)_3]$ structure [149]. It reacts with N-donor ligands under hydrothermal conditions in a generally analogous manner to the aluminium systems described above. In this way, *mer*-$[GaF_3(terpy)]{\cdot}3H_2O$, *mer*-$[GaF_3(2,2'\text{-bipy})(H_2O)]{\cdot}2H_2O$ (Fig. 43), *mer*-$[GaF_3(1,10\text{-phen})(H_2O)]$ [147] and *fac*-$[GaF_3(Me_3\text{-tacn})]{\cdot}3H_2O$ [20] were isolated.

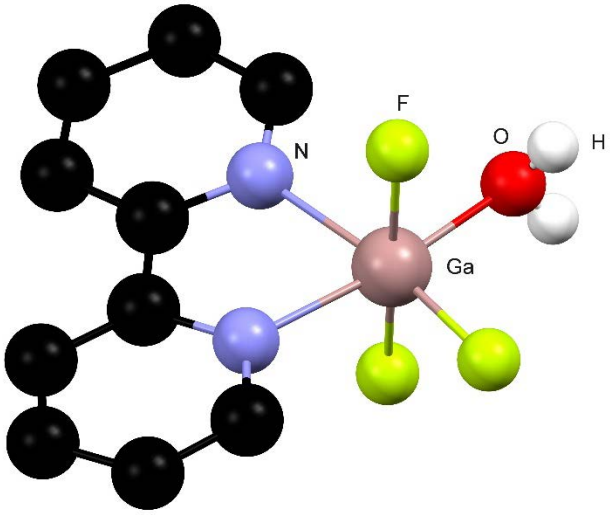

Fig. 43 Structure of $[GaF_3(2,2'\text{-bipy})(H_2O)]$ redrawn from Reference 147.

The *fac*-$[GaF_3(Me_3\text{-tacn})]$, *fac*-$[GaF_3(BnMe_2\text{-tacn})]$ and *mer*-$[GaF_3(terpy)]$ were also made by Cl/F exchange from the corresponding chloro-complexes and KF in H_2O/MeCN or $[NMe_4]F$ in CH_2Cl_2. The reaction of *mer*-$[GaF_3(terpy)]$ with $[NH_4][PF_6]$ in MeCN/H_2O generated orange crystals of $[\{GaF(terpy)\}_2(\mu\text{-}F)_2][PF_6]_2{\cdot}4H_2O$ with the structure shown in Fig. 44.

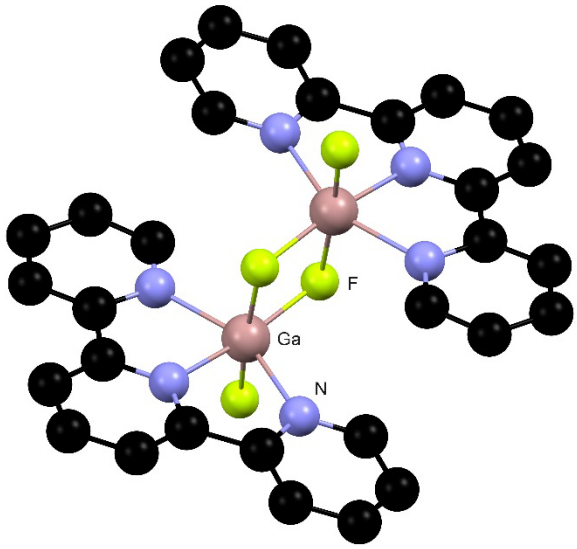

Fig. 44 Structure of the cation $[\{GaF(terpy)\}_2(\mu\text{-}F)_2]^{2+}$ redrawn from Reference 147.

The hydrothermal reaction of PMDTA with $GaF_3{\cdot}3H_2O$ resulted in the formation of the $[\subset\text{-}Me_2N(CH_2)_2NMe(CH_2)_2][Ga_2F_8(H_2O)_2]{\cdot}2H_2O$ salt [147,149], exactly analogous to the aluminium system. Refluxing $GaF_3{\cdot}3H_2O$ in dmf results in a complex mixture of products (largely unidentified), but a few crystals isolated from this reaction were identified as $[NMe_2H_2][\textit{trans}\text{-}GaF_4(H_2O)_2]$, the cation derived from cleavage of the solvent [149]. As with the aluminium system, $GaF_3{\cdot}3H_2O$ dissolved in hot dmso to form *mer*-$[GaF_3(dmso)(H_2O)_2]$ [Fig. 45] [149] and this is a useful synthon for making other gallium trifluoride complexes (Scheme 5); it also avoids the harsh conditions of the hydrothermal syntheses. Attempts to convert $[GaF_3(dmso)(H_2O)_2]$ to phosphine oxide complexes failed, but with pyNO crystals of composition $GaF_3(pyNO)_2(H_2O)_3$ formed; the structure of these crystals revealed two geometric isomers of $[GaF_3(pyNO)(H_2O)_2]$ linked by strong H-bonds, along with lattice water and lattice pyNO [Fig. 46] [149].

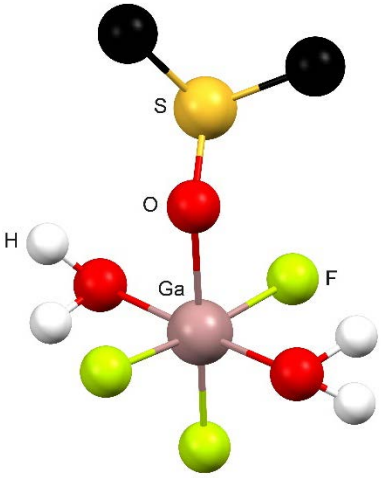

Fig. 45 Structure of $[GaF_3(dmso)(H_2O)_2]$ redrawn from Reference 149.

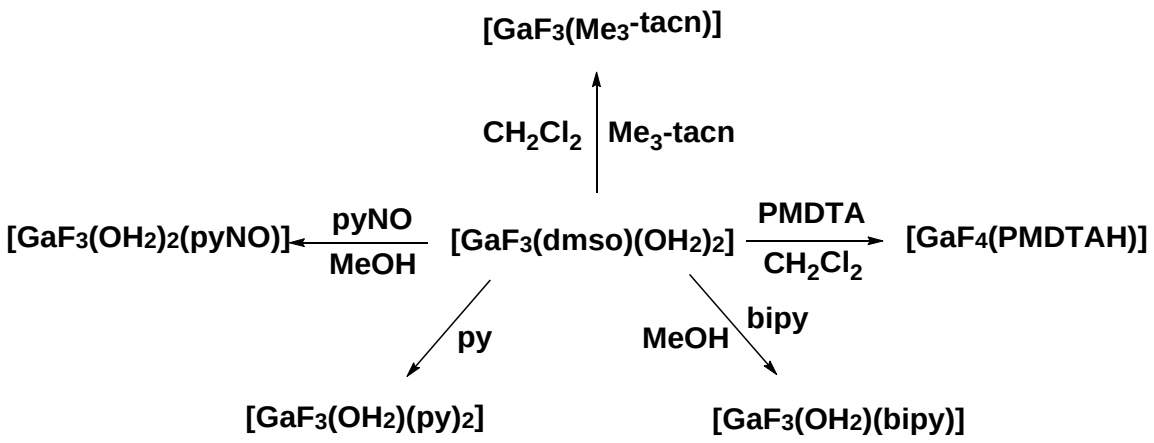

Scheme 5 Reactions of the synthon $[GaF_3(dmso)(OH_2)_2]$.

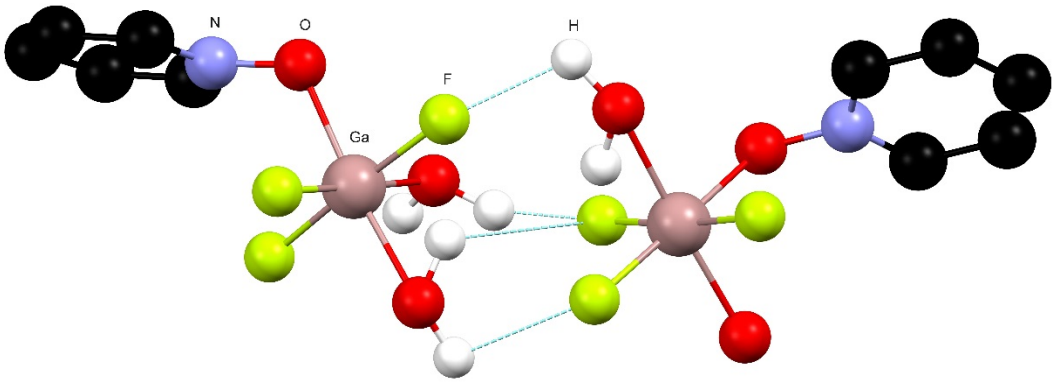

Fig. 46 Structure of $[GaF_3(pyNO)(H_2O)_2]$ showing the two geometric isomers and H-bonding interaction between the two. Figure redrawn from Reference 149.

The reaction of PMDTA, with $[GaF_3(dmso)(H_2O)_2]$ formed the zwitterionic $[GaF_4(PMDTAH)]\cdot 2H_2O$ with the PMDTA coordinated κ^2- and with the free Me_2N- group protonated to balance the charge [149]. Like the analogous aluminium systems, attempts to prepare phosphine or thioether complexes by Cl/F exchange failed with gallium fluoride polymer formed.

$[GaF_3(Me_3\text{-tacn})]$-$Gd^{III}$ species have also figured as a component of single molecule magnets [82]. Electrospray (ES^+) mass spectrometry studies found that *fac*-$[GaF_3(BnMe_2\text{-tacn})]$ behaved as a metalloligand towards Na^+, K^+, and $[NH_4]^+$ cations in aqueous solution, and crystals grown from such solutions revealed a supramolecular array of Na/K···F-Ga and H_3N-H···F-Ga coordination, for example as shown in Fig. 47 [151].

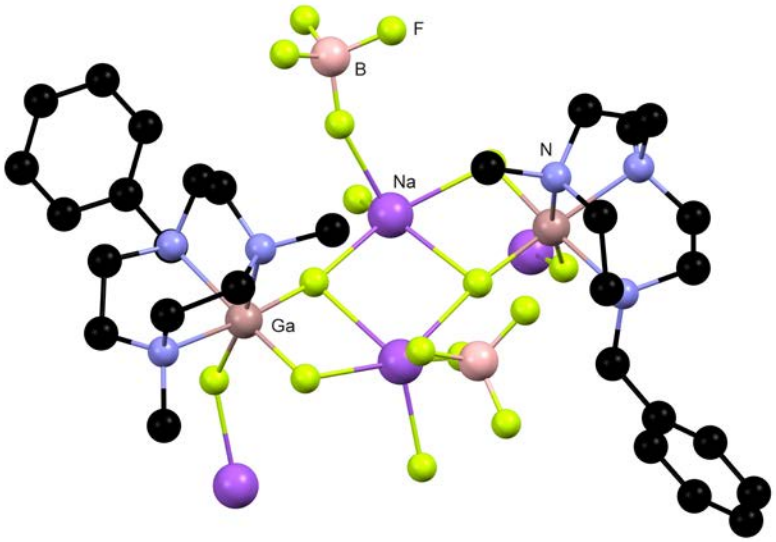

Fig. 47 Structure of [GaF_3($BnMe_2$-tacn)] acting as a metalloligand. From Reference 151.

The [GaF_3($BnMe_2$-tacn)] undergoes fast $^{18}F/^{19}F$ isotopic exchange in MeCN/H_2O or EtOH/H_2O at 80°C, making it a promising species to develop as a PET imaging agent (Section 7) [152]. The substituted R_3-tacn compound, 1-benzyl-1,4,7-triazacyclononane-4,7-dicarboxylic acid functions as a dianionic pentadentate (N_3O_2) ligand towards a $[GaF]^{2+}$ centre, which can also be easily radiofluorinated (Section 7) [153].

The gallium carbene complex [$GaCl_3$($NHCD^iPP_2$)] reacted with AgY (Y = BF_4 or PF_6) to form [$GaCl_2$($NHCD^iPP_2$)(κ^1-Y)] with the fluoroanion coordinated to the gallium centre, confirmed by the X-ray crystal structures [154]. If three equivalents of Ag[BF_4] were used the product was [GaF_3($NHCD^iPP_2$)] [154].

Indium

Indium trifluoride hydrate, $InF_3{\cdot}3H_2O$ has the polymeric β-aluminium trifluoride hydrate structure [149]. Analogous hydrothermal preparations to those used for Al and Ga systems resulted in *mer*-[InF_3(terpy)], *mer*-[InF_3(2,2'-bipy)(H_2O)]·$2H_2O$, *mer*-[InF_3(1,10-phen)(H_2O)] and *fac*-[InF_3(Me_3-tacn)]·$4H_2O$ [20,147]. Fluorination of [$InCl_3$(R_3-tacn)] (R_3 = Me_3 or $BnMe_2$) with [NMe_4]F in CH_2Cl_2 also proves a successful route to the trifluoride complexes. Both of the white aza-macrocycle complexes were characterised by X-ray crystallography [20]. There is clearly great similarity between the metal trifluoride N-donor diimine and aza-macrocycle complexes of Al, Ga and In: all the hydrated complexes are stable to water and show extensive hydrogen bonding and π-stacking (of the diimines) interaction in the crystals. Variable temperature ^1H and $^{19}F\{^1H\}$ NMR spectroscopy show that in CD_3OD solution reversible dissociation occurs in some of the gallium and indium complexes, suggesting the stability is Al > Ga > In as would be expected based upon the relative Lewis acidity of the metal centre [147]. $InF_3{\cdot}3H_2O$ dissolved slowly in hot dmso to give a poor yield of [InF_3(dmso)(H_2O)$_2$] [149].

Group 14

The coordination chemistry of SiF_4, GeF_4 and SnF_4 is well developed [7,155] and only a modest amount of new work has appeared.

Silicon

NHC complexes have attracted considerable interest and the area has been recently reviewed [140]. The new carbene complex *trans*-$[SiF_4(NHCIP_2)_2]$ was isolated during attempts to make SiF_2 adducts. The structures of this complex and its toluene solvate were determined [156]. In the former the carbenes are arranged parallel whilst in the solvate the carbenes are perpendicular to each other; this is presumably a packing effect and makes no difference to the bond lengths. The carbene NHCAAC reacted with SiF_4 in thf to form the five coordinate $[SiF_4(NHCAAC)]$ (Fig 48 C) [157]. Reduction of $[SiF_4(NHCAAC)]$ with two equivalents of KC_8 in thf in the presence of NHCAAC produced the dark purple Si(II) complex $[SiF_2(NHCAAC)_2]$ (Fig. 48 B) , whilst using one equivalent of KC_8 generated the yellow radical $[SiF_3(NHCAAC)]$ (Fig. 48 A)[157] (Fig. 48).

Although extremely moisture sensitive six-coordinate phosphine complexes, *trans*-$[SiX_4(PMe_3)_2]$ and $[SiX_4(diphosphine)]$ (diphosphine = $Me_2PCH_2CH_2PMe_2$, $Et_2PCH_2CH_2PEt_2$, *o*-$C_6H_4(PMe_2)_2$; X = Cl, Br), have been thoroughly characterised [158], attempts to prepare SiF_4 adducts have failed [159]. The failure to isolate phosphine complexes contrasts with the stability of the NHC complexes.

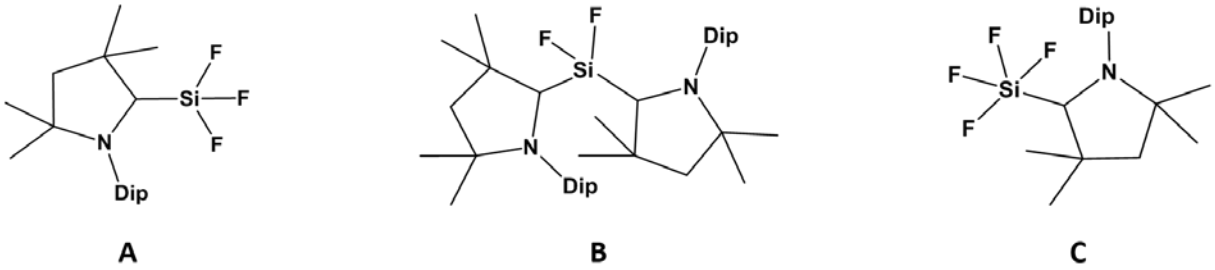

Fig. 48 $[SiF_3(NHCAAC)]$ (**A**), $[SiF_2(NHCAAC)_2]$ (**B**) and $[SiF_4(NHCAAC)]$ (**C**). Dip = 2,6-$^iPr_2C_6H_3$.

Low temperature IR spectroscopy and DFT calculations were used to explore the stability of nitrile and substituted pyridine complexes of SiF_4 [160]. The calculations and the IR data showed no significant adduct formation between SiF_4 and nitriles.

Germanium

Carbene complexes of GeF_4 and SnF_4 are included in recent reviews [19,140]. Oxidative addition of the appropriate bis(dialkylamino)difluoromethylenes to $[GeCl_2(dioxane)]$ gave the carbene complexes $[GeF_4(CAMe)]$ and $[GeF_4(SNHCMe_2)]$ [161]. The structures of both were determined and show trigonal bipyramidal geometries with equatorial carbene [161] (Fig. 49).

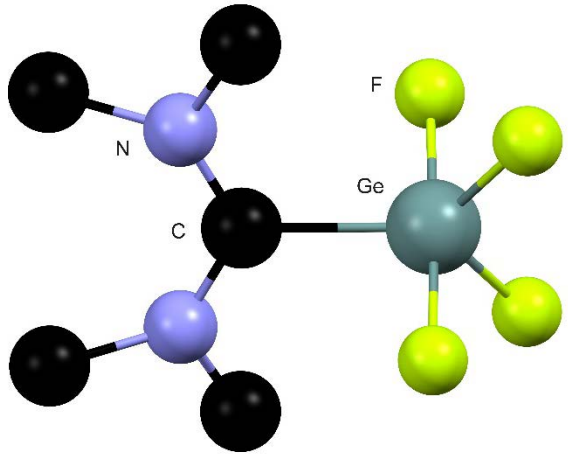

Fig. 49 Structure of [GeF_4(CAMe)] redrawn from Reference 161.

The acyclic carbene complex has a significantly longer Ge-C bond, but there is no difference in the Ge-F bond lengths between the two complexes. If excess of the cyclic difluoromethylene is used, the product is a six-coordinate anion $[GeF_5(SNHCMe_2)]^-$. The structure of $[GeF_4(FCH_2CN)_2]$ has been determined [162].

A new route to cationic germanium(IV) fluoride complexes is through oxidation of the corresponding germanium(II) adducts. The tetradentate N-donor, *tris*(1-ethyl-benzoimidazol-2-ylmethyl)amine ($BIMEt_3$) forms the Ge(II) complex $[Ge(BIMEt_3)][O_3SCF_3]_2$ on reaction with $[GeCl_2$(dioxane)] and $Me_3SiO_3SCF_3$, and subsequent treatment with XeF_2 or *Selectfluor* produced $[GeF_2(BIMEt_3)][O_3SCF_3]_2$ (Fig. 50) [163]. The X-ray structure reveals a distorted octahedron with *cis* fluorines. Treatment of $[GeF_2(BIMEt_3)][O_3SCF_3]_2$ with $Me_3SiO_3SCF_3$ generates $[GeF(BIMEt_3)][O_3SCF_3]_3$ in which a coordinated triflate completes the six-coordination at germanium [163].

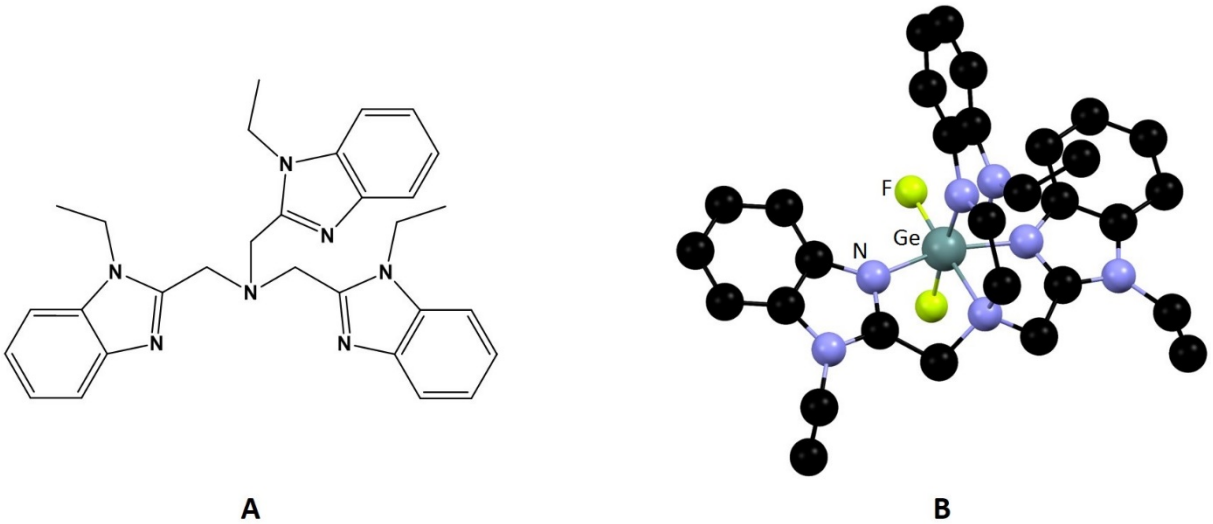

Fig. 50 **A**: the ligand $BIMEt_3$; **B**: Structure of the cation $[GeF_2(BIMEt_3)]^{2+}$ redrawn from Reference 163.

Tin

Oxidative addition of the bis(dialkylamino)difluoromethylenes to SnF_2 in MeCN gives the salts $[LF][SnF_5(L)]$ (L = CAMe, $SNHCMe_2$) directly and the neutral SnF_4 adducts could not be obtained (contrast with the germanium system above) [161]. Tin tetrafluoride reacts with the carbene $NHCMe_2^iPr_2$ in benzene to form *trans*-$[SnF_4(NHCMe_2^iPr_2)_2]$ [164]. Pentafluoroethylstannane adducts, including $[SnF_3(C_2F_5)_2(thf)]^-$, $[SnF_2(C_2F_5)_2(1,10\text{-phen})]$, $[SnF_3(C_2F_5)(1,10\text{-phen})]$ and $[SnF(C_2F_5)_3(1,10\text{-phen})]$, have been prepared by cleavage of the phenyl groups from $SnPh_n(C_2F_5)_{4-n}$ (n = 1-3) with HF, followed by addition of the neutral ligand [165].

In contrast to the germanium systems, attempted XeF_2 oxidation of $[Sn(BIMEt_3)][O_3SCF_3]_2$ results in a complex mixture, but reaction of SnF_4, $BIMEt_3$ and $Me_3SiO_3SCF_3$ in a 1:1:1 molar ratio in MeCN gave $[SnF_3(BIMEt_3)][O_3SCF_3]$, from which addition of one or two further equivalents of $Me_3SiO_3SCF_3$ gave $[SnF_2(BIMEt_3)][O_3SCF_3]_2$ and $[SnF(BIMEt_3)][O_3SCF_3]_3$, respectively [166]. Excess $Me_3SiO_3SCF_3$ generated the fluoride free cation $[Sn(BIMEt_3)][O_3SCF_3]_4$. All four complexes were characterised by ^{119}Sn NMR spectroscopy and X-ray diffraction. The Sn-N bonds shorten along the series from $[SnF_3(BIMEt_3)][O_3SCF_3]$ to $[Sn(BIMEt_3)][O_3SCF_3]_4$; the cations also interact either with triflate anions or in the case of the dication a dimer structure with fluorine bridges is present (Fig. 51) [166].

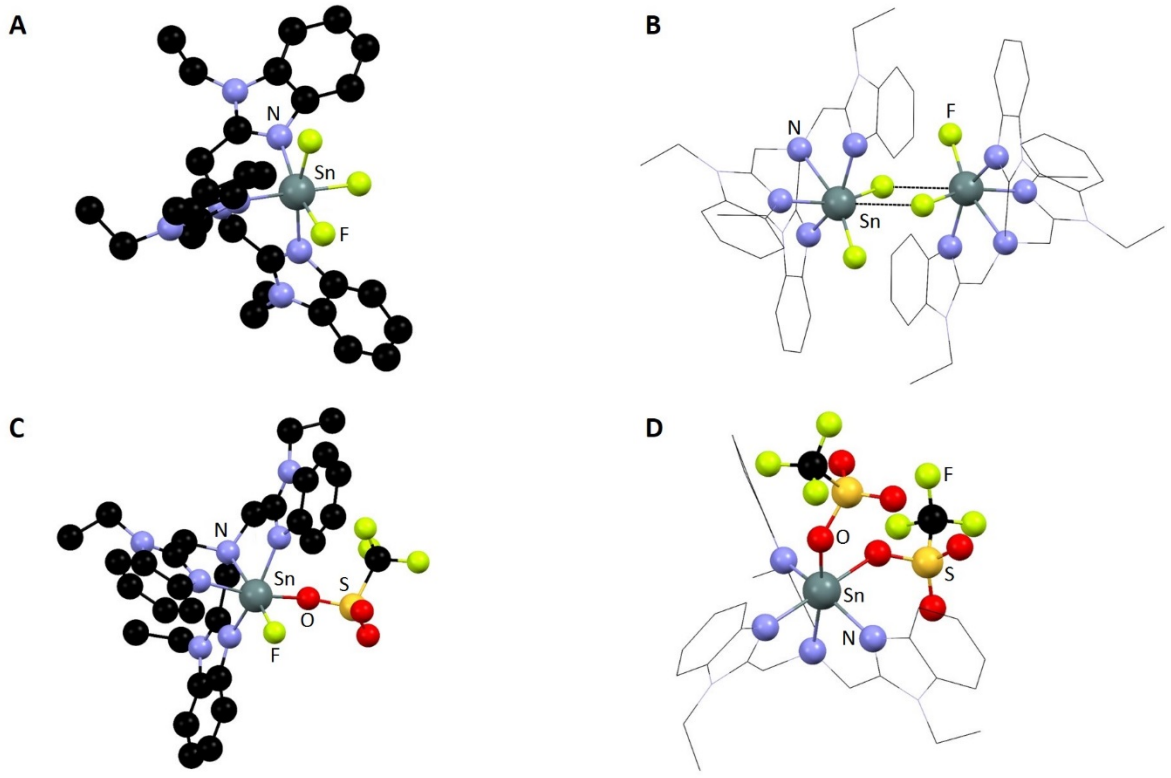

Fig. 51 Structures of the cations $[SnF_3(BIMEt_3)]^+$ (**A**), $[SnF_2(BIMEt_3)]^{2+}$ (**B**), $[SnF(BIMEt_3)(O_3SCF_3)]^{2+}$ (**C**) and $[SnF(BIMEt_3)(O_3SCF_3)_2]^+$ (**D**) redrawn from Reference 166.

Tin(IV) fluoride adducts with a range of fluoroalkylphosphoryl ligands $(R_2N)_nP(O)(OCH_2CF_3)_{3-n}$ (n = 0-2; R = Me or Et) and $P(O)(OCH_2CF_3)_3$ have been prepared from $[SnF_4(MeCN)_2]$ and the ligands in CH_2Cl_2 solution [167]. $^{19}F\{^1H\}$ NMR studies show the complexes exist as a mixture of *cis* and *trans* isomers in solution. Similar complexes of $(Me_2N)_3PO$, $(R_2N)_2FPO$ and $(R_2N)F_2PO$ have been described [168].

Group 15

Carbene adducts of phosphorus(V) fluorides have received considerable attention and the area has been reviewed recently [19,140,169]. In this section we have focussed on the synthesis and structures; the applications in organic synthesis are covered in these reviews. Some carbene complexes have been developed as possible ^{18}F carriers for PET imaging (Section 7). New work on antimony fluorides has also been reported, but no complexes of highly inert bismuth trifluoride are known.

Phosphorus

Addition of 4-dimethylaminopyridine to $PF_2(C_2F_5)_3$ produces the six-coordinate adduct $[PF_2(C_2F_5)_3(Me_2NC_5H_4N)]$ whose structure reveals *mer*-C_2F_5 groups with the pyridine *trans* to C_2F_5 [170]. Treatment of the complex with Brönsted acids (HX) (X = OH, OPh, OEt, OCH_2CF_3) leads to the corresponding anions $[PF_2(C_2F_5)_3X]^-$.

Thermolysis *in vacuo* of the corresponding imidazolium hexafluorophosphate salts gave the NHC complexes $[PF_5(NHC)]$ (NHC = $NHCMe_2$, NHCEtMe) [142]. Similar thermolysis of the *bis*(imidazolium) salt (Scheme 6) rather than generation of the corresponding carbene complex, gave a mixture of $[PF_5$(1-methylimidazole)] and the N-vinyl substituted carbene complex [171].

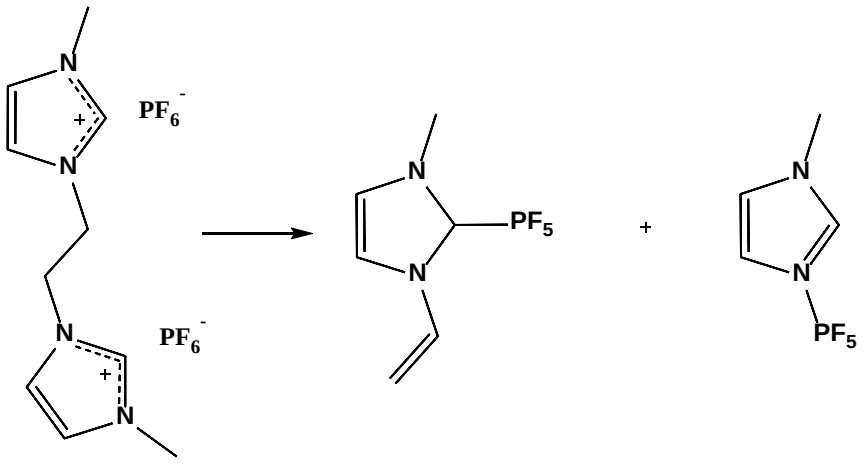

Scheme 6 Thermolysis of *bis*(imidazolium) hexafluorophosphate.

A convenient route to (amino)(aryl)carbene adducts of PF_5 is the fluorination of α-aroylphosphinic acids with morpholinesulfur trifluoride [172] (Scheme 7).

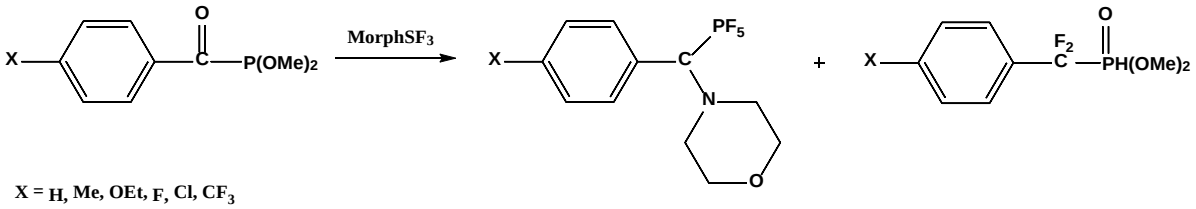

Scheme 7 Fluorination of α-aroylphosphinic acids with morpholinesulfur trifluoride

Xenon difluoride oxidation has been used to oxidise phosphine cations to difluorophosphorane cations (Fig. 52) [173]. Similar oxidation of $[PPh_2(SNHCMes_2)][B(C_6F_5)_4]$ produced $[PF_2Ph_2(SNHCMes_2)][B(C_6F_5)_4]$ which has a tbp geometry with axial fluorine [174]. Treatment of this with $[Et_3Si][B(C_6F_5)_4]$ removes one fluorine as Et_3SiF to generate the very unusual dication $[PFPh_2(SNHCMes_2)]^{2+}$ which is highly Lewis acidic.

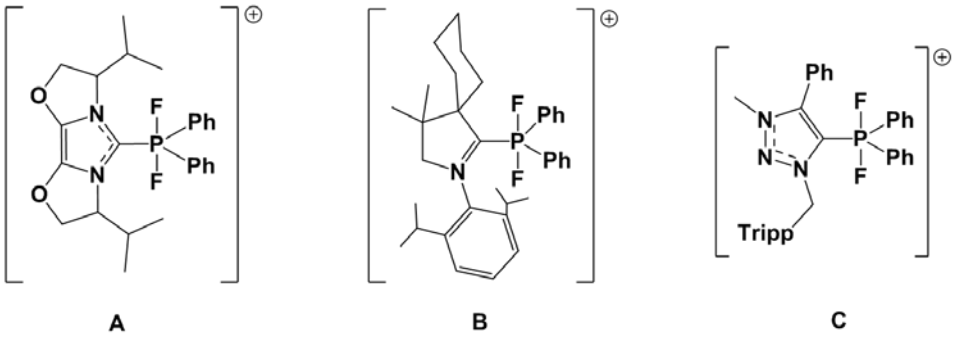

Fig. 52 Difluorophosphorane cations obtained from XeF_2 oxidation.

The high stability of some PF_5-NHC adducts towards hydrolysis means that they may have some potential as carriers for the ^{18}F radioisotope in PET imaging [175]. The new complex $[PF_4Ph(NHCMe_2)]$ was synthesised from $PhPCl_2$, which, on bromine oxidation in the presence of KF, forms $K[PF_5Ph]$; treatment of this with the imidazolium salt and $^{n}BuLi$, afforded the carbene complex [176]. New carbene complexes of P(V) containing fluoroalkyl groups have been prepared by oxidative addition of bis(dimethylamino)difluoromethylene to PX_2CF_3, $PX_2C_2F_5$ and $PX(C_2F_5)_2$ (X = F, Cl) which produce $[PF_4R(SNHCMe_2)]$ and $[PF_3(C_2F_5)_2(SNHCMe_2)]$ [177]. The complexes are air stable and can be recrystallised from boiling water, but anhydrous HF in CH_2Cl_2 cleaves the P-carbene bond to form imidazolium hexafluorophosphates. Similar oxidative addition to PF_3, $PMeCl_2$ and $PPhCl_2$ has been reported [178]. (Difluoroorganyl)dimethylamines RCF_2NMe_2 (R = H, Ph, ^{t}Bu) also oxidatively add to PF_3 to give sterically non-demanding asymmetric carbene complexes [178]. Phosphorus(V) fluoro-complexes containing carbenes with liquid crystal chains have been obtained [179].

Phosphorus(V) carbene complexes have been examined as additives to improve the function of Li-ion battery electrolytes [146].

The tetradentate $BIMEt_3$ (Fig. 50) cation in $[P^{III}(BIMEt_3)][O_3SCF_3]_3$ is oxidised by XeF_2 to $[P^{V}F_2(BIMEt_3)][O_3SCF_3]_3$, which is the first example of a phosphorus(V) trication; it has an octahedral phosphorus centre with *cis* fluorines [180].

Arsenic

Neutral ligand complexes of AsF_3 or AsF_5 are few [7] and merit further investigation. A series of adducts of HCN and various nitriles with AsF_5, $[AsF_5(L)]$ (L = HCN, PrCN, *c*-C_3H_5CN, ^tBuCN, PhCN, $NCCH_2CN$) and $[(AsF_5)_2(NCCH_2CN)]$ has been prepared from AsF_5 and the nitrile in liquid SO_2 at low temperatures [181]. The adducts are colourless solids at low temperatures, but decompose slowly turning brown when warmed to room temperature. They were characterised by IR, Raman, $^{19}F\{^1H\}$, ^{14}N NMR spectroscopy, and X-ray structures were reported for four examples: $[AsF_5(HCN)]$, $[AsF_5(PrCN)]$, $[AsF_5(c\text{-}C_3H_5CN)]$ and $[AsF_5(PhCN)]$ (Fig 53).

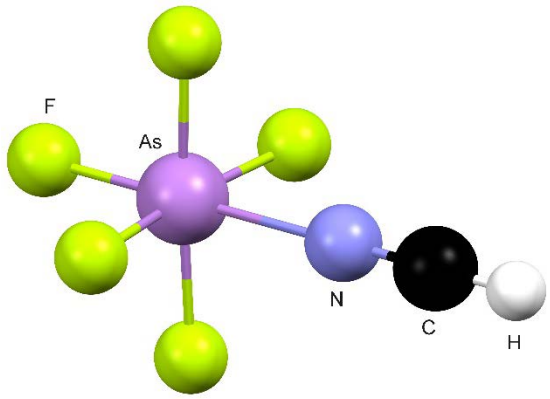

Fig. 53 Structure of $[AsF_5(NCH)]$ redrawn from Reference 181.

The As(V) carbene complex $[AsF_2Ph_2(NC^iPr_4)][BF_4]$ was made by XeF_2 oxidation of $[AsPh_2(NC^iPr_4)][BF_4]$; it has a trigonal bipyramidal geometry with axial fluorines (Fig. 54) [182].

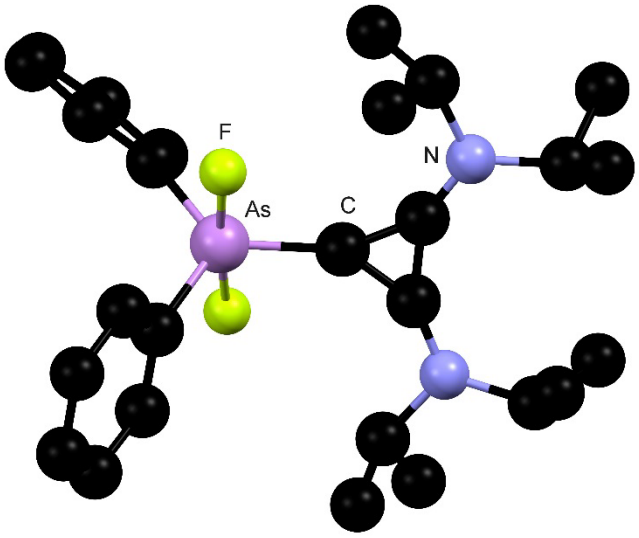

Fig. 54 Structure of the cation $[AsF_2Ph_2(NC^iPr_4)]^+$ redrawn from Reference 182.

Antimony

The nitrile complexes $[SbF_5(L)]$ (L = HCN, PrCN, *c*-C_3H_5CN, ^{t}BuCN, PhCN, $NCCH_2CN$) and $[(SbF_5)_2(NCCH_2CN)]$ were made from SbF_5 and the nitriles in liquid SO_2 and similarly characterised to their arsenic analogues (q.v.) including X-ray structures of $[SbF_5(HCN)]$ and $[SbF_5(PrCN)]$ [181]. Comparison of the spectroscopic data suggests that the nitriles interact more strongly with AsF_5 than SbF_5.

The reaction of SbF_3 with $Me_3SiO_3SCF_3$ in the molar ratios 1:1, 1:2 and 1:>3 in MeCN in the presence of 2,2'-bypyridyl results in evolution of Me_3SiF and formation of $[SbF_2(2,2'\text{-bipy})_2][O_3SCF_3]$, $[SbF(2,2'\text{-bipy})_2][O_3SCF_3]_2$, and $[Sb(2,2'\text{-bipy})_2][O_3SCF_3]_3$, respectively [183]. The structure of $[SbF_2(2,2'\text{-bipy})_2][O_3SCF_3]$ reveals a four-coordinate (SbN_2F_2) unit with contact to a triflate oxygen and a fluoride ligand from a neighbouring molecule completing a distorted octahedral geometry, whilst in $[Sb(2,2'\text{-bipy})_2][O_3SCF_3]_3$ the SbN_4 core has three long Sb···O contacts to triflate anions (Fig. 55).

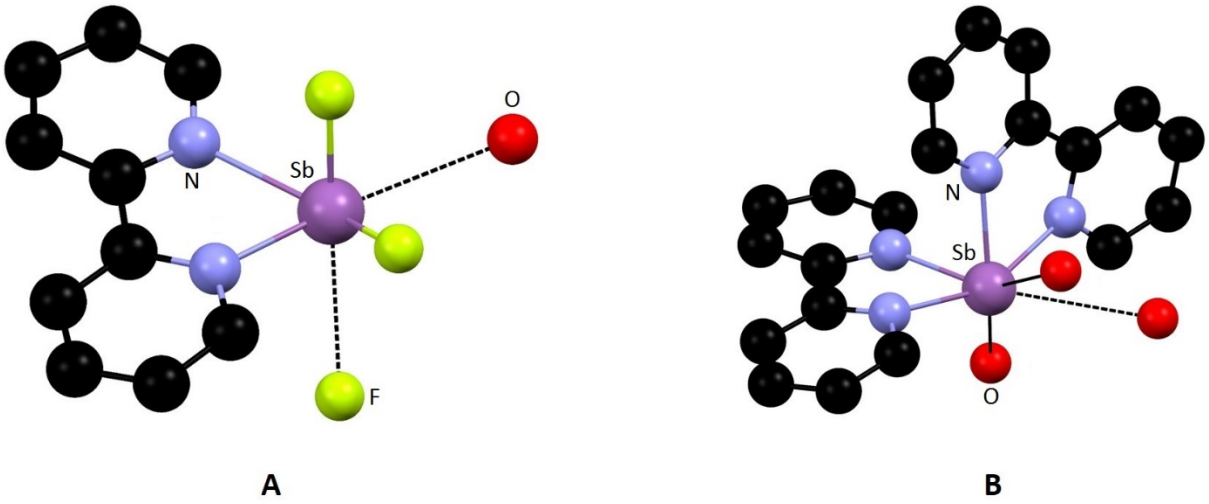

A **B**

Fig. 55 Structures of the cations $[SbF_2(2,2'\text{-bipy})]^+$ (**A**) and $[Sb(2,2'\text{-bipy})_2]^{3+}$ (**B**) redrawn from Reference 183. Triflate oxygen atoms and a fluoride ligand from a neighboring molecule complete the coordination environment around Sb.

New deep red complexes $[SbF(^{Dipp}BIAN)][O_3SCF_3]_2$ and $[SbF_2(^{Dipp}BIAN)][O_3SCF_3]$ ($^{Dipp}BIAN$ = 1,2-bis(2,6-diisopropylphenyl)imino)acenaphthene (Fig. 56) are formed by reacting $SbF_n(O_3SCF_3)_{3-n}$ (n =1,2) with the ligand in CH_2Cl_2 [184].

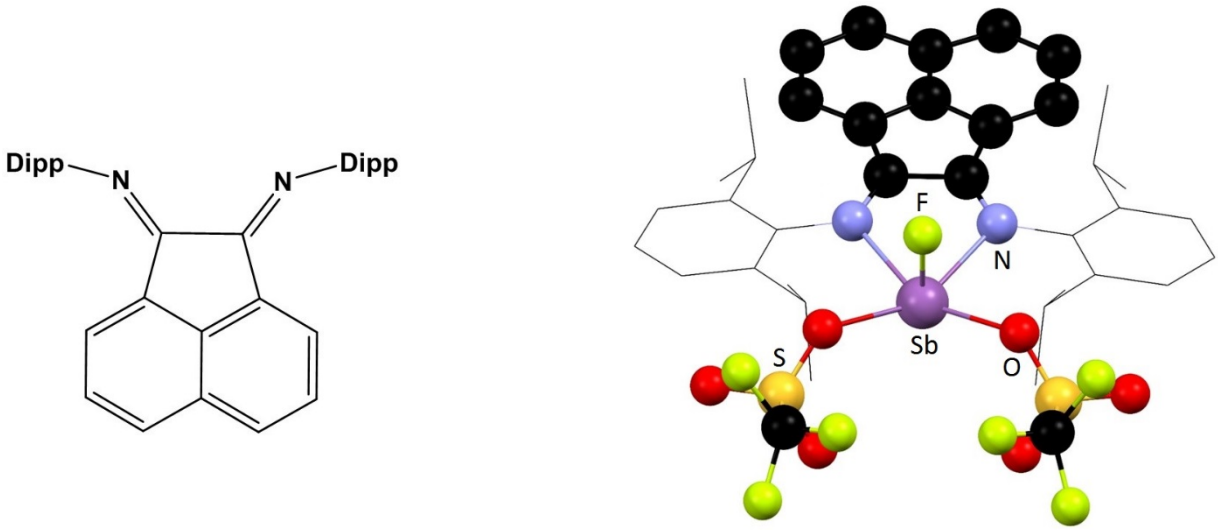

A **B**

Fig. 56 A: the ligand $^{Dipp}BIAN$; **B**: Structure of $[SbF(^{Dipp}BIAN)][O_3SCF_3]_2$ redrawn from Reference 184.

The reaction of $SbF(O_3SCF_3)_2$ with tris(2-pyridyl)phosphine in MeCN produces [SbF{tris(2-pyridyl)phosphine}][O_3SCF_3]$_2$ (Fig. 57) from which the fluoride can be abstracted with $Me_3SiO_3SCF_3$ to give [Sb{tris(2-pyridyl)phosphine}][O_3SCF_3]$_3$ [185].

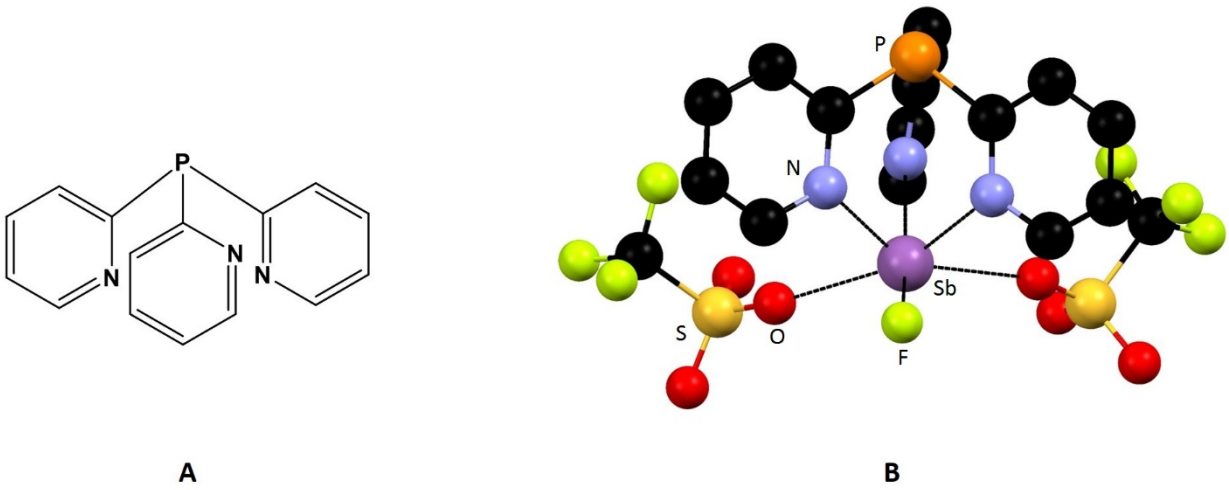

Fig. 57 A: the ligand tris(2-pyridyl)phosphine; **B**: structure of [SbF{tris(2-pyridyl)phosphine}][O_3SCF_3]$_2$ redrawn from Reference 185.

Tricyclohexylphosphine oxide forms 1:1 and 2:1 complexes with SbX_3 (X = F, Cl, Br) [186]. The structure of [$SbF_3(Cy_3PO)$] reveals a distorted square pyramidal environment at antimony composed of an OF_3 donor set and a weak association to the F of a second molecule, with a vacant vertex presumed to be occupied by a lone pair (Fig. 58) [186].

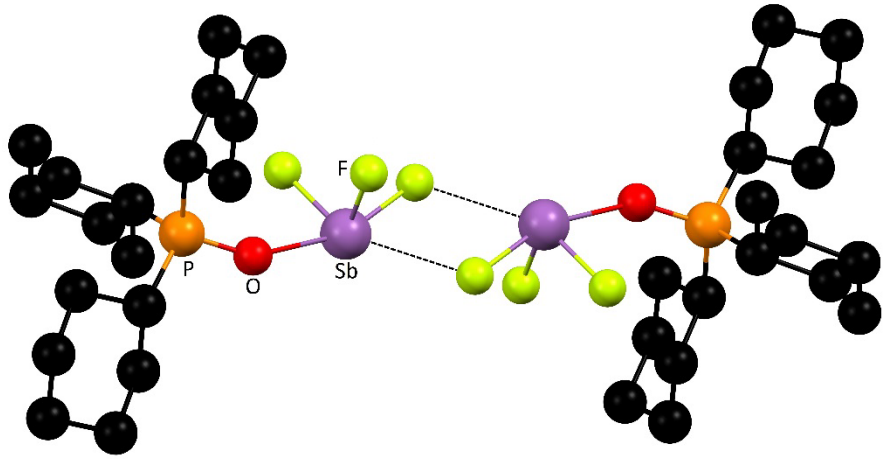

Fig. 58 Structure of [$SbF_3(Cy_3PO)$] redrawn from Reference 186.

The structure of [$SbF_3(Cy_3PO)_2$] was not determined, but it is likely to be a square pyramidal monomer with apical halide like [$SbCl_3(Cy_3PO)_2$] [186] or [$SbF_3(Me_3PO)_2$] [187]. Attempts to prepare SbF_3 complexes with Cy_3PS were unsuccessful, although the phosphine sulfide complexes with SbX_3 (X = Cl, Br).

Four crown complexes [SbF_3(crown)] (crown = 18-crown-6, [18]aneO_4S_2, [15]aneO_3S_2 and [18]aneO_4Se_2) were made by reaction in MeOH. The structure of [SbF_3([15]aneO_3S_2)] shows a pyramidal SbF_3 unit interacting with all five macrocyclic donor atoms (Fig 59) [188].

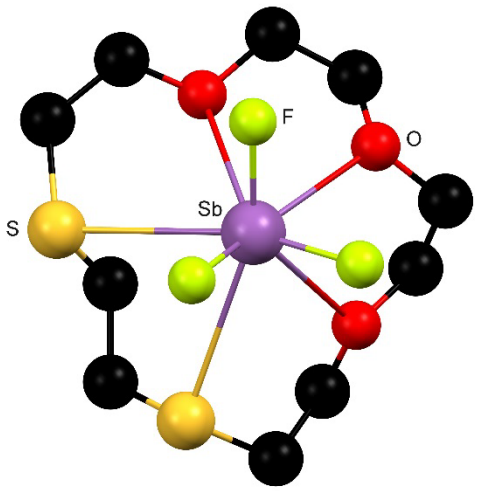

Fig. 59 Structure of $[SbF_3([15]aneO_3S_2)]$ redrawn from Reference 188.

The reaction of $BIMEt_3$ (Fig. 50) with SbF_3 and two equivalents of $Me_3SiO_3SCF_3$ gave the dication $[SbF(BIMEt_3)][Me_3SiO_3SCF_3]_2$, which has a tetragonal pyramidal geometry with two triflate anions interacting on the open face, forming a bridge to a second cation [180].

The direct reaction of SbF_3 with $NHCD^iPP_2$ in thf or MeCN gave the salt $[(NHCD^iPP_2)H][SbF_4]$. However, from reaction with $[SbF_3(tmeda)]$ in toluene, the product was $[SbF_2(NHCD^iPP_2)_2][SbF_4]$ [189]. The X-ray crystal structure shows the cation to have a disphenoidal ("saw-horse") geometry with axial fluorines, and most unexpectedly, one carbene has rearranged and coordinated in the mesoionic form (Fig. 60). The structure of the 2:1 SbF_3-glycine complex has been determined [190].

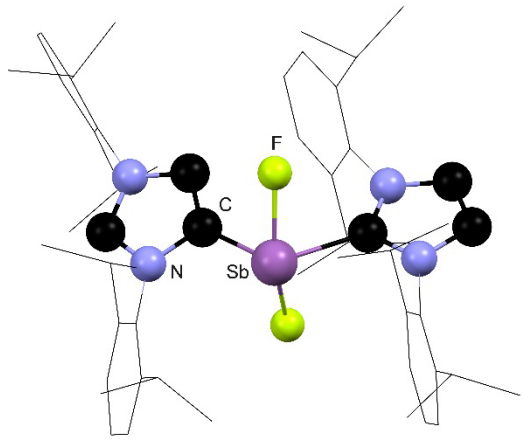

Fig. 60 Structure of the cation $[SbF_2(NHCD^iPP_2)_2]^+$ redrawn from Reference 189.

Group 16

Thermally unstable adducts of SF_4 with pyridines $[SF_4(Rpy)]$ (Rpy = py, 4-Mepy, 2,6-Me_2py, 4-Me_2Npy) were made by condensation of excess SF_4 onto the neat ligand at -45°C [191]. The structures show a square

pyramidal geometry with basal pyridines and long S-N bonds (~ 2.5 Å). $[SF_4(NEt_3)]$ which is only stable below -45°C has also been characterised by an X-Ray structure determination [192]. Weak adducts between oxygen ligands and SF_4 have been characterised more recently and include $[\{SF_4(thf]\}_2]$, $[SF_4(thf)_2]$, $[SF_4(cyclopentanone)_2]$ and $[SF_4(MeOCH_2CH_2OMe)]$ all of which contain distorted six-coordinate sulfur centres and decompose > -60°C [193]. The nature of the S-N and S-O bonds in these complexes [191-194] has been explored computationally. Unstable adducts of $Se(CN)_2F_2$, including $[Se(CN)_2F_2(L)_2]$ (L = MeCN, EtCN, thf) and $[Se(CN)_2F_2(L')]$ (L' = diglyme, 12-crown-4, 18-crown-6) have been synthesised and the structures determined (Fig. 61) [195]. They are unstable to air, moisture and temperature and the bonding is viewed as weak secondary bonding based upon the long Se-donor bonds and the results of DFT studies.

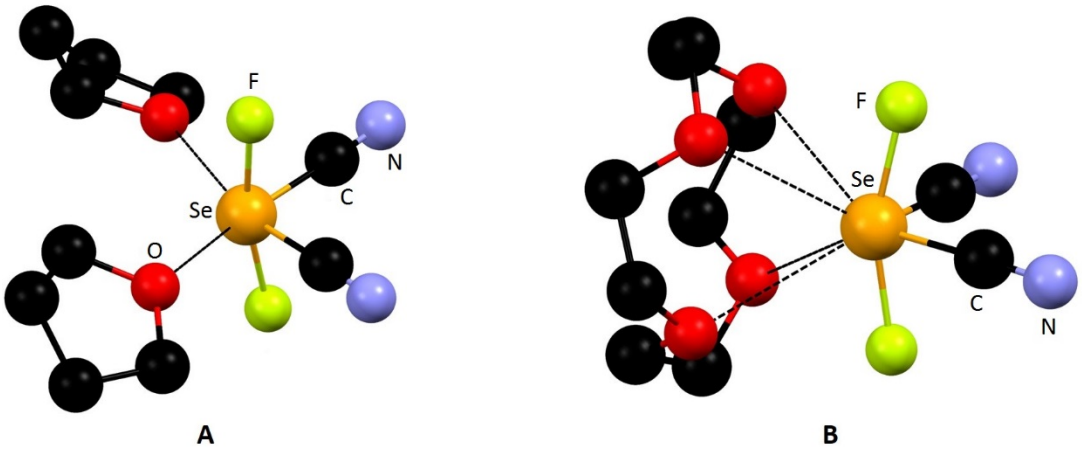

Fig. 61 Structure of $[Se(CN)_2F_2(thf)_2]$ (**A**) and $[Se(CN)_2F_2(12\text{-crown-4})]$ (**B**) redrawn from Reference 195.

Group 17

The first (and so far only) adduct of BrF_3 with a neutral ligand, $[BrF_3(py)]$ has been isolated as a white solid by combination of the reagents at low temperature [196]. The X-ray structure revealed a distorted square planar bromine centre (Fig 62).

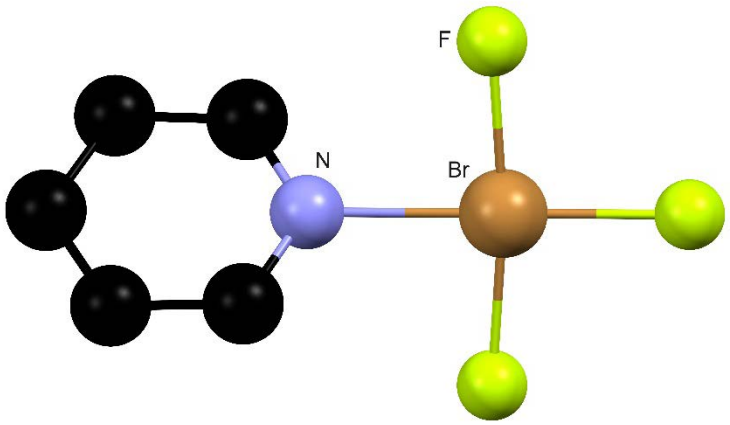

Fig. 62 Structure of $[BrF_3(py)]$ redrawn from Reference 196.

Group 18

Neutral ligand adducts of xenon fluorides are very rare, but include [$XeOF_3$(MeCN)] [197,198] and [$C_6F_5XeF_2$][BF_4]·xMeCN (x = 1, 2) [199], which are only stable at low temperatures and have weak Xe···NCMe contacts. A considerable *tour de force* is the isolation of the shock-sensitive [XeF_6(MeCN)] and [$XeF_6(MeCN)_2$]·MeCN [200]. The structures of both adducts were determined and detailed Raman spectroscopic characterisation reported. The Xe-N distances are long but significantly shorter than the sum of the appropriate Van der Waals radii; the bonding has been discussed in detail [201].

7. Complexes for ^{18}F Radiopharmaceutical Applications.

The increased amount of research into the coordination chemistry of metal/non-metal fluorides in recent years is tangible in the field of ^{18}F radiochemistry for PET imaging applications, in which several new systems have appeared as possible alternatives to organofluorine radiopharmaceuticals. Boron-, aluminium-, gallium-, silicon- and very recently, sulfur, phosphorus- and iron-fluoride compounds have all been investigated. Although many of these new systems have anionic ligands coordinated to the metal/non-metal fluoride, and hence formally fall outside the scope of this review, they will be presented, but not discussed in detail as they are already discussed in depth in several recent reviews [8,9,10,202,203,204,205,206,207,208]. These systems have attracted much interest due to their comparable or higher bond dissociation energies with fluorine compared to the C-F bond (Table 2), and their ability to incorporate [^{18}F]F^- under milder "physiologically friendly" conditions (e.g. aqueous solution, neutral/close to neutral pH and room temperature/moderate heating) and in the last step of the process. Moreover, given the increasing importance of targeting specific diseases through the use of biomolecules that deliver the radioactivity to the part of the body of interest, the mild reaction conditions also mean that the ^{18}F-labelling reactions can often be performed following bioconjugation, instead of first attaching [^{18}F]F^- to the organic molecule and then conjugating it to a biomolecule, resulting in a decrease of the total reaction time and of the number of steps of the process.

Table 2 Bond dissociation energies [209].

Bond type	Bond Dissociation Energy (kJ mol^{-1})
C-F	536
B-F	766
Al-F	664
Ga-F	577
Si-F	540
P-F	439

Fe-F	447

The most prominent alternatives to C-^{18}F radiopharmaceuticals comprising anionic ligands are:

- Silicon-fluoride-acceptors (SiFA) systems.

The SiFA chemistry has been developed by the Schirrmacher Group with the first example reported in 2006 [210]. In these molecules, the silicon atom has a tetrahedral coordination in which a single fluoride atom is present, along with a phenyl and two *tert*-butyl groups. The *tert*-butyl groups protect the silicon fluoride from hydrolysis and the aromatic group can be functionalised for biomolecule conjugation (Fig. 63).

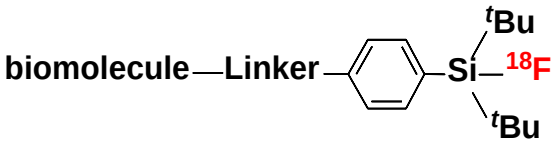

Fig. 63 SiFA system.

The [^{18}F]F$^-$ is incorporated into the system through isotopic exchange of the nonradioactive ^{19}F with [^{18}F]F$^-$ in water or in aqueous solution and it is usually followed by a simple solid-phase extraction (SPE) purification method (reagent and product are chemically identical and do not require HPLC purification). SiFA has been conjugated to several biomolecules [210, 211,212,213]. However, the need to have bulky groups around the hydrolytically unstable silicon atom have the major drawback of increasing the lipophilicity of the molecule, leading to very high liver uptake observed through *in vivo* studies [210]. The problem was overcome by introducing lipophilicity-reducing groups between the SiFA moiety and the biomolecule, such as an acetylated amino-sugar group attached to the amino acid asparagine, and making the system cationic overall [214,215].

- Organotrifluoroborate (RBF_3^-) systems.

The formation of the radiolabelled [^{18}F]RBF_3^- is achieved either by converting a boronic ester moiety into the trifluoroborate species [216, 217,218] or by an isotopic exchange reaction in acidic solution or aprotic solvents [218]. Isotopic exchange reactions sometimes require the use of a Lewis acid promoter (*e.g.* $SnCl_4$) [8]. Two main organotrifluoroborate species have been developed and successfully ^{18}F-fluorinated: aryl-trifluoroborate and the zwitterionic onium-trifluoroborate [8] (Fig. 64).

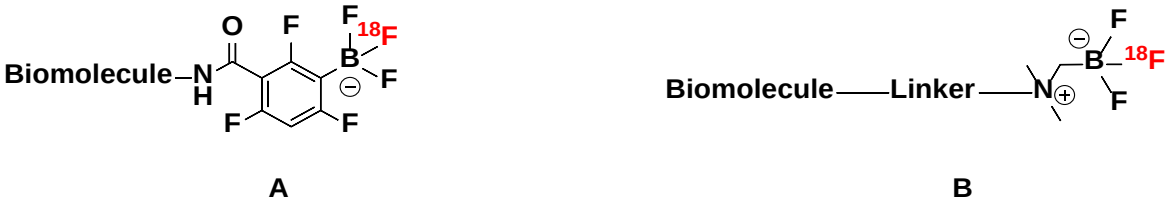

Fig. 64 Aryl-trifluoroborate (**A**) and zwitterionic ammonium-trifluoroborate (**B**) systems.

Since RBF_3^- anions also suffer from hydrolysis, forming the corresponding boronic acid, modifications to the aryl groups were explored. It was concluded that electron-withdrawing groups in the phenyl ring, such as F, confer the required stability to the trifluoroborate moiety. The development of the zwitterionic species is also related to the effort of improving the stability in water of the trifluoroborate unit; in this case the presence of a cationic group (*e.g.* ammonium, phosphonium) enhances the fluoride ion affinity of the borates, acting as an electrostatic anchor for the oppositely charged anion [219,220]. Both systems have been conjugated to biomolecules and their stability *in vivo* investigated [218,219,221,222,223].

- Aluminium ($[^{18}F]AlF$-NOTA) systems.

This chemistry was first reported by McBride *et al.* who investigated the possibility of attaching $[^{18}F]F^-$ to the Group 13 metal aluminium, exploiting their high bond dissociation energy [224,225,226,227]. Thermodynamic and kinetic stability is ensured by the presence of the anionic macrocycle, NOTA (Fig. 65). Despite the ligand being anionic, this chemistry is quite different from the other two examples presented above; this was the first metal-based chelate used for PET application, and the coordination environment does not involve C atoms, making the system and its chemistry quite different from the organo-B/Si chemistry discussed above. In this methodology, $[^{18}F]AlF^{2+}$ is first produced through $Cl/^{18}F$ halide exchange reactions, from $AlCl_3$ and $[^{18}F]KF$, and then reacted with the NOTA ligand (one carboxylic pendant arm is conjugated to a biomolecule), in water at pH 4 (CH_3COONa buffer) and T >100°C. The resulting product has the aluminium metal centre octahedrally coordinated with a N_3O_2F environment around the metal. Various modifications of the linker group and/or in the macrocycle backbone have been reported [228,229].

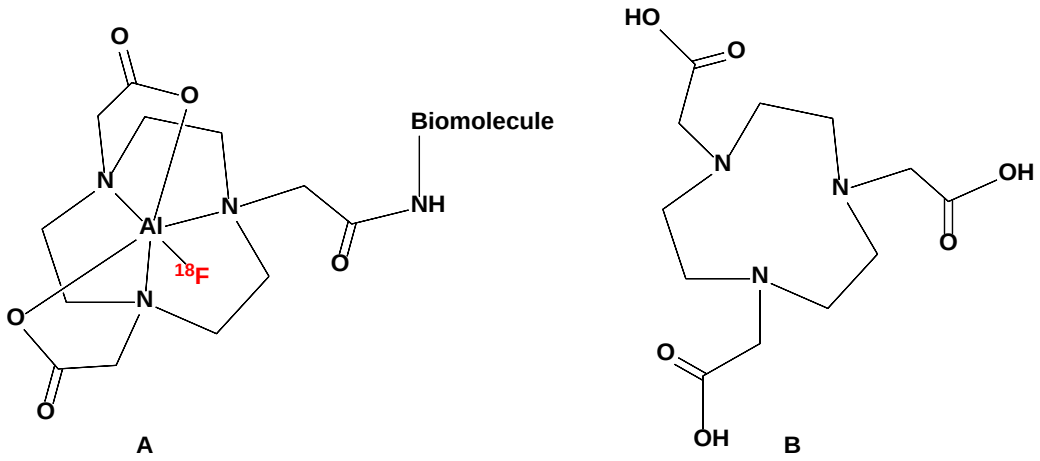

Fig. 65 [^{18}F]AlF-NOTA system (**A**) and H_3NOTA ligand (**B**).

The N_3O_2F coordination environment around the metal was confirmed by an X-ray study on [AlF(NODA-MPAA)] (NODA-MPAA = 1,4,7-triazacyclononane-1,4-diacetic acid-methylphenylacetic acid) [230]. Three nitrogen atoms of the ring and two oxygen atoms of the pendant carboxylate groups of the macrocycle complete the coordination around the metal along with a fluoride ion (Fig. 66).

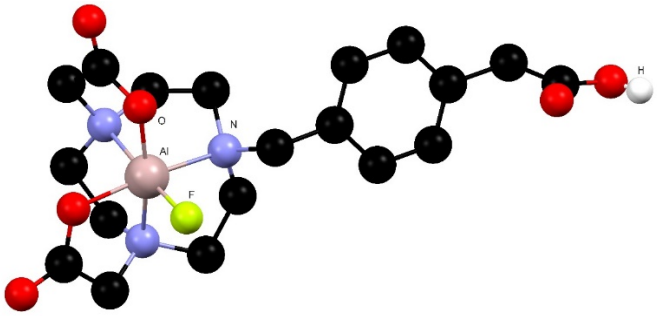

Fig. 66 Structure of [AlF(NODA-MPAA)] redrawn from Reference 228.

The high temperature required for complexation is a drawback when conjugating heat sensitive biomolecules, however, clinical *in vivo* studies of peptide conjugated [^{18}F]AlF-NOTA systems show the validity of this approach [231]. The use of open chain ligands has also been explored and allow for close to room temperature radiolabelling conditions and heat sensitive biomolecules to be employed [232,233].

Other systems successfully ^{18}F-radiolabelled include [^{18}F]BF_4^- [234,235,236], [^{18}F]SO_3F^- [237] and [^{18}F]PF_6^- [238] for imaging of the sodium-iodide symporter, the ^{18}F-fluorination of BODIPY dyes for PET/fluorescence dual modality imaging agents [8,239], and the Ga(III) complex with a dianionic N_3O_2 pentadentate ligand, [GaF(1-Bn-4,7-$(CH_3COO)_2$-tacn)] [153]. The latter was obtained from the chloride analogue in a one-step reaction through Cl/^{18}F halide exchange under aqueous conditions (pH 4) at 80°C for 30 minutes. This system reported good stability to at least pH 6 but defluorinates in phosphate buffered solution (PBS) and human serum albumin (HAS) at pH 7.4 [153]. [GaF(1-Bn-4,7-$(CH_3COO)_2$-tacn)] could also be obtained by reaction of

$Ga(NO_3)_3 \cdot 9H_2O$, [1-Bn-4,7-$(CH_3COO)_2$]$^{2-}$ and non-radioactive KF in water. The crystal structure of the fluoride complex is shown in Fig. 67. The X-ray structural characterisation shows a distorted octahedral coordination at gallium, through the pentadentate ligand and one terminal F^- ligand.

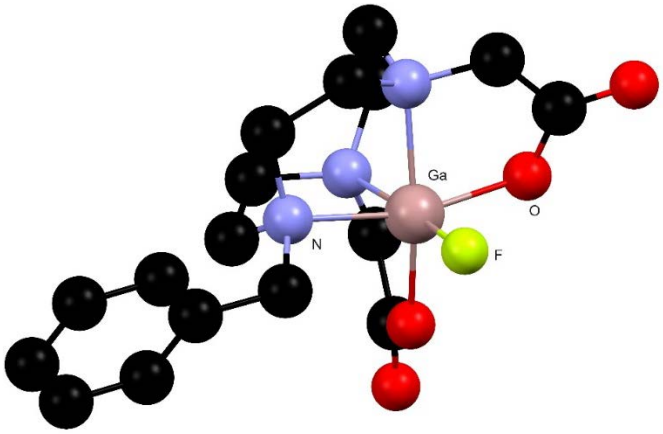

Fig. 67 Structure of [GaF(1-Bn-4,7-$(CH_3COO)_2$-tacn)] redrawn from Reference 153.

^{18}F-radiolabelling of systems with neutral ligands

^{18}F-fluorination of metal/non-metal fluorides coordinated to neutral ligands is less common. N-heterocyclic carbene boron trifluoride (NHC-BF_3) systems were successfully radiofluorinated by ^{18}F/^{19}F isotopic exchange reaction in one labelling step with azeotropically dried [^{18}F][Bu_4N]F (Scheme 8) [143,240].

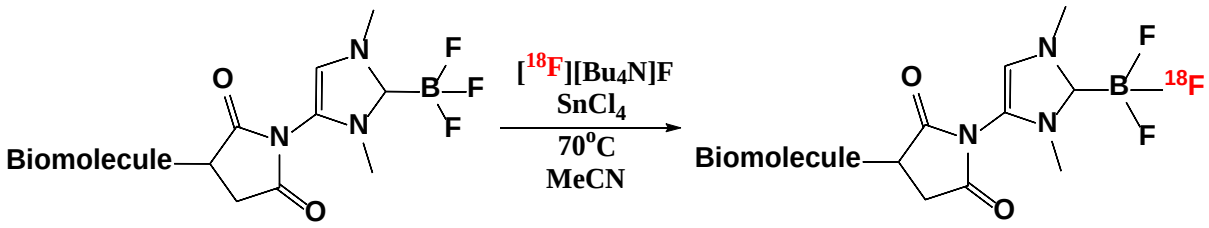

Scheme 8 Radiolabelling conditions of NHC-BF_3.

The exchange requires the presence of an excess of the Lewis acid promoter $SnCl_4$ and proceeds in anhydrous MeCN at 70°C, giving the desired product in good radiochemical yield (RCY) ~ 20-30%. The carbene was functionalised with a maleimide group to attach bioactive molecules prior to the radiolabelling reaction. The radioactive biomolecule-functionalised [^{18}F]NHC-BF_3, showed good *in vitro* and *in vivo* stability. Previously, a two-step radiosynthesis of an NHC-BF_3 adduct in which the biomolecule was attached following ^{18}F-labelling, was reported [143]. The same approach was employed for the ^{18}F-labelling of the analogue NHC-PF_5 (Scheme 9) [175].

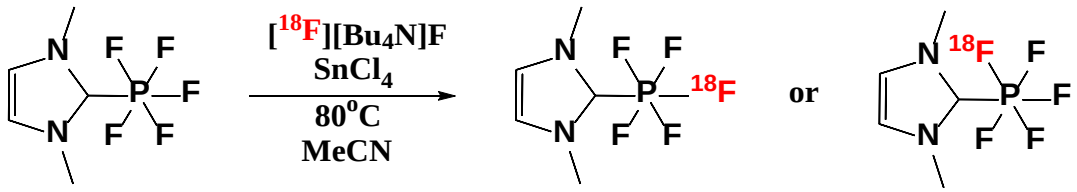

Scheme 9 Radiolabelling conditions of NHC-PF_5.

The RCY were rather poor (6.5%), a problem attributed to the stability of the P-F bond in the system which hinders the $^{18}F/^{19}F$ isotopic exchange. However, the purified radioproduct showed very good stability *in vitro* and *in vivo* [175].

The use of neutral triazacyclononane macrocycles with the Group 13 metal trihalides (M = Al, Ga) was also investigated. [MCl_3($BnMe_2$-tacn)] were successfully ^{18}F-radiolabelled through $Cl/^{18}F$ halide exchange reactions in which the M-F bonds being formed undoubtedly provide a significant thermodynamic driving force for rapid introduction of $[^{18}F]F^-$. The reactions were carried out in the presence of a slight deficit of non-radioactive KF, although in rather different reaction conditions (Scheme 10) [20,148].

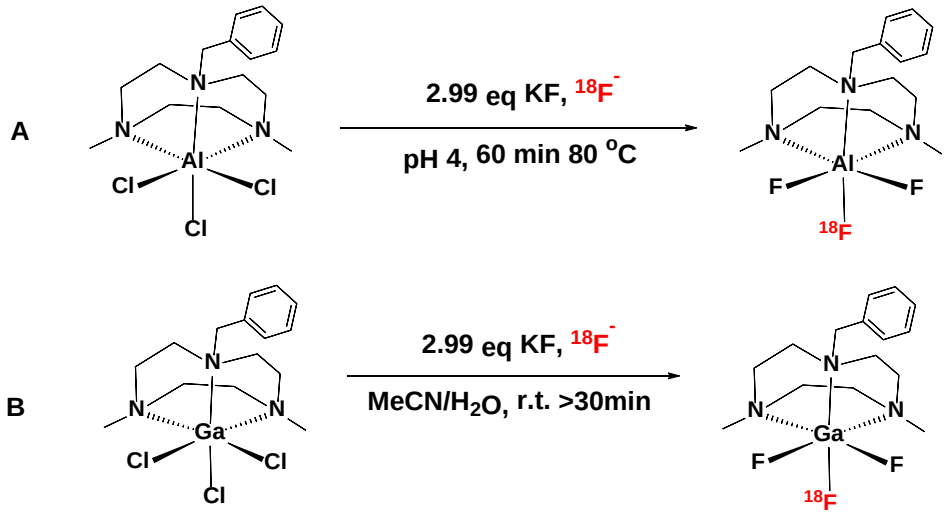

Scheme 10 Radiolabelling methods for [$AlCl_3$($BzMe_2$-tacn)] (**A**) and [$GaCl_3$($BnMe_2$-tacn)] (**B**).

While the Ga system was radiolabelled in aqueous MeCN solution at room temperature, the $AlCl_3$-chelate required a buffered pH 4 solution and 80°C to give a good RCY (30% and 24%, respectively) [20,148]. The RCYs were measured from the radio-HPLC chromatograms of the crude reactions and the product identified by comparison with the retention time (R_t) in the UV-chromatogram of the equivalent non-radioactive product used as reference standard (Fig. 68). The products from both reactions showed good stability *in vitro* (EtOH/PBS solution pH 7.4) with a radiochemical purity (RCP) >90% after 2/3 hours (Fig. 69).

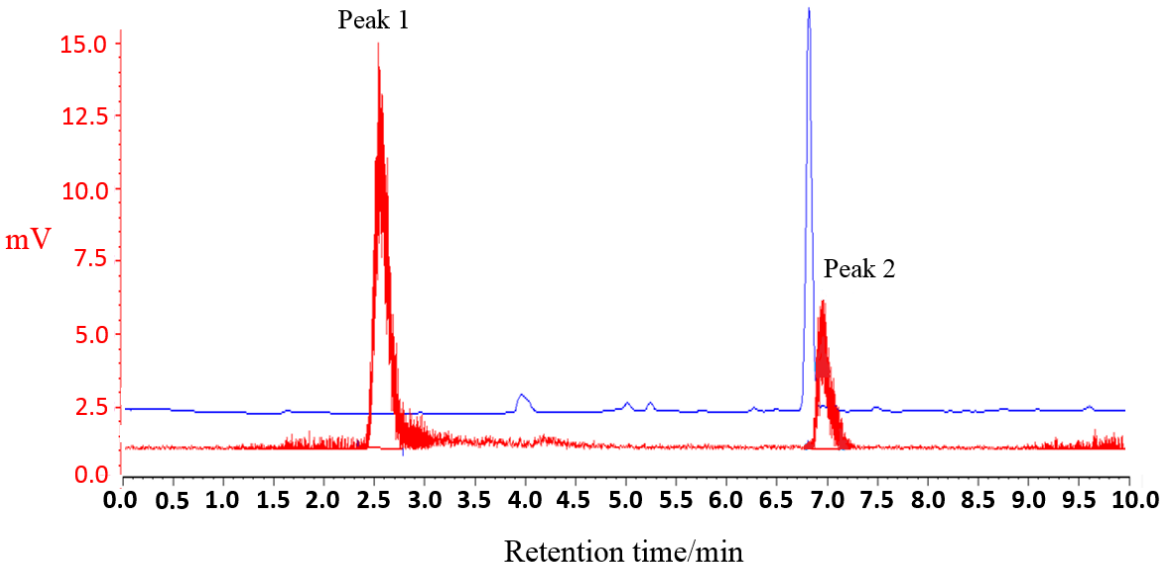

Fig. 68 Radio- (red) and UV-chromatogram (blue) of the crude from the reaction to form [Al^{18}F^{19}F$_2$(BzMe$_2$-tacn)]. Peak 1 = [^{18}F]F$^-$; peak 2 = [Al^{18}F^{19}F$_2$(BzMe$_2$-tacn)]. Reproduced from Ref. 148 with permission from the Royal Society of Chemistry.

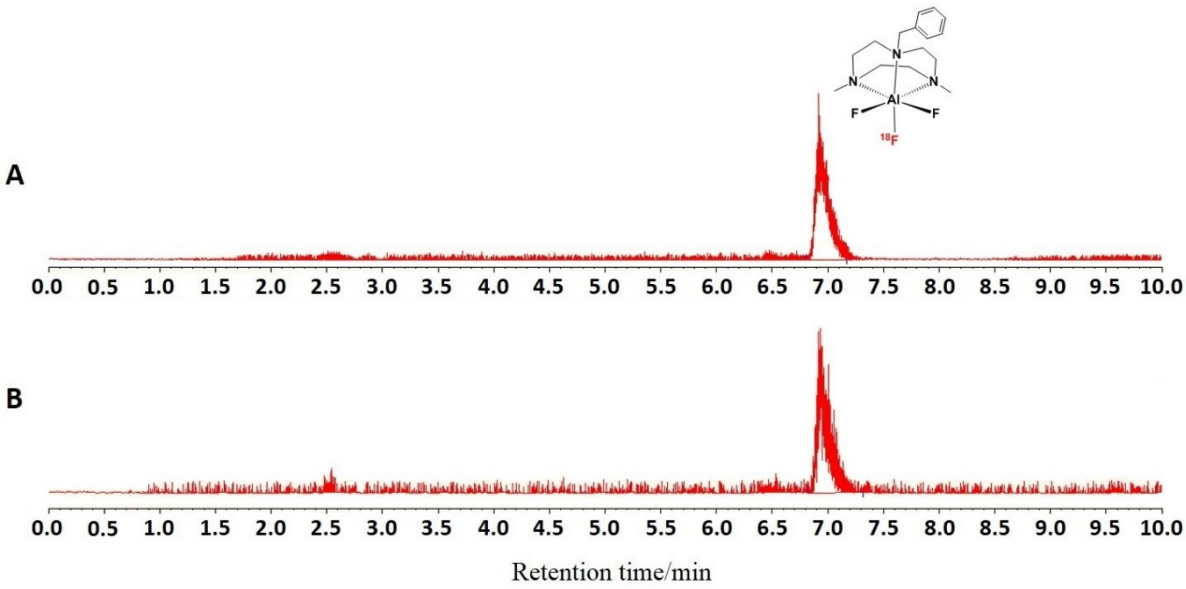

Fig. 69 Radio-chromatogram of the SPE purified [Al^{18}F^{19}F$_2$(BnMe$_2$-tacn)] after 20 minutes (**A**) and 3 hours (**B**) in 50% EtOH/PBS pH 7.4 (RCP 99%).

Both chloride complexes were radiolabelled using 1 mg per mL (2.63 µmol), however attempts to reduce the amount of the metal precursor complex employed were unsuccessful. This was attributed to hydrolysis, which competes with [^{18}F]F$^-$ ions at lower concentration. Likely factors contributing to the differences observed are the higher Al-F bond dissociation energy compared to Ga-F (Table 2) and the higher Lewis acidity and oxophilicity of the Al system. In consideration of the high stability of the [MF$_3$(RMe$_2$-tacn)] (R =

Bn, Me) complexes (they can be obtained in hydrothermal conditions, 180°C 15h) [20], $^{18}F/^{19}F$ isotopic exchange reactions were investigated. Indeed, [GaF_3($BnMe_2$-tacn)] was radiolabelled starting with 0.1 mg per mL (268 nmol) and also 0.01 mg per mL (27 nmol) in aqueous MeCN or EtOH solution at 80°C for 10 minutes, with good RCY (66±4% and 37±5% respectively) (Scheme 11and Fig. 70) [152].

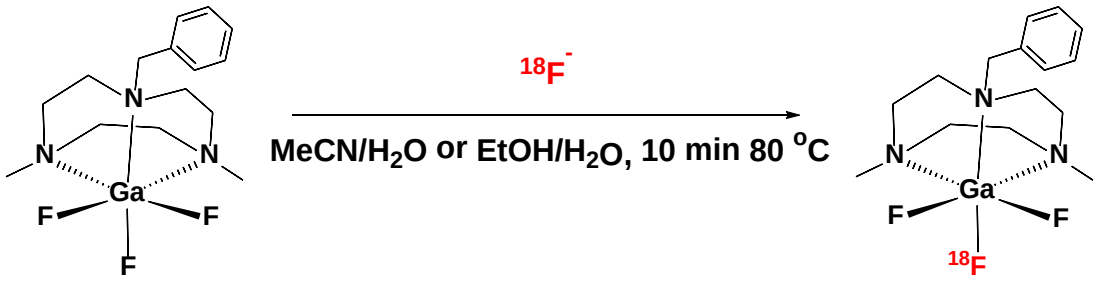

Scheme 11 $^{18}F/^{19}F$ Isotopic exchange method for [GaF_3($BnMe_2$-tacn)].

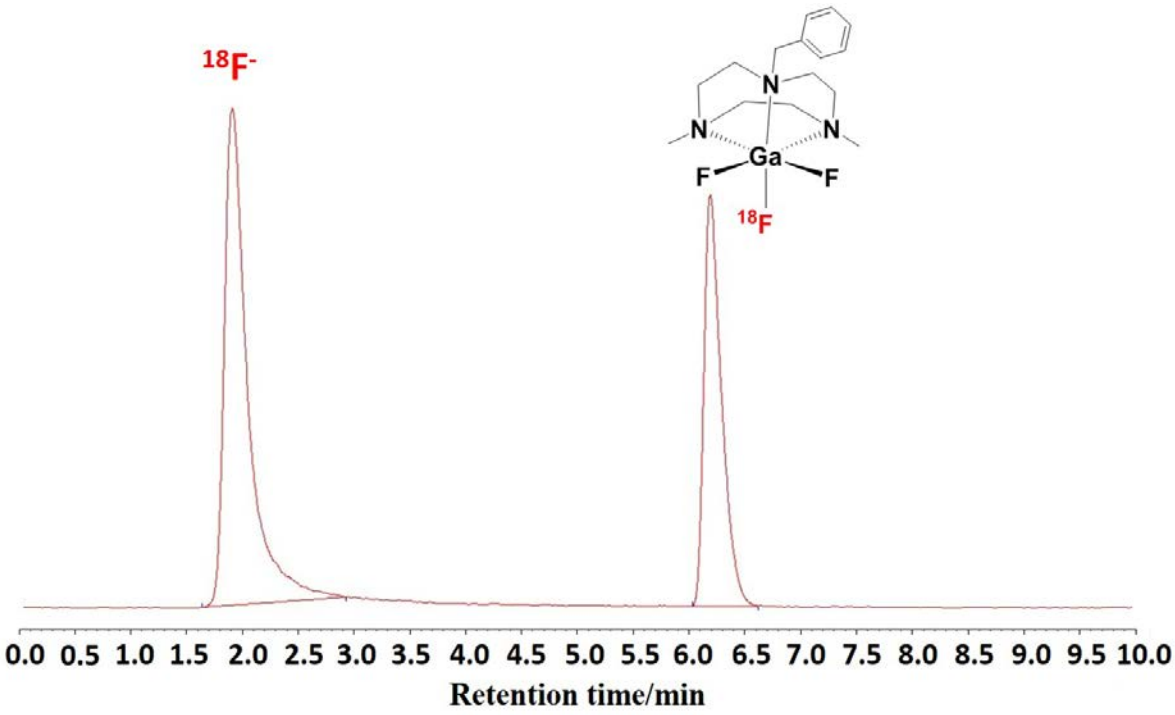

Fig. 70 Radio-chromatogram of the crude from the $^{18}F/^{19}F$ isotopic exchange reaction starting with 0.01 mg of [$Ga^{19}F_3$($BnMe_2$-tacn)] to form [$Ga^{18}F^{19}F_2$($BnMe_2$-tacn)] (38%).

The same method was successfully employed for the radiolabelling of [FeF_3($BnMe_2$-tacn)] which could be radiolabelled using 1 mg, 0.1 mg per mL (2.31 µmol, 230 nmol) in ~ 40% RCY and 0.01 mg per mL (23 nmol) in ~15% RCY [87].

The investigation of other transition metals in the 3+ oxidation state (Sc, Y, La, Cr, Mn, Co) with RMe_2-tacn (R = Me, Bz) was also reported [21,87]. The stability of the [$M^{19}F_3$(RMe_2-tacn)] was firstly investigated in the presence of common anions present in physiological conditions (phosphate, chloride, acetate, carbonate),

fluoride anions, pH and temperature range by means of $^{19}F\{^{1}H\}$ NMR, or UV spectroscopy in the case of the paramagnetic systems. The Y and La fluoride complexes were not obtained [21] and the Mn and Co systems did not show sufficient stability; the Cl/F exchange was too slow to be useful in the Cr system [87]. $[ScF_3(BnM_2\text{-tacn})]$ was stable in water over a range of temperatures and up until slightly basic pH (<8), as well as towards chloride and acetate anions. $[ScF_3(RM_2\text{-tacn})]$ could be formed from $[ScCl_3(RM_2\text{-tacn})]$ with $[Me_4N]F$ in anhydrous MeCN, representing a promising system worth further examination [21]. The complexes of MF_3 (M = Al, Ga, In, Sc, Cr, Mn, Fe, Co) with the tridentate acyclic ligand terpy were also reported, however these systems are generally less stable and are not considered to be suitable complexes for future PET applications [20,21,87].

It seems obvious that the possibility of using metal coordination complexes as ^{18}F PET radiotracers will be strongly dependant on the properties of the metal centre, which ultimately influence the reaction conditions to form the fluoride complexes and their stability. The main metal properties to consider are its size (dictating the coordination number), its redox chemistry and oxophilicity (the fluoride complex must be stable in water or in the presence of anions such as phosphates), its Lewis acidity and lability (allowing rapid Cl/F or $^{18}F/^{19}F$ substitution). Considering that stability tests and Cl/F halide exchange reactions on the non-radioactive complexes are usually performed using between 15-100 mg of material, whereas ^{18}F radiolabelling reactions require very small quantities of precursor and the amount of $[^{18}F]F^-$ is also extremely low, stability and reactivity of the complexes in the two regimes may be very different. At very low concentration, trace impurities, the vast excess of water and $^{19}F^-$ in the mixture can compete with $[^{18}F]F^-$ or disrupt the coordination around the metal, resulting in low RCY or a decrease in RCP over time. The use of neutral ligand systems is of recent origin and many other possibilities for suitable metal/ligand combinations for ^{18}F incorporation are conceivable, and will no doubt attract further studies.

8. Applications

It is evident from the work described in Sections 4-6, that the synthesis and study of metal and non-metal fluoride complexes containing neutral donor ligands is an area of significant current investigation. In addition to their inherent chemical interest, a number of potential applications of the complexes are beginning to emerge. A good example is the use of metal complexes as binding sites for ^{18}F in the drive towards new generations of PET imaging agents (Section 7). Examples now include complexes involving direct bonds from ^{18}F to P, Al, Ga, and Fe, as well as other inorganic anions based upon B and S. The next stages of this work are likely to focus on bioconjugation of peptides and PET imaging studies. A completely different application is the possible use of main group boron and phosphorus fluoride-carbene complexes as electrolyte additives to increase the stability and lifetime of Li-ion batteries [131,132,140,146,169].

The longest established use of non-metal fluorides is in organic and organometallic synthesis. For example, boron trifluoride or its more easily handled adducts, $[BF_3(L)]$ (L = Et_2O, Me_2S, MeOH, etc.) are very widely used as Lewis acids for many organic transformations [126]. More recently, carbene complexes of boron and phosphorus fluorides have attracted much interest as active Lewis acids [140]. Many other fluoride systems have been investigated as possible Lewis acids or catalysts for organic transformations, including olefin polymerisation and C-F bond formation. The different properties conferred on the central element by fluoride ligands usually results in clearly different behaviour compared to corresponding complexes with other anions. Species based upon Ti(IV) fluoride have numerous applications for stoichiometric or catalytic transformations, as described in a recent review [14]. These are typically metallocene based or contain anionic pincer co-ligands, with the catalyst or pre-catalyst prepared *in situ*; usually the active catalyst is not identified. Thus far neutral ligand complexes feature only as precursors to introduce the metal fluoride in a soluble form, e.g. as $[TiF_4(thf)_2]$, but further work can be expected to identify complexes that are themselves active. The specific effects of fluoride ligands are illustrated by olefin polymerisation using the pincer ligand in (Fig. 71) [241]. This complex, prepared from $[TiF_4(thf)_2]$ and the pincer by HF elimination, and activated with MAO (methylaluminoxane), produces ultra-high molecular weight polyethylene. The corresponding chloro-complex is also highly active, but gives a different molecular weight distribution. Other metal systems, including for example, simple complexes of NbF_5, achieve ethylene polymerisation, but the activity is low [66].

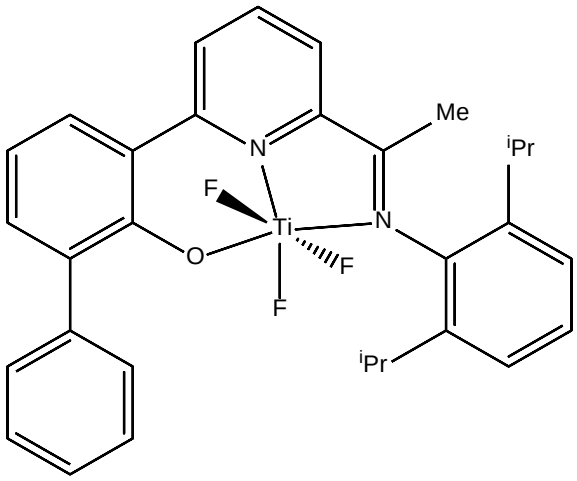

Fig. 71 The (anionic) pincer ligand pre-catalyst for olefin polymerisation [241].

Late d-block fluoride complexes, including those of nickel, palladium and gold, have also been investigated in connection with C-C coupling, C-H activation or C-F bond formation, and described in recent reviews [119,242,243]. The active species are often proposed to be M-F compounds in higher oxidation states, but it is rare for these to be identified and they have been isolated in only a few cases – see for example [116,117,118].

9. Conclusions and Outlook.

Over the approximately eight years covered by this article, there have been many advances in the coordination chemistry of metal fluorides, including the first N-base complexes of AuF_3, phosphine and arsine complexes of the highest oxidation states of the heavy group 5 and 6 elements, NbF_5, TaF_5 and WF_6, and an impressive number of carbene (NHC) complexes with many element fluorides across the Periodic Table. In the p-block, several series of fluorocations with mostly N-donor or NHC ligands have been described, including for P(V), Sb(III), Sn(IV) and Ge(IV), as well as neutral complexes of Group 13 metal fluorides, nitrile adducts of XeF_6 and a pyridine complex with the violently oxidising BrF_3. However, many other significant areas await development. Whilst lanthanide chemistry remains very limited, the chemistry of uranium fluoride complexes is developing, and there are sufficient examples to indicate that a substantial coordination chemistry with N- and O-donor ligands will exist for Pa, U, Np, Pu and Am, although the need for high level radioactivity facilities obviously greatly limits work on the post-uranium elements. In the early d-block, in addition to the absence of detailed study of vanadium(V) and (IV) fluorides, virtually nothing has been reported on complexes of the lower fluorides, including TiF_3, NbF_4, MoF_5 and MoF_4. The binary tri- and tetra- fluorides are intractable polymers, but many chloride complexes are known, and Cl/F exchange may provide a route to some fluoride complexes, although it is likely that in some cases Cl/F exchange from the chloride complexes will promote loss of the neutral ligand and formation of the metal fluoride polymer. The existence of complexes of ZrF_4 and HfF_4 with some neutral N- and O-donor ligands (the parent tetrafluorides are inert polymers), suggests that some further complexes may be accessible and this area merits careful investigation. The platinum metal hexafluorides are too oxidising to co-exist with neutral ligands (and also do not generally form fluoroanions), and no examples with MoF_6 are known, but ReF_6 and possibly ReF_7 appear worth investigation. The tri-, tetra- and possibly penta-fluorides of the platinum metals may complex with nitrile or pyridyl ligands, although this will require elemental fluorine to produce the binary fluoride precursors, as well as fluoroplastic or metal equipment, which limits such studies to a small number of laboratories. Even the complexes of the 3d metal trifluorides were little studied until late, but this has changed as a result of their potential applications in molecular magnets and as ^{18}F carriers for PET applications, and it seems that a wider range of ligand types could be incorporated.

Within the p-block, areas worthy of investigation include cationic fluoro complexes of the Group 13 metals which will have enhanced Lewis acidity compared to the neutral analogues, and detailed studies of the NHC complexes of AsF_5 and SbF_5 to compare with the large amount of work on PF_5 systems. Sulfur tetrafluoride forms only a few thermally unstable adducts, but complexes of TeF_4 have been little studied, and SeF_4 does not seem to have been examined. Nitrile and pyridyl complexes of Group 17 are also possible – while this is

hazardous chemistry, the recent synthesis of [BrF_3(py)] may lead to further examples (some complexes of iodine fluorides were reported over 40 years ago, but lack structural authentication).

Oxide fluoride chemistry is more limited, but recent work has included systematic studies of vanadium, molybdenum, niobium and tungsten oxide fluoride complexes with N- and O-donor ligands, and even for tungsten, some phosphine examples. A significant number of oxide fluorides exist for Re and Os and isolated examples of nitrile complexes have been characterised, but most have not been explored; again the need for fluorine and specialised equipment is a significant barrier. Molecular oxide fluorides in the p-block are mostly with the lighter non-metallic elements, and these appear to have little or no Lewis acidity.

It seems likely that the next few years will see some at least of this new chemistry attempted and a number of exciting new developments are to be expected.

Acknowledgements

We thank EPSRC for a Doctoral Prize EP/R513325/1 (F.M.M.), and the Cambridge Crystallographic Data Centre for access to the files used to draw the structures.

Declaration of Interest: None.

References

[1] Comprehensive Coordination Chemistry, G. Wilkinson, R. D. Gillard, J. A. McCleverty (Eds), Pergamon, Oxford 1987.

[2] Comprehensive Coordination Chemistry II, J. A. McCleverty, T. J. Meyer (Eds), Elsevier, Oxford 2004.

[3] N. M. Doherty, N. W. Hoffman, Chem. Rev. 91 (1991) 553.

[4] H. C. S. Clark, J. H. Holloway, in Advanced Inorganic Fluorides, T. Nakajima, B. Žemva, A. Tressaud (Eds), Elsevier, Oxford 2000, Chapter 3.

[5] H. W. Roesky, Inorg. Chem. 38 (1999) 5934.

[6] B. R. Jagirdar, E. F. Murphy, H. W. Roesky, Progr. Inorg. Chem. 48 (1999) 351.

[7] S. L. Benjamin, W. Levason, G. Reid, Chem. Soc. Rev. 42 (2013) 1460.

[8] K. Chansaenpak, B. Vabre, F. P. Gabbaï, Chem. Soc. Rev. 45 (2016) 954.

[9] P. J. Blower, Dalton Trans. 44 (2015) 4819.

[10] G. E. Smith, H. L. Sladen, S. C. G. Biagini, P. J. Blower, Dalton Trans. 40 (2011) 6196.

[11] K. S. Pedersen, M. A. Sørensen, J. Bendix, Coord. Chem. Rev. 299 (2015) 1.

[12] J. S. Miller, D. Gatteschi (Eds), Chem. Soc. Rev. 40 (2011) issue 6 – themed issue on molecular magnets.

[13] B. L. Pagenkopf, E. M. Carreira, Chem. Eur. J. 5 (1999) 3437.

[14] G. B. Nikiforov, H. W. Roesky, D. Koley, Coord. Chem. Rev. 258-259 (2014) 16.

[15] W. Levason, F. M. Monzittu, G. Reid, W. Zhang, Chem. Commun. 54 (2018) 11681.

[16] S. L. Benjamin, Y. P. Chang, C. Gurnani, A. L. Hector, M. Huggon, W. Levason, G. Reid, Dalton Trans. 43 (2014) 16640.

[17] M. Leblanc, V. Maisonneuve, A. Tressaud, Chem. Rev. 115 (2015) 1191.

[18] K. Seppelt, Chem. Rev. 115 (2015) 1296.

[19] T. Böttcher, G.-V. Röschenthaler, J. Fluor. Chem. 171 (2015) 4.

[20] R. Bhalla, C. Darby, W. Levason, S. K. Luthra, G. McRobbie, G. Reid, G. Sanderson, W. Zhang, Chem. Sci. 5 (2014) 381.

[21] E. Curnock, W. Levason, M. E. Light, S. K. Luthra, G. McRobbie, F. M. Monzittu, G. Reid, R. N. Williams, Dalton Trans. 47 (2018) 6059.

[22] S. L. Benjamin, W. Levason, D. Pugh, G. Reid, W. Zhang, Dalton Trans. 41 (2012) 12548.

[23] Y.-P. Chang, L. Furness, W. Levason, G. Reid, W. Zhang, J. Fluorine Chem. 191 (2016) 149.

[24] E. F. Murphy, R. Murugavel, H. W. Roesky, Chem. Rev. 97 (1997) 3425.

[25] M. F. Davis, M. Jura, A. Leung, W. Levason, B. Littlefield, G. Reid, M. Webster, Dalton Trans. (2008) 6265.

[26] W. Levason, G. Reid, W. Zhang, J. Fluorine Chem. 184 (2016) 50.

[27] W. Levason, G. Reid, J. Trayer, W. Zhang, Dalton Trans. 43 (2014) 3649.

[28] L. Arnaudet, R. Bougon, B. Buu, M. Lance, A. Navaza, M. Nierlich, J. Vigner, J. Fluorine Chem. 59 (1992) 141.

[29] A. L. Hector, A. Jolleys, W. Levason, G. Reid, Dalton Trans. 41 (2012) 10988.

[30] I. Ruppert, V. Bastian, Angew. Chem. Int. Ed. 17 (1978) 214.

[31] F. A. Cotton, J. Lu, Inorg. Chem. 34 (1995) 2639.

[32] F. Kraus, S. A. Baer, Z. Naturforsch. 66B (2011) 868.

[33] F. Kraus, S. A. Baer, Chem. Eur. J. 15 (2009) 8269.

[34] M. J. D. Champion, W. Levason, G. Reid, J. Fluorine Chem. 157 (2014) 19.

[35] P. Woidy, F. Kraus, Z. Anorg. Allg. Chem. 640 (2014) 1547.

[36] G. Gotthelf, M. A. Stuber, A. Y. Kornienko, T. J. Emge, J. G. Brennan, Chem. Commun. 54 (2018) 12018.

[37] P. Woidy, A. J. Karttunen, S. S. Rudel, F. Kraus, Chem. Commun. 51 (2015) 11826.

[38] P. Woidy, A. J. Karttunen, F. Kraus, Z. Anorg. Allg. Chem. 638 (2012) 2044.

[39] B. Scheibe, S. S. Rudel, M. R. Buchner, A. J. Karttunen, F. Kraus, Chem. Eur. J. 23 (2017) 291.

[40] O. J. Cooper, D. P. Mills, W. Lewis, A. J. Blake, S. T. Liddle, Dalton Trans. 43 (2014) 14275.

[41] Q.-J. Pan, Y.-M. Wang, R.-X. Wang, H.-Y. Wu, W. Yang, Z.-M. Sun, H.-X. Zhang, RSC Adv. 3 (2013) 1572.

[42] B. J. Kagan, A. G. Lichtscheidl, K. A. Erickson, M. J. Monreal, B. L. Scott, A. T. Nelson, J. L. Kiplinger, Eur. J. Inorg. Chem. (2018) 1247.

[43] M. Carravetta, M. Concistre, W. Levason, G. Reid, W. Zhang, Inorg. Chem. 55 (2016) 12890.

[44] A. Doddi, C. Gemel, R. W. Seidel, M. Winter, R. A. Fischer, Polyhedron 52 (2013) 1103.

[45] E. G. Il'in, A. V. Tyuremnov, Russ. J. Inorg. Chem. 58 (2013) 1330.

[46] E. G. Il'in, A. S. Parshakov, V. G. Yarzhemskii, V. V. Danilov, G. V. Bodrin, E. I. Goryunov, E. E. Nifant'ev, Doklady Chem. 465 (2015) 272.

[47] E. G. Il'in, A. S. Parshakov, V. I. Privalov, V. V. Danilov, G. V. Bodrin, E. I. Goryunov, E. E. Nifant'ev, Doklady Chem. 467 (2016) 122.

[48] E. G. Il'in, A. S. Parshakov, G. G. Aleksandrov, V. G. Yarzhemskii, V. V. Danilov, G. V. Bodrin, E. I. Goryunov, E. E. Nifant'ev, Doklady Chem. 470 (2016) 255.

[49] R. L. Davidovich, D. V. Marinin, V. Stavila, K. H. Whitmire, Coord. Chem. Rev. 257 (2013) 3074.

[50] R. L. Davidovich, M. A. Pushilin, V. B. Logvinova, A. V. Gerasimenko, J. Struct. Chem. 54 (2013) 541.

[51] R. L. Davidovich, M. A. Pushilin, V. B. Logvinova, A. V. Gerasimenko, J. Struct. Chem. 54 (2013) 741.

[52] V. V. Kovalev, E. G. Il'in, Russ. J. Inorg. Chem. 61 (2016) 63.

[53] Z. Zupanek, M. Tramsek, A. Kokalj, G. Tavcar, Inorg. Chem. 57 (2018) 13866.

[54] J. Kohl, D. Wiedemann, Acta Crystallog. C69 (2013) 1482.

[55] F. H. Aidoudi, C. Black, K. S. A. Arachchige, A. M. Z. Slawin, R. E. Morris, P. Lightfoot, Dalton Trans. 43 (2014) 568.

[56] G. A. Senchyk, V. O. Bukhan'ko, A. B. Lysenko, H. Krautscheid, E. B. Rusanov, A. N. Chernega, M. Karbowiak, K. V. Domasevitch, Inorg. Chem. 51 (2012) 8025.

[57] M. Nicolaou, M. G. Papanikolaou, A. C. Tsipis, T. A. Kabanos, A. D. Keramidas, S. Sproules, H. N. Miras, Chem. Eur. J. 24 (2018) 3836.

[58] S. S. Passadis, C. Tsiafoulis, C. Drouza, A. C. Tsipis, H. N. Miras, A. D. Keramidas, T. A. Kabanos, Inorg. Chem. 55 (2016) 1364.

[59] C. Black, P. Lightfoot, Acta Crystallog. C72 (2016) 80.

[60] P. Woidy, F. Kraus, Z. Naturforsch. 70B (2015) 161.

[61] J. Kohl, D. Wiedemann, S. I. Troyanov, E. Palamidis, M. Lerch, Dalton Trans. 44 (2015) 13272.

[62] S. A. Baer, M. Lozinsek, F. Kraus, Z. Anorg. Allg. Chem. 639 (2013) 2586.

[63] G. Bresciani, T. Funaioli, S. Zacchini, M. Hayatifar, F. Marchetti, G. Pampaloni, Inorg. Chim. Acta 482 (2018) 498.

[64] R. Haiges, P. Deokar, K. O. Christe, Z. Anorg. Allg. Chem. 640 (2014) 1568.

[65] E. G. Il'in, N. A. Ovchinnikova, M. E. Ignatov, Russ. J. Inorg. Chem. 58 (2013) 788.

[66] M. Hayatifar, F. Marchetti, G. Pampaloni, Y. Patil, A. M. R. Galletti, Inorg. Chim. Acta 399 (2013) 214.

[67] F. Marchetti, G. Pampaloni, C. Pinzino, S. Zacchini, Eur. J. Inorg. Chem. (2013) 5755.

[68] R. Haiges, P. Deokar, K. O. Christe, Angew. Chem. Int. Ed. 53 (2014) 5431.

[69] W. Levason, G. Reid, W. Zhang, J. Fluorine Chem. 172 (2015) 62.

[70] W. Levason, M. E. Light, G. Reid, W. Zhang, Dalton Trans. 43 (2014) 9557.

[71] M. Bortoluzzi, F. Marchetti, G. Pampaloni, M. Pucino, S. Zacchini, Dalton Trans. 42 (2013) 13054.

[72] P. A. Petrov, T. S. Sukhikh, M. N. Sokolov, Dalton Trans. 46 (2017) 4902.

[73] M. Bortoluzzi, E. Ferretti, F. Marchetti, G. Pampaloni, S. Zacchini, Dalton Trans. 45 (2016) 6939.

[74] M. Hayatifar, F. Marchetti, G. Pampaloni, S. Zacchini, Polyhedron 70 (2014) 6.

[75] M. Jura, W. Levason, E. Petts, G. Reid, M. Webster, W. Zhang, Dalton Trans. 39 (2010) 10264.

[76] N. Bartalucci, M. Bortoluzzi, G. Pampaloni, C. Pinzino, S. Zacchini, F. Marchetti, Dalton Trans. 47 (2018) 3346.

[77] M. Bortoluzzi, E. Ferretti, F, Marchetti, G. Pampaloni, S. Zacchini, J. Coord. Chem. 69 (2016) 2766.

[78] J. Sala-Pala, J. Y. Calves, J. Guerchais, J. Inorg. Nucl. Chem. 37 (1975) 1294.

[79] C. A. Thuesen, K. S. Pedersen, M. Schau-Magnussen, M. Evangelisti, J. Vibenholt, S. Piligkos, H. Weihe, J. Bendix, Dalton Trans. 41 (2012) 11284.

[80] J. Dreiser, K. S. Pedersen, C. Piamonteze, S. Rusponi, Z. Salman, M. E. Ali, M. Schau-Magnussen, C. A. Thuesen, S. Piligkos, H. Weihe, H. Mutka, O. Waldmann, P. Oppeneer, J. Bendix, F. Nolting, H. Brune, Chem. Sci. 3 (2012) 1024.

[81] T. Birk, K. S. Pedersen, C. A. Thuesen, T. Weyhermüller, M. Schau-Magnussen, S. Piligkos, H. Weihe, S. Mossin, M. Evangelisti, J. Bendix, Inorg. Chem. 51 (2012) 5435,

[82] K. S. Pedersen, G. Lorusso, J. J. Morales, T. Weyhermüller, S. Piligkos, S. K. Singh, D. Larsen, M. Schau-Magnussen, G. Rajaraman, M. Evangelisti, J. Bendix, Angew. Chem. Int. Ed. 53 (2014) 2394.

[83] D. Moon, K. S. Ryoo, J.-H. Choi, Acta Crystallog. 70E (2014) m280.

[84] D. Moon, J.-H. Choi, Acta Crystallog. 69E (2013) m514.

[85] D. Moon, J.-H. Choi, Acta Crystallog. 70E (2014) m290.

[86] J.-H. Choi, D. Moon, J. Mol. Struct. 1059 (2014) 325.

[87] P. J. Blower, W. Levason, S. K. Luthra, G. McRobbie, F. M. Monzittu, T. O. Mules, G. Reid, M. N. Subhan, Dalton Trans., in press. DOI: 10.1039/c8dt03696a.

[88] W. Levason, F. M. Monzittu, G. Reid, W. Zhang, E. G. Hope, J. Fluorine Chem. 200 (2017) 190.

[89] R. Kergoat, J. E. Guerchais, Bull. Chem. Soc. Fr., (1970) 2932.

[90] M. F. Davis, W. Levason, R. Ratnani, G. Reid, T. Rose, M. Webster, Eur. J. Inorg. Chem. (2007) 306.

[91] D. W. Aldous, P. Lightfoot, J. Fluorine Chem. 144 (2012) 108.

[92] M. Wang, T. Weyhermüller, J. England, K. Weighardt, Inorg. Chem. 52 (2013) 12763.

[93] G. C. Stephan, C. Näther, G. Peters, F. Tuczek, Inorg. Chem. 52 (2013) 5931.

[94] D. Turnbull, N. Kostiuk, S. D. Wetmore, M. Gerken, J. Fluorine Chem. 215 (2018) 1.

[95] S. El-Kurdi, A.-A. Al-Terkawi, B. M. Schmidt, A. Dimitrov, K. Seppelt, Chem. Eur. J. 16 (2010) 595.

[96] J. W. Emsley, W. Levason, G. Reid, W. Zhang, G. De Luca, J. Fluorine Chem. 197 (2017) 74.

[97] J. Nieboer, W. Hillary, X. Yu, H. P. A. Mercier, M. Gerken, Inorg. Chem. 48 (2009) 11251.

[98] J. Nieboer, X. Yu, P. Chaudhary, H. P. A. Mercier, M. Gerken, Z. Anorg. Allg. Chem. 638 (2012) 520.

[99] L. Arnaudet, R. Bougon, B. Buu, J. Fluorine Chem. 74 (1995) 223.

[100] E. Houton, B. Kelly, S. Sanz, E. J. L. McInnes, D. Collison, E. U. Brechin, A.-L. Barra, A. G. Ryder, L. F. Jones, Eur. J. Inorg. Chem. (2016) 5123.

[101] K. S. Pedersen, M. Sigrist, H. Weihe, A. D. Bond, C. A. Thuesen, K. P. Simonsen, T. Birk, H. Mutka, A.-L. Barra, J. Bendix, Inorg. Chem. 53 (2014) 5013.

[102] N. Montenegro-Pohlhammer, D. Paez-Hernandez, C. J. Calzado, R. Arratia-Perez, New. J. Chem. 42 (2018) 13847.

[103] H. Kropp, A. Scheurer, F. W. Heinemann, J. Bendix, K. Meyer, Inorg. Chem. 54 (2015) 3562.

[104] H. Lu, T. Yamamoto, W. Yoshimune, N. Hayashi, Y. Kobayashi, Y. Ajiro, H. Kageyama, J. Am. Chem. Soc. 137 (2015) 9804.

[105] T. Huxel, S. Leone, Y. Lan, S. Demeshko, J. Klingele, Eur. J. Inorg. Chem. (2014) 3114.

[106] I. Abdi, J. Lhoste, M. Leblanc, V. Maisonneuve, J.-M. Greneche, G. Viau, A. B. Ali, J. Fluorine Chem. 173, (2015) 23.

[107] M. Smida, J. Lhoste, V. Pimenta, A. Hemon-Ribaud, L. Jouffret, M. Leblanc, M. Dammak, J.-M. Greneche, V. Maisonneuve, Dalton Trans. 42 (2013) 15748.

[108] V. Pimenta, Q. H. H. Le, L. Clark, J. Lhoste, A. Hemon-Ribaud, M. Leblanc, J.-M. Greneche, G. Dujardin, P. Lightfoot, V. Maisonneuve, Dalton Trans. 44 (2015) 7951.

[109] S. Bouketaya, M. Smida, M. S. M. Abdelbaky, M. Dammak, S. Garcia-Granda, J. Solid State Chem. 262 (2018) 343.

[110] S. Dammers, T. P. Zimmermann, S. Walleck, A. Stammler, H. Bögge, E. Bill, T. Glaser, Inorg. Chem. 56 (2017) 1779.

[111] M. Albino, L. Clark, J. Lhoste, C. Payen, J.-M. Greneche, P. Lightfoot, V. Maisonneuve, M. Leblanc, Dalton Trans. 46 (2017) 5352.

[112] M. Wozniak, T. Braun, M. Ahrens, B. Braun-Cula, P. Wittwer, R. Herrmann, R. Laubenstein, Organometallics 37 (2018) 821.

[113] H. Baumgarth, G. Meier, T. Braun, B. Braun-Cula, Eur. J. Inorg. Chem. (2016) 4565.

[114] J. Fawcett, D. A. J. Harding, E. G. Hope, Dalton Trans. 39 (2010) 5827.

[115] J. Fawcett, D. A. J. Harding, E. G. Hope, K. Singh, G. A. Solan, Dalton Trans. 39 (2010) 10781.

[116] F. D'Accriscio, P. Borja, N. Saffon-Merceron, M. Fustier-Boutignon, N. Mezailles, N. Nebra, Angew. Chem. Int. Ed. 56 (2017) 12898.

[117] T. Furuya, T. Ritter, J. Am. Chem. Soc. 130 (2008) 10060.

[118] N. D. Ball, M. S. Sandford, J. Am. Chem. Soc. 131 (2010) 3796.

[119] J. Miró, C. del Pozo, Chem. Rev. 116 (2016) 11924.

[120] M. A. Ellwanger, S. Steinhauer, P. Golz, H. Beckers, A. Wiesner, B. Braun-Cula, T. Braun, S. Riedel, Chem. Eur. J. 23 (2017) 13501.

[121] M. A. Ellwanger, S. Steinhauer, P. Golz, T. Braun, S. Riedel, Angew. Chem. Int. Ed. 57 (2018) 7210.

[122] M. A. Ellwanger, C. von Radow, S. Steinhauer, Y. Zhou, A. Wiesner, H. Beckers, T. Braun, S. Riedel, Chem. Commun. 54 (2018) 9301.

[123] M. Albayer, R. Corbo, J. L. Dutton, Chem. Comm. 54 (2018) 6832.

[124] N. P. Mankad, F. D. Toste, J. Am. Chem. Soc. 132 (2010) 12859.

[125] N. P. Mankad, F. D. Toste, Chem. Sci. 3 (2012) 72.

[126] Boron Science: New Technologies and Applications; N. S. Hosmane (Ed), CRC Press: Boca Raton, FL, 2012.

[127] I. B. Sivaev, V. I. Bregadze, Coord. Chem. Rev. 270-271 (2014) 75.

[128] E. V. Carino, C. E. Diesendruck, J. S. Moore, L. A. Curtiss, R. S. Assary, F. R. Brushett, RSC Adv. 5 (2015) 18822.

[129] E. Chenard, A. Sutrisno, L. Zhu, R. S. Assary, J. A. Kowalski, J. L. Barton, J. A. Bertke, D. L. Gray, F. R. Brushett, L. A. Curtiss, J. S. Moore, J. Phys. Chem. C 120 (2016) 8461.

[130] M. Nie, J. Xia, J. R. Dahn, J. Electrochem. Soc. 162 (2015) A1693.

[131] M. Nie, J. Xia, J. R. Dahn, J. Electrochem. Soc. 162 (2015) A1186.

[132] M. Nie, J. Xia, L. Ma, J. R. Dahn, J. Electrochem. Soc. 162 (2015) A2066.

[133] J. Burt, J. W. Emsley, W. Levason, G. Reid, I. S. Tinkler, Inorg. Chem. 55 (2016) 8852.

[134] U. Monkowius, S. Nogai, H. Schmidbaur, Dalton Trans. (2003) 987.

[135] V. K. Greenacre, W. Levason, G. Reid, Organometallics, 37 (2018) 2123.

[136] D. A. Dickie, U. Chadha, R. A. Kemp, Inorg. Chem. 56 (2017) 7292.

[137] A. Gallen, S. Orgue, G. Muller, E. C. Escudero-Adan, A. Riera, X. Verdaguer, A. Grabulosa, Dalton Trans. 47 (2018) 5366.

[138] C. K. Y. A. Okio, W. Levason, F. M. Monzittu, G. Reid, J. Organomet. Chem. 848 (2017) 232.

[139] C. K. Y. A. Okio, W. Levason, F. M. Monzittu, G. Reid, J. Organomet. Chem. 854 (2018) 140.

[140] V. Nesterov, D. Reiter, P. Bag, P. Frisch, R. Holzner, A. Porzelt, S. Inoue, Chem. Rev. 118 (2018) 9678.

[141] T. Böttcher, S. Steinhauer, L. C. Lewis-Alleyne, B. Neumann, H.-G. Stammler, B. S. Bassil, G.-V. Röschenthaler, B. Hoge, Chem. Eur. J. 21 (2015) 893.

[142] C. Tian, W. Nie, M. V. Borzov, P. Su, Organometallics 31 (2012) 1751.

[143] K. Chansaenpak, M. Wang, Z. Wu, R. Zaman, Z. Li, F. P. Gabbaï, Chem. Commun. 51 (2015) 12439.

[144] D. N. Lastovickova, C. W. Bielawski, Organometallics 35 (2016) 706.

[145] S. Sarmah, A. K. Guha, A. K. Phukan, Eur. J. Inorg. Chem. (2013) 3233.

[146] P. Janssen, B. Streipert, R. Krafft, P. Murmann, R. Wagner, L. Lewis-Alleyne, G.-V. Röschenthaler, M. Winter, I. Cekic-Laskovic, J. Power Sources 367 (2017) 72.

[147] R. Bhalla, W. Levason, S. K. Luthra, G. McRobbie, F. M. Monzittu, J. Palmer, G. Reid, G. Sanderson, W. Zhang, Dalton Trans. 44 (2015) 9569.

[148] W. Levason, S. K. Luthra, G. McRobbie, F. M. Monzittu, G. Reid, Dalton Trans. 46 (2017) 14519.

[149] R. Bhalla, J. Burt, A. L. Hector, W. Levason, S. K. Luthra, G. McRobbie, F. M. Monzittu, G. Reid, Polyhedron, 106 (2016) 65.

[150] A. Dimitrov, D. Heidemann, K. I. Khallow, E. Kemnitz, Inorg. Chem. 51 (2012) 11612.

[151] R. Bhalla, W. Levason, S. K. Luthra, G. McRobbie, G. Reid, G. Sanderson, W. Zhang, Chem. Commun. 50 (2014) 12673.

[152] F. M. Monzittu, I. Khan, W. Levason, S. K. Luthra, G. McRobbie, G. Reid, Angew. Chem. Int. Ed. 57 (2018) 6658.

[153] R. Bhalla, W. Levason, S. K. Luthra, G. McRobbie, G. Sanderson, G. Reid, Chem. Eur. J. 21 (2015) 4688.

[154] C. Bour, J. Monot, S. Tang, R. Guillot, J. Farjon, V. Gandon, Organometallics 33 (2014) 594.

[155] W. Levason, G. Reid, W. Zhang, Coord. Chem. Rev. 255 (2011) 1319.

[156] F. Uhlemann, R. Köppe, A. Schnepf, Z. Anorg. Allg. Chem. 640 (2014) 1658.

[157] S. Sinhababu, S. Kundu, A. N. Paesch, R. Herbst-Irmer, D. Stalke, I. Fernandez, G. Frenking, A. C. Stückl, B. Schwederski, W. Kaim, H. W. Roesky, Chem. Eur. J. 24 (2018) 1264.

[158] W. Levason, D. Pugh, G. Reid, Inorg. Chem. 52 (2013) 5185.

[159] K. George, A. L. Hector, W. Levason, G. Reid, G. Sanderson, M. Webster, W. Zhang, Dalton Trans. 40 (2011) 1584.

[160] N. J. Hora, B. M. Wahl, C. Soares, S. A. Lara, J. R. Lanska, J. A. Phillips, J. Mol. Struct. 1157 (2018) 679.

[161]T. Böttcher, B. S. Bassil, G.-V. Röschenthaler, Inorg. Chem. 51 (2012) 763.

[162] A. W. Waller, N. M. Weiss, D. A. Decato, J. A. Phillips, J. Mol. Struct. 1130 (2017) 984.

[163] R. Suter, A. Swidan, C. L. B. Macdonald, N. Burford, Chem. Commun. 54 (2018) 4140.

[164] M. Göhner, F. Herrmann, N. Kuhn, M. Ströbele, Z. Anorg. Allg. Chem. 638 (2012) 2196.

[165] J. Klösener, M. Wiesemann, B. Neumann, H.-G. Stammler, B. Hoge, Eur. J. Inorg. Chem. (2018) 3960.

[166] R. Suter, A. Swidan, H. S. Zijlstra, C. L. B. Macdonald, J. S. McIndoe, N. Burford, Dalton Trans. 47 (2018) 16729.

[167] M. A. Sanhoury, M. T. B. Dhia, M. R. Khaddar, J. Fluorine Chem. 146 (2013) 15.

[168] M. A. Sanhoury, M. T. B. Dhia, M. R. Khaddar, J. Fluorine Chem. 132 (2011) 865.

[169] P. A. Gray, N. Burford, Coord. Chem. Rev. 324 (2016) 1.

[170] J. Bader, N. Ignat'ev, B. Hoge, Inorg. Chem. 53 (2014) 7547.

[171] C. Tian, W. Nie, Q. Chen, G. Sun, J. Hu, M. V. Borzov, Russ. Chem. Bull. Int. Ed. 63 (2014) 2668.

[172] O. I. Guzyr, S. V. Zasukha, Y. G. Vlasenko, A. N. Chernaga, A. B. Rozhenko, Y. G. Shermolovich, Eur. J. Inorg. Chem. (2013) 4154.

[173] M. Mehta, T. C. Johnstone, J. Lam, B. Bagh, A. Hermannsdorfer, M. Driess, D. W. Stephan, Dalton Trans. 46 (2017) 14149.

[174] M. H. Holthausen, M. Mehta, D. W. Stephan, Angew. Chem. Int. Ed. 53 (2014) 6538.

[175] B. Vabre, K. Chansaenpak, M. Wang, H. Wang, Z. Li, F. P. Gabbaï, Chem. Commun. 53 (2017) 8657.

[176] T. Böttcher, S. Steinhauer, N. Allefeld, B. Hope, B. Neumann, H. G. Stammler, B. S. Bassil, M. Winter, N. W. Mitzel, G.-V. Röschenthaler, Dalton Trans. 43 (2014) 2979.

[177] T. Böttcher, O. Shyshkov, M. Bremer, B. S. Bassil, G.-V. Röschenthaler, Organometallics 31 (2012) 1278.

[178] T. Böttcher, B. S. Bassil, L. Zhechkov, G.-V. Röschenthaler, Inorg. Chem. 52 (2013) 5651.

[179] R. Pajkert, T. Böttcher, M. Ponomarenko, M. Bremer, G.-V. Röschenthaler, Tetrahedron 69 (2013) 8943.

[180] A. Swidan, R. Suter, C. L. B. Macdonald, N. Burford, Chem. Sci. 9 (2018) 5837.

[181] T. Saal, K. O. Christe, R. Haiges, Dalton Trans. 48 (2019) 99.

[182] J. W. Dube, Y. Zheng, W. Thiel, M. Alcarazo, J. Am. Chem. Soc. 138 (2016) 6869.

[183] S. S. Chitnis, N. Burford, M. J. Ferguson, Angew. Chem. Int. Ed. 52 (2013) 2042.

[184] R. Suter, H. Sinclair, N. Burford, R. McDonald, M. J. Ferguson, E. Schrader, Dalton Trans. 46 (2017) 7681.

[185] R. Suter, C. Frazee, N. Burford, R. McDonald, M. J. Ferguson, Chem. Eur. J. 23 (2017) 17363.

[186] K. L. Bamford, A. P. M. Robertson, H. A. Jenkins, B. O. Patrick, N. Burford, Can. J. Chem. 93 (2015) 375.

[187] W. Levason, M. E. Light, S. Maheshwari, G. Reid, W. Zhang, Dalton Trans. 40 (2011) 5291.

[188] P. Farina, W. Levason, G. Reid, Polyhedron 55 (2013) 102.

[189] B. Alic, A. Stefancic, G. Tavcar, Dalton Trans. 46 (2017) 3338.

[190] N. V. Makarenko, V. Ya. Kavun, A. A. Udovenko, E. V. Kovaleva, L. A. Zemnukhova, J. Fluorine Chem. 213 (2018) 56.

[191] P. Chaudhary, J. T. Goettel, H. P. A. Mercier, S. Sowlati-Hashjin, P. Hazendonk, M. Gerken, Chem. Eur. J. 21 (2015) 6247.

[192] J. T. Goettel, P. Chaudhary, P. Hazendonk, H. P. A. Mercier, M. Gerken, Chem. Commun. 48 (2012) 9120.

[193] J.T. Goettel, M. Gerken, Inorg. Chem. 55 (2016) 12441.

[194] V. de P. N. Nziko, S. Scheiner, J. Phys. Chem. A. 118 (2014) 10849.

[195] S. Fritz, C. Ehm, D. Lentz, Inorg. Chem. 54 (2015) 5220.

[164] S. I. Ivlev, M. R. Buchner, A. J. Karttunen, F. Kraus, J. Fluorine Chem. 215 (2018) 17.

[197] D. S. Brock, V. Bilir, H. P. A. Mercier, G. J. Schrobilgen, J. Am. Chem. Soc. 129 (2007) 3598.

[186] E. Makarewicz, J. Lundell, A. J. Gordon, S. Berski, J. Comput. Chem. 37 (2016) 1876.

[199] K. Koppe, J. Haner, H. P. A. Mercier, H.-J. Frohn, G. J. Schrobilgen, Inorg. Chem. 53 (2014) 11640.

[200] K. Matsumoto, J. Haner, H. P. A. Mercier, G. J. Schrobilgen, Angew. Chem. Int. Ed. 54 (2015) 14169.

[201] J. Haner, K. Matsumoto, H. P. A. Mercier, G. J. Schrobilgen, Chem. Eur. J. 22 (2016) 4833.

[202] D. M. Perrin, Acc. Chem. Res. 49 (2016) 1333.

[203] D. M. Perrin, Curr. Opin. Chem. Biol. 45 (2018) 86.

[204] B. P. Burke, G. S. Clemente, S. J. Archibald, Contrast Media Mol. Imaging 10 (2015) 96.

[205] P. Laverman, W. J. McBride, R. M. Sharkey, D. M. Goldenberg, O. C. Boerman, J. Label. Compd. Radiopharm. 57 (2014) 219.

[206] W. J. McBride, R. M. Sharkey, D. M. Goldenberg, EJNMMI Research 3 (2013) 36.

[207] V. Bernard-Gauthier, J. J. Bailey, Z. Liu, B. Wängler, C. Wängler, K. Jurkschat, D. M. Perrin, R. Schirrmacher, Bioconjugate Chem. 27 (2016) 267.

[208] V. Bernard-Gauthier, M. L. Lepage, B. Wängler, J. J. Bailey, S. H. Liang, D. M. Perrin, N. Vasdev, R. Schirrmacher, J. Nucl. Med. 59 (2018) 568.

[209] J. G. Speight, Lange's Handbook of Chemistry, McGraw-Hill Education, 2015.

[210] R. Schirrmacher, G. Bradtmöller, E. Schirrmacher, O. Thews, J. Tillmanns, T. Siessmeier, H. G. Buchholz, P. Bartenstein, B. Wängler, C. M. Niemeyer, K. Jurkschat, Angew. Chem. Int. Ed. 45 (2006) 6047.

[211] P. Rosa-Neto, B. Wängler, L. Iovkova, G. Boening, A. Reader, K. Jurkschat, E. Schirrmacher, ChemBioChem 10 (2009) 1321.

[212] L. Iovkova, D. Könning, B. Wängler, R. Schirrmacher, S. Schoof, H. Arndt, K. Jurkschat, Eur. J. Inorg. Chem. (2011) 2238.

[213] A. P. Kostikov, J. Chin, K. Orchowski, S. Niedermoser, M. M. Kovacevic, A. Aliaga, K. Jurkschat, B. Wängler, C. Wängler, H.-J. Wester, R. Schirrmacher, Bioconjugate Chem. 23 (2012) 106.

[214] C. Wängler, S. Niedermoser, J. Chin, K. Orchowski, E. Schirrmacher, K. Jurkschat, L. Iovkova-Berends, A. P. Kostikov, R. Schirrmacher, B. Wängler, Nat. Protoc. 7 (2012) 1946.

[215] S. Niedermoser, J. Chin, C. Wängler, A. Kostikov, V. Bernard-Gauthier, N. Vogler, J.-P. Soucy, A. J. McEwan, R. Schirrmacher, B. Wängler, J. Nucl. Med. 56 (2015) 1100.

[216] R. Ting, C. Harwig, U. auf dem Keller, S. McCormick, P. Austin, C. M. Overall, M. J. Adam, T. J. Ruth, D. M. Perrin, J. Am. Chem. Soc. 130 (2008) 12045.

[217] Z. Liu, Y. Li, J. Lozada, P. Schaffer, M. J. Adam, T. J. Ruth, D. M. Perrin, Angew. Chem. Int. Ed. 52 (2013) 2303.

[218] Y. Li, Z. Liu, J. Lozada, M. Q. Wong, K. S. Lin, D. Yapp, D. M. Perrin, Nucl. Med. Biol. 40 (2013) 959.

[219] Z. Li, K. Chansaenpak, S. Liu, C. R. Wade, P. S. Conti, F. P. Gabbaï, MedChemComm 3 (2012) 1305.

[220] C. R. Wade, H. Zhao, F. P. Gabbaï, Chem. Commun. 46 (2010) 6380.

[221] Y. Li, J. Guo, S. Tang, L. Lang, X. Chen, D. M. Perrin, J. Nucl. Med. Mol. Imaging 3 (2013) 44.

[222] Z. Liu, M. Pourghiasian, F. Benard, J. Pan, K.-S. Lin, D. M. Perrin, J. Nucl. Med. 55 (2014) 1499.

[223] Z. Liu, M. Pourghiasian, M. A. Radtke, J. Lau, J. Pan, G. M. Dias, D. Yapp, K.-S. Lin, F. Benard, D. M. Perrin, Angew. Chem. Int. Ed. 53 (2014) 11876.

[224] W. J. McBride, R. M. Sharkey, H. Karacay, C. A. D'Souza, E. A. Rossi, P. Laverman, C.-H. Chang, O. C. Boerman, D. M. Goldenberg, J. Nucl. Med. 50 (2009) 991.

[225] P. Leverman, W. J. McBride, R. M. Sharkey, A. Eek, L. Joosten, W. J. G. Oyen, D. M. Goldenberg, O. C. Boerman, J. Nucl. Med. 51 (2010) 454.

[226] I. Dijkgraaf, G. M. Franssen, W. J. McBride, C. A. D'Souza, P. Laverman, C. J. Smith, D. M. Goldenberg, W. J. G. Oyen, O. C. Boerman, J. Nucl. Med. 53 (2012) 947.

[227] K. L. S. Chatalic, G. M. Franssen, W. M. van Weerden, W. J. McBride, P. Laverman, E. de Blois, B. Hajjaj, L. Brunel, D. M. Goldenberg, J.-A. Fehrentz, J. Martinez, O. C. Boerman, M. de Jong, J. Nucl. Med. 55 (2014) 2050.

[228] W. J. McBride, C. A. D'Souza, R. M. Sharkey, H. Karacay, E. A. Rossi, C.-H. Chang, D. M. Goldenberg, Bioconjugate Chem. 21 (2010) 1331.

[229] W. J. McBride, C. A. D'Souza, H. Karacay, R. M. Sharkey, D. M. Goldenberg, Bioconjugate Chem. 23 (2012) 538.

[230] C. A. D'Souza, W. J. McBride, R. M. Sharkey, L. J. Todaro, D. M. Goldenberg, Bioconjugate Chem. 22 (2011) 1793.

[231] W. Wan, N. Guo, D. Pan, C. Yu, Y. Weng, S. Luo, H. Ding, Y. Xu, L. Wang, L. Lang, Q. Xie, M. Yang, X. Chen, J. Nucl. Med. 54 (2013), 691.

[232] F. Cleeren, J. Lecina, E. M. F. Billaud, M. Ahamed, A. Verbruggen, G. M. Bormans, Bioconjugate Chem. 27 (2016) 790.

[233] F. Cleeren, J. Lecina, M. Ahamed, G. Raes, N. Devoogdt, V. Caveliers, P. McQuade, D. J. Rubins, W. Li, A. Verbruggen, C. Xavier, G. Bormans, Theranostics 7 (2017) 2924.

[234] J. O'Doherty, M. Jauregui-Osoro, T. Brothwood, T. Szyszko, P. K. Marsden, M. J. O'Doherty, G. J. R. Cook, P. J. Blower, V. Lewington, J. Nucl. Med. 58 (2017) 1666.

[235] A. Khoshnevisan, M. Jauregui-Osoro, K. Shaw, J. B. Torres, J. D. Young, N. K. Ramakrishnan, A. Jackson, G. E. Smith, A. D. Gee, P. J. Blower, EJNMMI Research 6 (2016) 34.

[236] H. Jiang, A. Bansal, M. K. Pandey, K.-W. Peng, L. Suksanpaisan, S. J. Russell, T. R. DeGrado, J. Nucl. Med. 57 (2016) 1454.

[237] A. Khoshnevisan, K. Chuamsaamarkkee, M. Boudjemeline, A. Jackson, G. E. Smith, A. D. Gee, G. O. Fruhwirth, P. J. Blower, J. Nucl. Med. 58 (2017) 156.

[238] H. Jiang, A. Bansal, R. Goyal, K.-W. Peng, S. J. Russell, T. R. DeGrado, Bioorg. Med. Chem. 26 (2018) 225.

[239] S. Liu, T.-P. Lin, D. Li, L. Leamer, H. Shan, Z. Li, F. P. Gabbaï, P. S. Conti, Theranostics 3 (2013) 181.

[240] K. Chansaenpak, M. Wang, H. Wang, B. C. Giglio, F. P. Gabbaï, Z. Wu, Z. Li, RSC Adv. 7 (2017) 17748.

[241] L. A. Wright, E. G. Hope, G. A. Solan, W. B. Cross, K. Singh, Organometallics, 35 (2016) 1183.

[242] M. G. Campbell, T. Ritter, Chem. Rev. 115 (2015) 612.

[243] T. Ahrens, J. Kohlmann, M. Ahrens, T. Braun, Chem. Rev. 115 (2015) 931.